Three-Dimensional Analysis of the Perforators of the Integument in the Human Thigh

by

Ali Mohammed Alshareef Alkhawaji

Submitted in partial fulfillment of the requirements

for the degree of Master of Science

at

Dalhousie University

Halifax, Nova Scotia

December 2013

DEDICATION

To my grandfather's peaceful soul,

To my parents Mohammed and Fatimah for their unconditional love and support,

To my bride Mona for her patience and steadfastness through the difficult stages of this thesis which included long absences from home

TABLE OF CONTENTS

LIST OF TABLES

LIST OF FIGURES

ABSTRACT

Soft tissue defects resulting from trauma, cancer surgery or congenital abnormalities can occur throughout the body, and are reconstructed with surgical flaps by plastic surgeons. Perforator flaps are the most recent applications of surgical tissue transfers. These tissue transfers are reliant on a single artery and vein, which perfuse a portion of tissue with the blood required for survival. As a result of diminished flap bulk, minimal donor site morbidity, and more donor site choices, perforator flaps are considered to be an advanced form of tissue transfer.

Fifteen thighs obtained from 10 fresh human cadavers were studied. This study employed the 3D imaging software, Materialise's Interactive Medical Image Control System (MIMICS), to create 3D models of the vascular anatomy of the thigh.
In total there is an average of 88 ± 16 arterial perforators supplying the integument of the thigh from nine source arteries.

There is a correlation between the average area perfused per perforator and the diameter of the potential perforator. Based on this vascular anatomy, a "safe" limit of can be estimated based on the ratio of perforator diameter and flap area. The lateral circumflex femoral artery (LCFA), superficial femoral artery (SFA), and profunda femoral artery (PFA), in descending order, were found to be the most reliable vascular territories for large flap harvest. This virtual digital dissection technique yields opportunities for preoperative simulation and can be a valuable educational and training tool.

LIST OF ABBREVIATIONS AND SYMBOLS USED

^{0}C: Celsius degree

3D: Three-dimension

AL: Anterolateral

ALT: Anterolateral thigh flap

AM: Anteromedial

AMT: Anteromedial thigh flap

CAD: Computer aided design

CFA: Common femoral artery

CT: Computed tomography

D-IGA: Descending branch of inferior gluteal artery

DGA: Descending genicular artery

DICOM: Digital imaging and communications in medicine

HU: Hounsfield unit

kg: Kilogram

kPa: Kilopascal

kVp: Kilovolt peak

LCFA: Lateral circumflex femoral artery

LSGA: Lateral superior genicular artery

mAs: Milliampere second

MCFA: Medial circumflex femoral artery

MIGA: Medial inferior genicular artery

MIGA: Medial inferior genicular artery

MIMICS: Materialise's interactive medical image control system

ml: Milliliter

mm: Millimeter

MSGA: Medial superior genicular artery

PA: Popliteal artery

Pb_3 O_4: Lead oxide

PFA: Profunda femoral artery

PL: Posterolateral

PM*l*: Posteromedial

PM*n*: Posteromedian

SFA: Superficial femoral artery

STL: Stereolithography

TFL: Tensor fascia lata muscle

GLOSSARY

Angiography: Medical imaging technique used to visualize arteries, veins and the heart chambers.

Angiosome: Three-dimensional composite block of tissue supplied by a source vessel. The concept correlates the blood supply to the skin from a source artery with its supply to the underlying muscles tendons, nerves and bones.

Computed tomography (CT) scanner: Radiologic imaging that uses computer processing to generate an image of tissue density in slices through the patient's body.

Cutaneous perforator: General term used to define the perforating vessels through different deep tissue to supply subcutaneous fat and overlying skin.

Direct or axial perforator: Type of perforator that exclusively pierces the deep fascia en route to supplying subcutaneous fat and overlying skin.

Fasciocutaneous flap: Surgical flap consists of deep fascia and skin.

Free flaps: Vascularized tissue transfer, which is detached from the donor site, along with its blood supply, then reattached at the recipient site.

Hounsfield scale: is a quantitative scale for describing radiodensity.

Integument: Commonly called skin, is an anatomically and physiologically specialized boundary lamina essential to life. The integument consists of the epidermis - superficial layer, and the dermis - the deep moderately dense layer.

Musculocutaneous flap: Surgical flap comprised of muscle and skin.

Musculocutaneous perforator: Type of perforator that courses through muscle and the deep fascia en route to supplying subcutaneous fat and overlying skin.

Pedicled flap: Vascularized tissue transfer, which remains attached to the pedicle of the donor site.

Perforator flap: A skin transfer that relies on a single artery and vein, which perfuse a portion of tissue.

Posterior thigh: Loosely defined as a sub-region bordered by the inferior gluteal fold superiorly, the iliotibial tract laterally, the posterior border of the gracilis muscle medially, and a horizontal line along the superior pole of the patella inferiorly.

Septocutaneous perforator: Type of perforator that courses through the intramuscular septum and the deep fascia en route to supplying subcutaneous fat and overlying skin.

Subcutaneous tissue fat: Adipose tissue located between the overlying dermis layer and the underlying deep fascia. Generally considered as part of the skin.

Thigh region: Defined as a region extending distally from the inguinal ligament line anteriorly and posteriorly from the gluteal fold to a horizontal line along the superior pole of the patella.

Three-dimensional computerized modeling: Technique used to create three-dimensional models of body components using three-dimensional scans and specialized software.

ACKNOWLEDGEMENTS

I would like to express the deepest appreciation to my supervisor Professor Steven Morris, who has assiduously guided me throughout this thesis providing deep insights and mentorship. He has always infused a spirit of adventure and excitement in me with regard to research, scholarship and teaching. Without his persistent and yet welcome guidance, this thesis would not have proceeded as efficaciously as it has.

Special thanks to my committee chair, Dr. Kazue Semba, who has always enthusiastically supported this thesis. Her timely advice throughout the thesis proceeded was very helpful in keeping the study on schedule.

Special gratitude to my thesis committee members, Dr. Michael Bezuhly, Dr. Boris Kablar and the external examiner Dr. William Currie; together their knowledge and insights have infused this study.

Last but not least, I am eternally grateful to the King Saud Bin Abdulaziz University for Health Sciences (KSU-HS), College of Medicine, for the sponsorship and financial support in this master of sciences (MSc) program.

CHAPTER 1 INTRODUCTION

Anatomical research related to the identification of innovative autologous tissue transfers and characterization of components of known flaps is essential to the advancement of reconstructive surgery. The goal in the reconstruction of complex defects resulting from trauma, congenital causes, or large tumor ablation is to restore the normal anatomy using available donor tissues. Defects can be highly variable, which necessitates an extensive knowledge of the available reconstructive options for tissue transfer. This, in turn, requires a detailed knowledge of the underlying vascular anatomy of both potential donor sites and recipient areas. Perforator flaps have become a popular option for reconstruction because of their advantages including longer pedicle length, more extensive donor site options, reduced donor site morbidity and an increased opportunity to "customize" the reconstructive result.

The thigh region is considered the largest donor site available for perforator flap harvest. Each thigh contributes 10.5% of total body surface area.[1] The integument (the skin and the underlying subcutaneous tissue) of this region is supplied by a mixture of musculocutaneous and septocutaneous perforators, the majority of which originate from the profunda femoral artery (PFA) and related primary branches - the medial circumflex femoral artery (MCFA) and the lateral circumflex femoral artery (LCFA).[1] These vessels provide versatile reconstructive options that may be utilized in many surgical scenarios. The initial quantification of PFA, MCFA and LCFA perforators,[1] and description of anatomical landmarks used to facilitate flap dissection[2] have advanced the field of perforator flap surgery.

The increasing use of perforator flaps based on PFA, LCFA and MCFA perforators of the thigh requires detailed knowledge of the vascular anatomy. The thigh is used for both free and pedicled flaps because the thigh can be concealed by clothing and can be closed primarily.[3] However, this region exhibits vascular anomalies and vessel disease, especially among Western socities.[3] A comprehensive understanding of the underlying vascular anatomy is therefore essential to the safe design of existing perforator flaps; it may also lead to the identification of other suitable donor site options not previously described.

This study develops a digitized, interactive visual model of the vascular anatomy of the thigh region using three-dimensional (3D) angiography and Materialise's Interactive Medical Image Control System (MIMICS) software to provide morphological data, including detailed information regarding dimensions, localization and description of vascular territories. Data collected and subsequent analysis and discussion is intended to facilitate the utilization of thigh perforator flaps as reliable and viable surgical options.

CHAPTER 2 LITERATURE REVIEW

Anatomical research into vascular architecture has expanded the understanding of blood vessel orientation. Vascular anatomical knowledge underpins effective flap surgery; detailed understanding of the underlying arterial anatomy involved is required for safe flap design.

2.1 Overview of the historical development of vascular anatomical descriptions

The investigation of blood supply to the integument has made slow progress due to technical challenges in past methods and availability of human cadavers. Historically, shortages of cadavers have limited anatomical teaching and research, and prompted illegal acquisition of human cadavers.[4] While methods used to assess microvascular anatomy have improved, low body donation can still limit anatomical research today. Each new era of anatomical research relevant to reconstructive surgery has been led by the innovative efforts of a few investigators. Anatomists have had an integral role in the advancement of flap surgery, providing surgeons with many suitable donor sites for flap surgery.

2.1.1 Pioneering descriptions

Early knowledge of vascular anatomy was attained through dissection.[5] Manchot, relying on extensive dissection, provided the first description of skin vasculature in *Skin arteries of the human body.*[6] This description defining 40 vascular territories, remains the standard for defining blood supply to the integument (Figure 1). A century later, the work of Manchot was expanded and published under the title *The cutaneous arteries of the*

human body, where the work of Manchot was described as “plastic surgery’s missed opportunity”.[7]

Spalteholz initially documented two major types of blood vessels which supply the skin (perforators): musculocutaneous arteries supply muscles, and have “indirect” branches that terminate in the skin; septocutaneous arteries perforate “directly” to the skin between the body tissues. These vessels then anastomose to form the cutaneous plexus.[8] Salmon then developed the use of a radiographic agent and radiography to study the cutaneous arteries.[9] Lead oxide injection and two-dimensional angiography (2D) were pioneered to assess the vascular anatomy of human integument (Figure 2).[9] More than 80 cutaneous vascular territories, covering the entire body, were defined. The equilibrium law governing the relationship between arteries supplying the same cutaneous territory was proposed.[9] Essentially the law states that if the vascular territory of one artery is larger, the territory of the adjacent arteries will be smaller.[9]

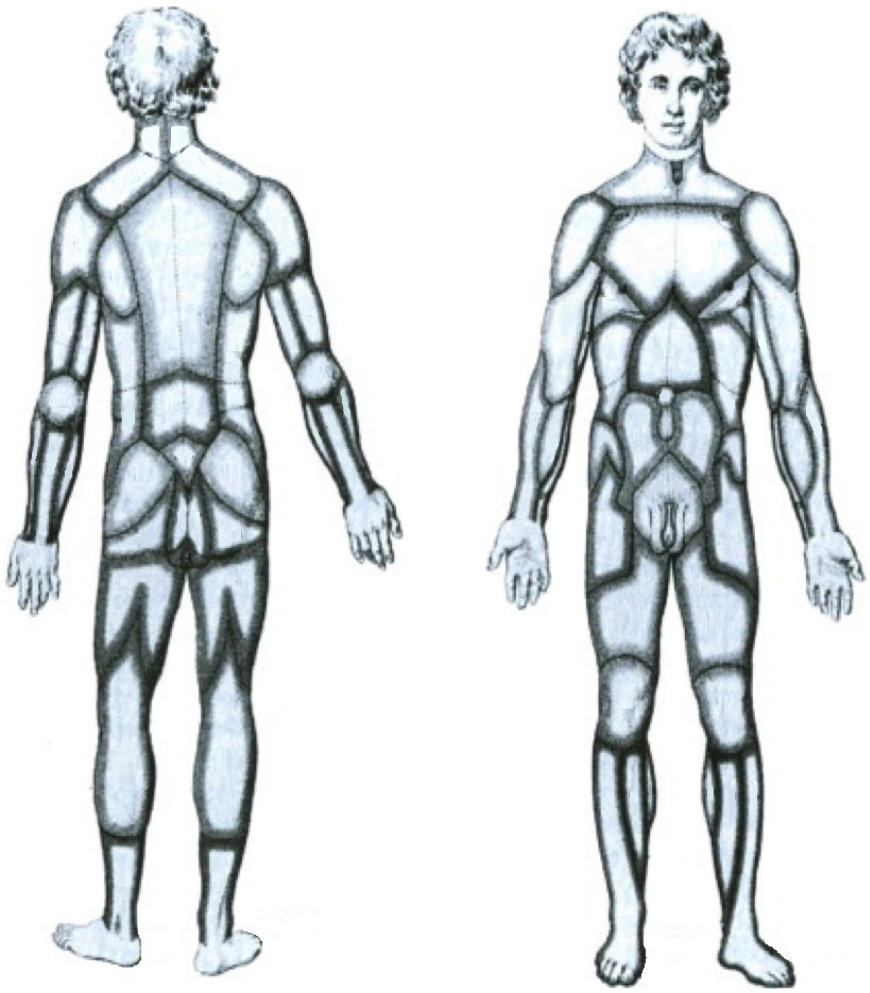

Figure 1: Carl Manchot's description of the vascular territories of the human body.[10] (Modified from Morris et al.[10])

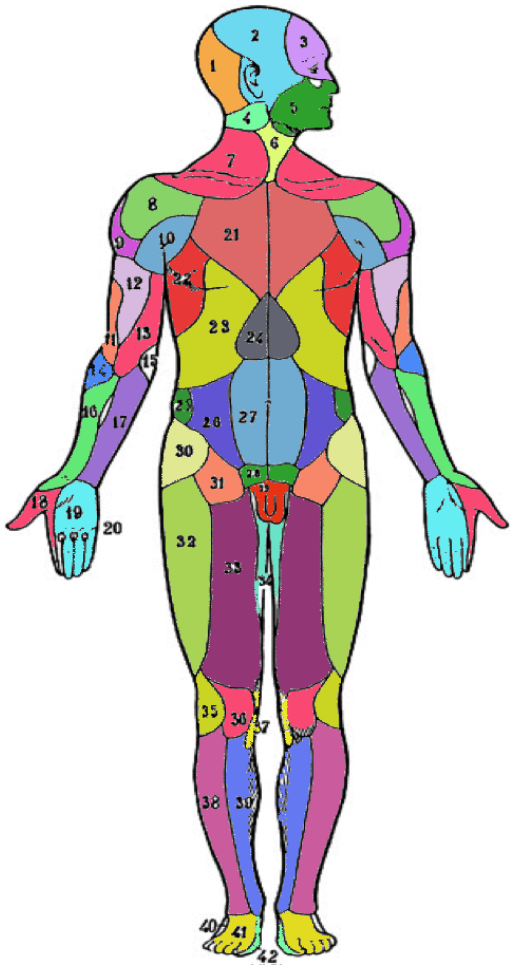

Figure 2: Michel Salmon's description of the vascular territories of the human body.[11] (Modified from Taylor et al.[11])

2.1.2 The angiosome and perforasome concepts

The term "angiosome" is a compound term derived from two Greek words, *angeion* meaning vessel and *somite* meaning section of the body.[12] The "angiosome" concept anatomically describes the body as 3D composite blocks of tissue supplied by source arteries.[12,] This concept correlates the blood supply to the skin from a source artery with its supply to the underlying muscles tendons, nerves and bones. It was proposed to define the 3D vascular territories of primary source vessels.[12] These angiosomes, connected through anastomotic or "choke vessels",[3,12] were documented from two-dimensional angiograms using the refined radio-contrast injection methodology,[13] combined with dissection.

In addition to the two major types of perforators intially described Spalteholz,[8] a third type of perforator, which course directly to the integument, was subsequently proposed to be the primary blood supply to the integument in addition to musculocutaneous or septocutaneous vessels.[12] This knowledge led to an explosion in the application of perforator flaps, becoming the fundamental basis of flap surgery, and allowing for the design of a flap at any donor site where a suitable perforator could be identified (Figure 3 + Table 1).[3,12]

Subsequently, the "perforasome" or "perforator angiosome" concept defines the boundaries of cutaneous territories supplied by a perforator by lines drawn through the anastomotic zone connecting that perforator with adjacent 'perforasomes' in all directions. These perforasome are linked together like a *patchwork quilt* (Figure 4).[14] Extrapolation from a surgical study performed on animal models revealed the possibility of the safe harvest of the anatomical territory of radially contiguous perfraosomes (without their

perforators), all of which will survive relying on the perforator of the central perforasome.[14,15]

Further study of the arterial anatomy led to improved understanding of the anatomical basis of perforator flaps. Cutaneous perforators of the human body were mapped with more detail as a result of research combining cadaver injection studies, tedious dissection and 2D angiography,[1,16-19] representing the most comprehensive study of the cutaneous fine arterial anatomy up to date. In addition these studies filled a fundamental deficiency in previous studies by quantifying perforators, introducing dimensional analysis (diameter, pedicle length) of perforators obtained by dissection, and describing the zones of cutaneous blood supply used for flap surgery design (Figure 5 + Table 2).[1,16-19]

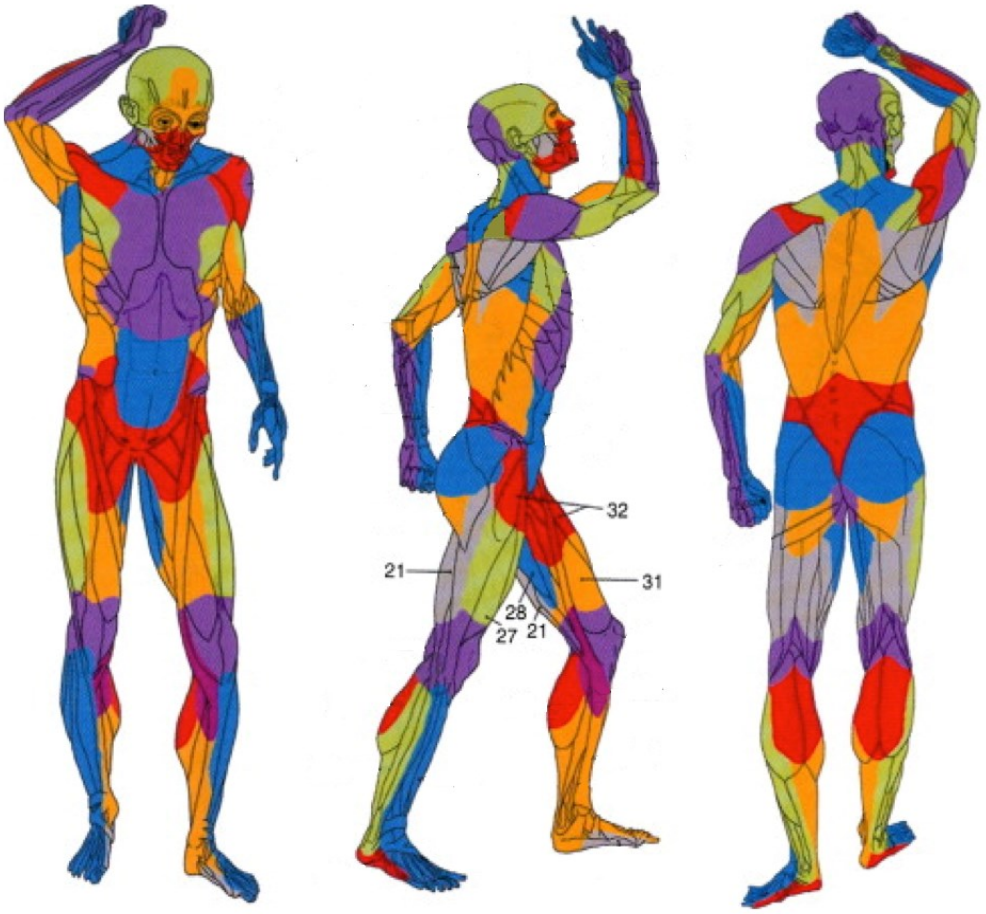

Figure 3: G. Ian Taylor's description of the vascular territories of the human body.[11] Each vascular territory supply a three-dimensional (3D) composite block of tissue (angiosome). Vascular territories of profunda femoral artery (21); lateral circumflex femoral (27); adductor (profunda) (28); superficial femoral (31) and common femoral (32).[11] (Modified from Taylor et al.[11])

Table 1: Several potential perforator flaps of the thigh region based on the classification of angiosomes by Taylor and Palmer.[11]

Source artery	Major superficial muscle(s) supplied	Angiosome	Perforator flap
Profunda femoral	Sartorius Vastus medialis Rectus femoris Adductor longus	21. Profunda femoral	PFAPF
Lateral circumflex femoral	Tensor fascia lata Vastus lateralis	27. Lateral circumflex femoral	LCFAPF
Adductor branch of profunda femoral	Adductor longus Gracilis Adductor brevis Adductor magnus	28. Adductor (profunda)	PFAPF
Superficial femoral	Adductor longus Adductor magnus Adductor brevis Gracilis Vastus medialis	31. Superficial femoral	SFAPF
Common femoral	Sartorius Vastus medialis Rectus femoris Adductor longus	32. Common femoral	CFAPF

The source artery, perforated and supplied muscles, corresponding angiosome and potential perforator flap name are listed. See Figure 3 for diagram of angiosomes of the profunda femoral artery (21); lateral circumflex femoral (27); adductor (profunda) (28); superficial femoral (31) and common femoral (32).[11]

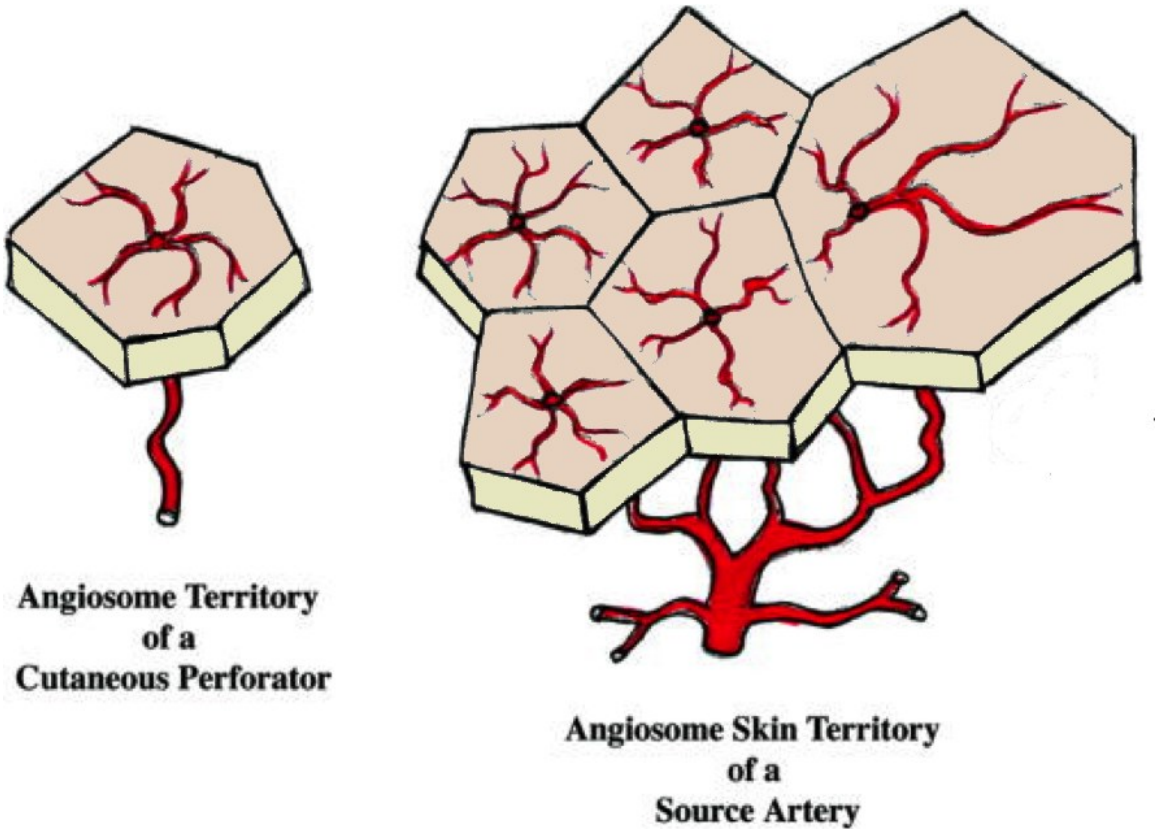

Figure 4: Schematic representations of the cutaneous perforasome and angiosome.[14] On the left, cutaneous perforator angiosomes (*perforasome*) and on the right, several perforasomes combined to represent the cutaneous territory of a source artery (*angiosome*).[14] (Modified from Taylor et al.[14])

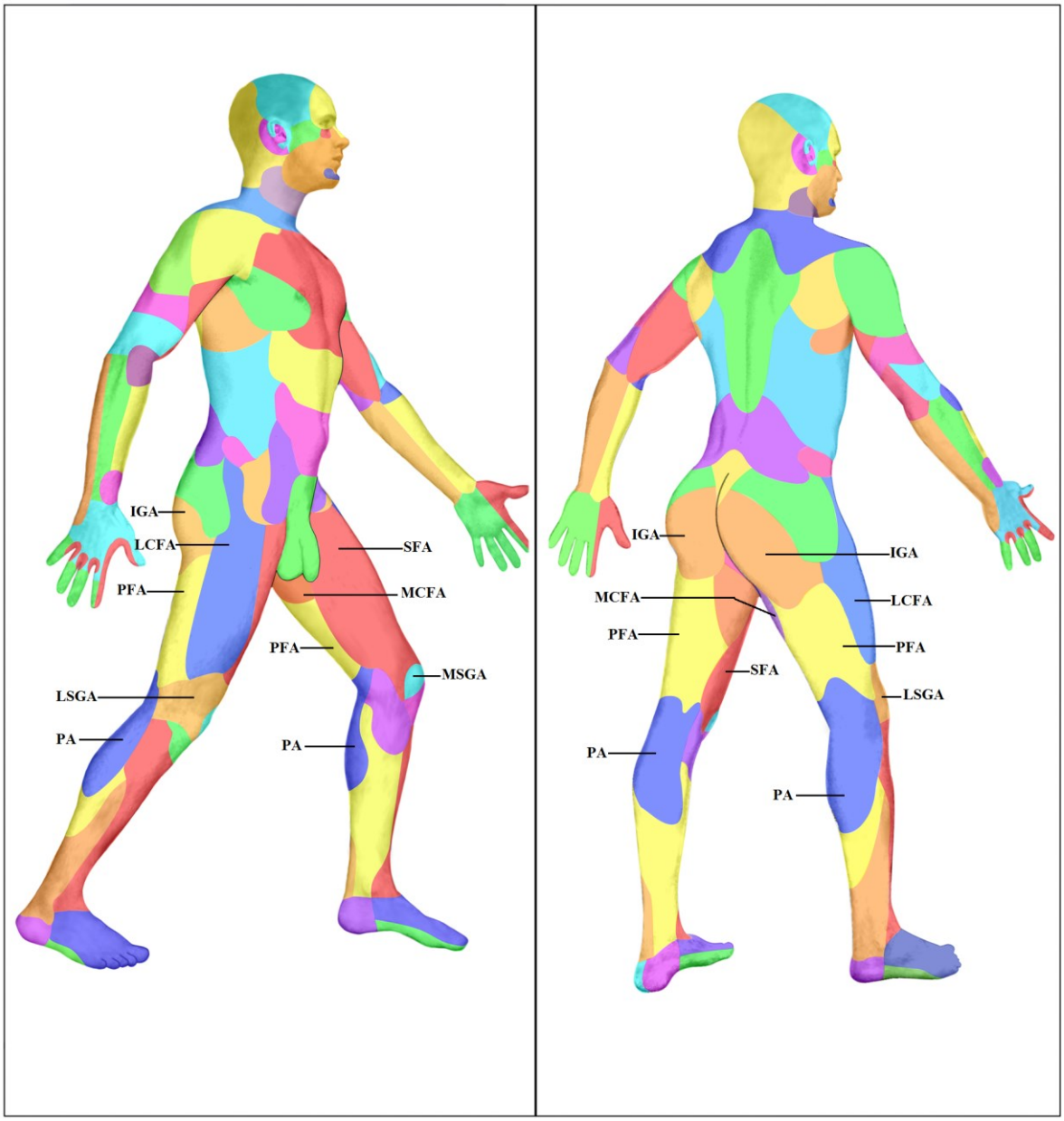

Figure 5: Composite diagram showing vascular territories of the human body that correspond to source arteries.[10] Vascular territories of descending genicular artery (DGA); inferior gluteal artery (IGA); lateral circumflex femoral artery (LCFA); lateral superior genicular artery (LSGA); medial circumflex femoral artery (MCFA); medial superior genicular artery (MSGA); popliteal artery (PA); profunda femoral artery (PFA); superficial femoral artery (SFA). (Modified from Morris et al.[10])

Table 2: The abbreviations of vascular territories of the thigh that correspond to source arteries, associated with Figure 5.[10]

Source artery	Abbreviation
Inferior gluteal artery	IGA
Superficial femoral artery	SFA
Profunda femoral artery	PFA
Medial circumflex femoral artery	MCFA
Lateral circumflex femoral artery	LCFA
Popliteal artery	PA
Descending genicular artery	DGA
Lateral superior genicular artery	LSGA
Medial superior genicular artery	MSGA

2.1.3 Modern three-dimensional (3D) digitized modeling

Technological advancements in health biomedical sciences have provided new research tools for exploring human anatomy. Previous anatomical studies used cadaveric dissection and two-dimensional (2D) angiography as the standard for investigating the vascular supply of muscles, skin and bones.[1-3,9-12,16-19] The visualization of microvascular anatomy of the integument was limited by representation in 2D, complicating the interpretation of the spatial locations of vessels in relationship to nearby structures.[20]

Materialise's Interactive Medical Imaging Control System (MIMICS) software (Materialise, Leuven, Belgium) was initially developed to provide medical image segmentation tools for engineering in anatomy, and used in the field of orthopedics to simulate prosthetic surgery. In 2008, a pilot study combined 3D angiography of human cadavers arterially injected with lead oxide mixture combined with MIMICS software.[20] The creation of a digitized, interactive, visual 3D model of the arterial vascular anatomy was possible, marking a significant advancement in anatomic, plastic and reconstructive surgery research,[20] as it allows for spatially accurate depictions of the complex vascular anatomy of the area of interest, and facilitates data collection. Rotating reconstructed models resolve ambiguities associated with assessing vascular anatomy in 2D permitting the ability to measure actual length of pedicle, diameter of perforators, and a better understanding of perforator course and type classification. Evaluating the relationship of perforators to surrounding structures is important to developing anatomical landmarks that can be used clinically to locate these vessels. Many recent anatomical cadaveric studies[21-25] have used the 3D modeling technique to study the vascular anatomy of various surgical flaps.

2.2 Review of vascular injection methods for angiography

Shortly after the invention of X-rays, originally referred to as Roentgen rays, in 1895, Teichann's mixture of petroleum, mercury and chalk was used to inject the upper limbs of human cadavers marking the first attempt to use a radiopaque material to produce an arterial angiogram.[26] The ideal radiopaque material for whole body angiography as well as isolated organ perfusion was believed to have the following characteristics:[27]

(a) Perfect homogeneity in order to avoid formation of coarse granules, which would block the fine arterioles, and consequently interfere with the completeness of the perfusion.

(b) Adequately thin, to perfuse into the fine arterioles.

(c) Miscible with formalin and other solvents to prevent the "separation out" of the material after mixing with formalin, blood or saline (used for washing out the blood contained within vessels prior to injection).

(d) The mass must "set" in the arteries after injection to facilitate subsequent dissection without oozing and staining.

(e) The material should cast a high contrast shadow on X-rays.

(f) Perfusion procedure must be performed without heat.

(g) Permit easy manipulation.

Many radiopaque media have been assessed including barium salts, bismuth salts, lead salts, metallic mercury, calcium salts, and colloids.[27,28] Lead oxide and barium sulfate have emerged as the most reliable and consistent radiopaque materials used to date. Tables 3, 4 and 5 present the historical development of contrast media from 1907-2013.

Barium

Barium, first used by Gough, was a standard for angiographic studies of basic vascular anatomy for much of the past century.[27] Three years after the initial use, the barium technique was modified to include sodium bromide, with gelatin as a suspension medium.[28] Many scientists continued to use barium for angiography between 1950-1975.[28-30] In 2013, however, epoxy emerged as a suspension medium, and barium sulfate resurfaced as a radiopaque agent.[31]

Lead oxide

Lead oxide is the most widely used material for visualizing the micro and macro vascular anatomy for surgical research.[28] Jamin and Merkel pioneered the use of lead oxide and gelatin in 1907.[28] Thirty years later, colophony, ether and phenol, as suspending mediums, were used to enhance lead oxide perfusion in the study of muscle and integument vascular anatomy.[9] This technique was subsequently simplified by re-employing the gelatin to harden the mixture after the injection, in order to assist in the subsequent dissection.[13]

Currently, the modified lead oxide injection technique has gained popularity in vascular anatomy research. This technique,[32] a refinement of the simplified lead oxide injection,[13] minimizes lead oxide volume, and modifies gelatin quantity in order to optimize the angiography. By the addition of powdered milk as a minor modification, the effectiveness of the mixture's perfusion through the microvasculature is improved giving rise to the technique of micro-angiography. Micro-angiography is a recently developed technique used for visualizing microvasculature, for example, in the lymphatic vessels.[33]

Table 3: The development of lead as contrast media for vascular anatomical studies.

Compound	Researcher	Suspending medium	Year
Lead oxide	Jamin and Markel	Gelatin	1906
Lead chromate	Parker	N/A	1913
Lead oxide	Salmon	Oil, colophony, ether, phenol	1936
Lead phosphate	Schlesinger	Agar or gelatin	1938
White lead	Olovson	Acacia	1941
Lead oxide	Rees and Taylor	Gelatin	1986
Lead oxide	Taylor and Palmer	Gelatin	1987
Lead oxide	Tang et al.	Gelatin	2002
Lead Oxide	Suami et al.	Gelatin and milk powder	2011

Adopted and modified.[28]

Table 4: The history of barium as contrast media for vascular anatomical studies.

Compound	Researcher	Suspension medium	Year
Barium	Gough	N/A	1920
Barium and sodium bromide	Hinman et al.	Gelatin	1923
Barium	Lindbom	Acacia and gelatin	1950
Barium silver iodide	Trueta and Harrison	Latex	1953
Barium	Shehata	Starch	1974
Barium sulfate	Bulla et al.	Epoxy	2013

Adopted and modified.[28]

Table 5: The history of other contrast media for vascular anatomical studies.

Material	Researcher	Suspension medium	Year
Chalk	Haschek & Linderthal	N/A	1896
Calcium sulfate	Dutto	N/A	1896
Mercury	Braus	N/A	1896
Bismuth	Baumgrten	N.A	1899
Colloidal silver	Frank and Alwens	N/A	1910
Strontium bromide	Berberich and Hirsch	N/A	1923
Vermillion	Ferguson	N/A	1924
Iodized oils	Cadenat	N/A	1924

Adopted and modified.[28]

2.3 History and evolution of perforator flaps

For many decades, physicians have sought to treat wounds with tissue transfer. Initial flap surgeries were used to reconstruct facial defects mostly resulting from wartime injury.[34] Early flaps were designed with a lack of anatomical knowledge of blood supply. Their designs were mostly random, with little consideration of the vascularity in the transferred flap. These randomly designed flaps had poor survival rates, emphasizing the need for better understanding of the underlying vascular anatomy in order to improve outcomes.

Experimental flap studies[35-38] revealed the importance of considering local blood supply to the donor tissue in the design of flaps. Subsequent use of axial flaps, such as the deltopectoral[39] and groin[40,41] flaps, which were based on axial blood supply, improved survival of transferred flaps.

Later, musculocutaneous flaps[42-44] became widely used for pedicled flap reconstruction of large defects and wound closure. The reliable arterial anatomy of the muscle, the available bulk to fill large soft tissue defects and maintain an aesthetic appearance at the reconstruction site, popularized these flaps. Musculocutaneous flaps are still considered as surgical options for cases involving large defects.[45-47] A classification system for muscle based on their vascular supply was developed flaps.[44,48,49] This provided a standard nomenclature across anatomic and surgical disciplines. Each muscle, and consequently musculocutaneous flap, is categorized into one of five muscle types.[44,48,49] While musculocutaneous flaps have a reliable vascular supply, the volume provided by some, such as the latissimus dorsi musculocutaneous flap, may be unnecessarily bulky for reconstruction, leading to poor aesthetic results. Another disadvantage of

musculocutaneous flaps is the loss of donor site muscle function. Perforator flaps have subsequently emerged as an alternative to musculocutaneous flaps because they have equally reliable vascular pedicles, but avoid the unnecessary bulk and loss of function associated with the harvest of muscle from the donor site.

2.3.1 Anatomical knowledge and perforator flaps

The use of perforator flaps clinically has changed plastic surgery by allowing for improved options for recostructions.[50] Comprehensive vascular anatomical knowledge has allowed for more precise isolation of vessels supplying the integument and the underlying subcutaneous fat, consequently sparing the unnecessary use of tissue. Lack of comprehensive anatomical knowledge in the early era of perforator flaps limited flap design, and surgeons were forced to work within the constraints of contemporary reliable knowledge of muscle vascular anatomy.

Kroll and Rosenfield,[51] and Koshima and Soeda[52] were the first to introduce flaps nourished by musculocutaneous perforator arteries, and composed exclusively of skin and subcutaneous fat. They dissected through muscle to harvest the vessels supplying the overlying skin, positing that the exclusion of the passive muscle carrier does not affect the integrity of the perforating arteries.

The perforator flap concept, therefore, allows for the exclusion of muscle as mere passive vessel carriers from the flap design (Figure 6). This has contributed to reduced donor site morbidity, as well as decreased flap bulk. Improved postoperative recovery is another advantage of perforator flaps due to the conservation of muscle in the donor site,

consequently, the preservation of donor site function and aesthetic appearance, have been the primary benefits of perforator flap technique.

The term “perforator flap” is theoretically defined as vascularized skin and subcutaneous tissue transfer supplied by musculocutaneous or septocutaneous perforators. Clinically, the term perforator flap (local, loco-regional, or free) refers to vascularized skin and subcutaneous tissue based on a cutaneous perforator vessel that penetrates the outer layer of deep fascia to reach the skin. The cutaneous perforator is either musculocutaneous, septocutaneous, or direct axial. Enhancements in methods used to evaluate vascular territories have also induced a revolution in flap surgery and expanded its application to the transfer of a variety of other tissues, such as bone and functioning muscle.[53-59]

2.3.2 Refinements in perforator flap surgery and wound closure

Technology influences research and science. Advances in technology have therefore provided modern tools, equipment, and instruments to enable the refinement of perforator flap use.

Flap thinning and free flap transfer

Research into flap volume reduction has led to the introduction of several new surgical techniques. Flap thinning is a surgical procedure to mechanically remove excess subcutaneous tissue from the perforator flap. This technique customizes the flap bulkiness to fit particular surgical needs. The technique depends on an intimate knowledge of the detailed microvascular anatomy of individual perforators.[60,61] There are a number of different options to close wounds including the local transfer of pedicled flaps and free tissue transfer, also known as free flaps. Tissue is transplanted and reattached with

microvascular anastomosis of donor site artery and vein to reconstruction site of recipient vessels. Current interest has reconsidered the thigh as a potential donor site for these free flaps.[3] The success of these complicated procedures demand detailed knowledge of the vascular anatomy in both donor and recipient sites to assure adequate blood circulation and provide metabolites and gases required for transplanted tissue survival.[62,63]

In 1973, the era of microsurgical tissue transfer was born, when Daniel and Taylor[62,63] performed the first vascularized free tissue transfer for skin defect reconstruction. This free tissue transfer was preceded by transplant of organs, such as the kidney and liver, but the vessels anastomosed for organ transplants are much larger than the delicate cutaneous perforators. One year after Daniel and Taylor's initial success, Harii et al.[64-66] and Harii and Ohmori[67] performed a series of clinical microsurgical transfers, several of them from the thigh region. Since these pioneering efforts, many free microvascular transfers of skin, muscle, bone, nerve, tendon, and various combinations thereof, have been performed and documented.

The development of super-microsurgery techniques has further expanded reconstructive possibilities. Super-microsurgery allows for microvascular dissection and anastomosis of vessels of 0.3 to 0.8 mm diameter. Applications of this technique include fingertip replantation, free perforator-to-perforator flap surgeries and lymphatico-venular anastomoses in the surgical treatment for lymphedema.[68] Due to increased anatomical knowledge, refinement of surgical techniques and improved surgical instruments, the transplant tissue survival rate has increased to 96-98 percent.[68]

Reliability of perforator anatomy

Flap surgery generally, involves two sites: the donor site and the reconstruction site. The main goal of successful flap surgery is the optimal coverage of a defect, leaving minimal or no donor site morbidity and no obvious scars. Pertaining to free flaps, the perforators of both donor and recipient sites should be dimensionally compatible in pedicle length and diameter in order to permit easy manipulation of the flap and facilitate anastomosis, respectively. Regarding pedicled flaps, the perforator pedicle length is the most important variable, because a long pedicle increases the versatility of flap transpositioning.

The harvest of adequate donor tissue must be accomplished viadissection that limits complications such as tissue necrosis, muscle dysfunction or loss of sensory function. These complications may occur due to the interference with normal functioning of other systems at the site, such as, the muscular, nervous and circulatory systems. At the reconstruction site, successful flap surgery, and subsequent aesthetic appearance, entails the use of the available tissue for full coverage of the defect. This establishes an intrinsic blood circulation to ensure survival of the flap as well as restoration of vital functions.

Together these factors constitute reliable flap surgery. However, cadaveric research is limited by the fact that not all of the reliability factors can be investigated anatomically. Factors that can be investigated on human cadavers are: facilitated dissection, which is reliant on arterial, innervational, muscular and lymphatic knowledge and the relevant quantitative data of the region; prediction of flap size related to flap survival with implementation of safe design rules extrapolated from physiological research on animal models in order to predict flap behavior.[14,15]

Generally, reliability of any perforator of a particular vascular territory can be defined by the level of confidence that surgeons possess in the anticipation of complications during and after flap surgeries based on that perforator.

Figure 6: Anterolateral thigh perforator flap (ALT) dissected after lead oxide injection. This Figure shows the exclusion of unnecessary muscular component. The bright color of the lead oxide facilitates the visibility of the vessels, aiding in the dissection.

2.4 History of thigh region flaps and perforator anatomy

The thigh region has been extensively used as a donor site for perforator flaps.[2] The presence of reliable perforators from several source vessels provides a rich vascular donor site for many potential surgical flaps. Two seminal clinical reports revolutionized perforator flap surgery in the region: two new perforator flaps in this region, medial and lateral thigh free flaps, were pioneered in 1983, and documented on a perforator of the SFA and the third lateral perforator of the PFA respectively;[69] a year later, three free flaps designed on septocutaneous perforators - a new free flap concept - were documented.[70] The first flap was the anterolateral thigh (ALT) flap nourished by a septocutaneous perforator of the descending branch of the LCFA, the second flap was an anteromedial thigh (AMT) flap based on a perforator of the "innominate" descending branch of the LCFA, and the third was the posterior thigh flap based on a branch of the PFA.[70]

As the principal artery in the thigh, the PFA diverges from the common femoral artery (CFA) and then gives off the major lateral branch, the LCFA. The ascending, transverse and descending branches of the LCFA supply the skin overlying the anterolateral (AL) thigh and trochanteric sub-regions, and provide the vascular basis for both the ALT and tensor fascia lata (TFL) flaps.[71,72] Medially, the PFA gives off the medial circumflex femoral artery (MCFA) that supply the superior aspect of the gracilis muscle and the overlying skin and provide the vascular basis for the MCFA or the medial groin perforator flap.[73] Then the vessel continues in the posterior thigh to supply posterior thigh muscles and the overlying skin, providing the vascular basis of posterior thigh flaps.[74] The clinical applications of the thigh region flaps are summarized in Table 6.

2.4.1 Anterolateral (AL) thigh

The anterolateral thigh (ALT) perforator flap

The ALT perforator flap since its introduction,[70] has become the most popular flap in the thigh and one of the most common flaps used to reconstruct various defects throughout the whole body. The increasing interest in this flap encouraged further researchers to re-evaluate the course of the potential vessel. A study found that 60% of the potential perforators were musculocutaneous while 40% were septocutaneous.[76] Currently, the ALT perforator flap is a superb soft tissue flap,[77-81] described by some as the "ideal flap".[82]

Despite the highly variable arterial anatomy in this area,[83-92] the main pedicle of this flap is very consistent and comes from the LCFA. The majority of perforators supplying the area are musculocutaneous[76,78,82,89,93] with a higher incidence of septocutaneous perforators towards proximal areas.[75] The term 'musculoseptocutaneous', or 'semiseptocutaneous' was proposed to describe a septocutaneous vessel, with a short intramuscular course[85] after observation of the intramuscular length of the potential perforator.[85,90]

With a potentially long pedicle and large diameter that are suitable for anastomosis, this perforator enhances the flap's versatility,[93,94] giving this flap extensive favorable comparisons with other free flaps in the literature.[79,93-96] The harvest of fasciocutaneous, musculocutaneous, subcutaneous, sensate (with the inclusion of the lateral femoral cutaneous nerve of the thigh), and adipofascial flaps has also been well described.[84,93-99] Thinning the flap, as an added modification, has also been proposed,[61,100,101] while limiting donor site morbidity with the use of the ALT perforator flap, emphasized.[102]

The Bailout perforator artery of the ALT perforator flap

The variable vascular anatomy increases the chances of accidental pedicle injury during flap elevation, emphasizing the importance of a back-up approach to prevent total flap damage. Recommendations for using a proximal perforator in the case of pedicle damage[103] led to the documentation of an oblique branch of the LCFA supplying the ALT perforator flap, noting its incidence in 35 percent of cases.[90]

This "ideal"[82] flap is a versatile reconstructive workhorse that is widely known and commonly used by surgeons for different reconstructions. The AL thigh is a suitable donor site to reconstruct defects of the head and neck, upper and lower extremity, abdomen, and breast.[70, 71,79,80,75,83-86,89,96-98,104]

The tensor fascia lata (TFL) perforator flap

The use of the TFL muscle and the overlying skin in the trochanteric sub-region for free flap transfer was pioneered and found to be reliable in 1978.[105] This reliability was confirmed with the use of the musculocutaneous flap.[106] However, potential drawbacks including bulkiness and potential loss of knee stability, have limited the use of the TFL musculocutaneous flap.[107-111] To address these disadvantages, some modifications were made to the this flap design.[112-114] Without the muscular component, the TFL flap was transferred as a free perforator flap.[115] Noticing that the cutaneous perforator orientation was directly toward the sub-dermal plexus, micro-dissection was performed to remove any unnecessary fat in order to thin the flap.[116] The TFL perforator flap including the iliotibial tract, was successfully transferred for simultaneous reconstruction of the achilles tendon and an overlying cutaneous defect.[117] Previous clinical application of the pedicled TFL muscle or musculocutaneous flaps was primarily for soft tissue coverage of inguinal and

supra-trochanteric defects, abdominal wall defects, trochanteric decubitus ulcers and ischial pressure sores.[118-122] Recent clinical application considered the TFL muscle as an alternative donor for functioning muscle transplantation.[123] In 2011, the use of this flap was extended for breast reconstruction in some unusual situations.[124]

The anatomical descriptions of the vascular anatomy of this flap have until now been confusing. Early,[105] and more recent,[125] studies have described the transverse branch of the LCFA as the source artery. The ascending branch has also been described as the source vessel.[126,111] Consequently, owing to the frequency of anatomic anomalies of perforators to this donor site, the TFL flap has made slow progress in clinical applications.[72]

The Lateral superior genicular artery (LSGA) perforator flap

From a cadaveric study, the anatomy of the lower posterolateral (PL) thigh flap illustrated the blood supply of this flap to be provided by perforators from both popliteal artery (PA) and LSGA.[127] The anatomical basis of perforator flaps designed on the LSGA were documented, and used to cover skin defects within the knee region.[128] Further clinical applications of this flap confirmed the reliable arterial anatomy, long vessel pedicles, easy dissection and primary donor closure make this flap a good option for regional reconstructions,[129] for example in soft tissue defect coverage after total knee arthroplasty.[130]

2.4.2 Anteromedial (AM) and medial thigh

The anteromedial thigh (AMT) perforator flap and the superficial femoral artery (SFA)

The AMT flap nourished by a single perforator from an unnamed branch of the SFA was described in 1983.[69] A year later, another AMT flap designed on a septocutaneous perforator of an innominate branch of LCFA, and back up musculocutaneous perforators off the SFA through the gracilis and sartorius muscles were reported.[70] Extensive study of the LCFA system indicated that the descending branch is divided into lateral and medial branches,[131] and in confirmation of earlier research,[70] the septocutaneous perforator to this flap was shown to arise from this medial branch and course through the medial intramuscular septum between the rectus femoris and sartorius muscles.[131] Yet three years later, the vascular anatomy to this flap was revised,[132] as a synthesis of earlier seemingly contradictory findings.[69,70] The revision revealed that the main perforators are large cutaneous arteries branching off a muscular branch of the SFA and supplying the gracilis and sartorius muscles.

Observations from 8 clinical cases provided an overview of the anatomy that still lacked an exact description of the underlying vasculature of the flap.[133,134] They indicated that the vascular anatomy was different in each case and explained that the perforators to this flap could originate from either the SFA or from the LCFA.[133,134] Yet there still persisted the earlier idea[131] that the perforator to this flap prevalently courses as a septocutaneous perforator at the medial border intersection of the rectus femoris muscle and the sartorius muscles.[135]

Several advantages can be achieved in the clinical use of the AMT or the SFA perforator flap. This flap can be combined with other flaps in the medial or anterior thigh,

thus enabling the reconstruction of wide defects in a single maneuver.[132] Compared to the AL thigh, the integument of the AM thigh is more pliable, has less hair and allows for more fat tissue harvest in the area of the flap design.[135] In addition, the location of the great saphenous vein allows its inclusion in the flap thereby increasing venous drainage (vein supercharges).[132] The anterior cutaneous branch of the femoral nerve can also be included in the flap if sensory potential is needed at the reconstruction site.[132]

Although the benefits of the AMT flap or SFA perforator flap are numerous, there are a few disadvantages: the variable vascular anatomy, including anatomical irregularities, and relatively short perforator pedicles supplying these flaps, make this flap undesirable in certain situations;[134,136] the AMT flap is thicker than the ALT flap, a bulkiness that may require thinning;[136] the limited width of this flap makes it useful in covering only small to medium sized defects if primary donor site closure is needed - the elevation of a larger flap would necessitate skin grafting, which would leave non-aesthetic results.[136]

The introduction of microsurgery has increased the use of the SFA flaps.[132] The clinical use of this flap as a free flap has extended to the covering of distant defects: cephalically, massive defects within head and neck region have been reconstructed,[131,134,136] and caudally, to reconstruct posttraumatic defects of the foot.[134,136]

The medial superior genicular artery (MSGA) perforator flap

This flap has not been studied or utilized extensively, possibly due to the reluctance of surgeons in clinical practice to harvest flaps which cross joints. Clinical applications and study of the anatomical basis of the MSGA flap were presented describing a triangle where perforators from the MSGA were prevalently found.[137] This flap was deemed useful for reconstruction of burns over the popliteal fossa.[137]

The descending genicular artery (DGA): the saphenous artery perforator flap

The first documented work on the DGA was the saphenous branch perforator flap positioned within the distal third of the thigh, also called Acland flap.[138] The study elaborated on the advantages of using the medial area of the knee as a potential donor site,[138] which include: limited subcutaneous fat, a consistent perforator and distinct sensory nerve supply.[139] All of these advantages encouraged the acceptance of utilizing this perforator flap. However, the design of the flap based on a reversed flow from the medial inferior genicular artery (MIGA) has been documented,[140] but, the main perforator of this flap comes from the DGA. This flap has since been used widely to reconstruct head and neck defects post hemiglossectomy,[139] and has been considered a good option for upper leg, regional knee, popliteal fossa and distal posterior thigh reconstruction.[140,141] A cadaveric study was performed subsequent to the documentation of the Acland flap with presentation of clinical cases of ankle and foot reconstructions.[142]

The medial circumflex femoral artery (MCFA) perforator flap

The MCFA perforator flap in the proximal medial thigh area has been posited as an ideal flap because it provides a medium to large cutaneous flap, functioning muscle that can, but need not, be included in harvest, specific skin area that can be elevated reliably, the donor site is easily hidden by clothing and the perforator is consistent in this location.[73] The advantages of this flap are: this donor site can be closed primarily and the flap provides an adiposal flap, which could be used to augment subcutaneous bulk and restore normal body contours after deformities. In addition, the flap can be used as a sensory flap, and the resulting scar at the donor site is concealed at the inner thigh.[143]

Historically, this concept of superior medial thigh as a donor site for flaps had been first documented in the transfer of a large musculocutaneous flap comprised of the gracilis muscle and overlying skin,[144] and in reconstructing local defects.[145] This flap was widely known as a musculocutaneous flap dependent on a musculocutaneous perforator until 1987, when the flap was elevated on a suprafascial perforator[146] relying on previous insights[147] which had earlier defined the MCFA musculocutaneous perforators. These investigations underpinned the initiation of this perforator flap into clinical use. Summation of the planar coordinates of the perforators through the gracilis muscle performed through a vector analysis showed that the cutaneous territories of these perforators have a transverse orientation parallel to the medial groin crease.[148] These findings contributed to reliability of the initially described flaps from this area.[144,145] In 2009, a published a report of an anatomical study and clinical refinements of a distally extended "fascioadipocutaneous" flap asserted that the main pedicle of the gracilis muscle originates from the MCFA or PFA while the second pedicle of this muscle is provided by the SFA, and anastomoses with the descending branch of the main pedicle.[149] The flap, described as a medial groin free flap, was transferred as a free perforator flap designed on a musculocutaneous perforator.[150]

Applications of this flap have included autologous breast reconstruction using a free gracilis perforator flap with complete preservation of the muscle,[151] femoral triangle and perineal defects closure, using the flap locally.[152,153] The transverse musculocutaneous gracilis flap has also been reported as fast and reliable for breast reconstruction.[154]

2.4.3 Posterior thigh

Descending branch of the inferior gluteal artery (D-IGA)

The initial clinical use of the posterior thigh dates back to 1980, when a massive defect of the pelvic cavity was covered by the posterior thigh flap, "the gluteal thigh" musculocutaneous flap, based on a perforator of the descending branch of the inferior gluteal artery (D-IGA).[155] A year later, after successful coverage of perineal and buttock wounds, this flap was described as reliable and sensate.[156]

An anatomic descriptive study of the free inferior gluteal flap designed on a perforator of the D-IGA, based on unembalmed cadavers, revealed the perforators to be septocutaneous.[136] To address posterior thigh and popliteal region sensibility loss as a consequence of elevation of the this flap (this flap was used for breast reconstruction), further studies focused on the anatomy of the posterior femoral cutaneous nerve and the relationship with the D-IGA.[157] Multiple applications of the posterior thigh flap were documented based on the D-IGA.[158]

Profunda femoral artery (PFA)

The first documentation of flaps based on a perforating branch of the PFA was the use of the *V-Y advancement technique* in a "hamstring musculocutaneous flap" for coverage of ischial sores in1981.[159]

Analysis of the anatomy of "the extensive gluteus maximus flap", led to use of the "first deep femoral perforating vessel", and the documentation of a PL fascia lata flap.[160] Within the PL thigh, fasciocutaneous flaps with blood supply from the first,[161] "third", [93,94] terminal fourth[162] branches of the PFA were reported. In 2007, a simplified anatomical

description of the lateral perforators of the PFA facilitated the clinical use of flaps based on these perforators.[2]

Medially, a musculocutaneous perforator, the adductor flap, was elevated on the "first medial branch" of the PFA in 2001.[163] Recently, this pedicle has been used to design an elliptical flap, inferior to the gluteal crease, for breast reconstruction.[164] Since then, further studies to evaluate the PFA medial perforators, and facilitate the location of these perforators, have been performed through clinical trials (preoperative 3D angiography),[165] and cadaveric study (dissection).[166]

However, the main issue with the posterior sub-region as a donor site is that, repositioning of patients is often required if defects are located anteriorly. Nevertheless, flap surgery in the posterior thigh sub-region has developed despite the absence of accurate and thorough descriptions of the PFA perforators.

The popliteo-posterior thigh perforator flap and the popliteal artery (PA)

The popliteo-posterior thigh fasciocutaneous island flap on a perforator of the PA was first used to repair skin defects around the knee.[167] A few years later, the same technique was employed to raise this distally based flap to cover amputation stumps and defects of the knee.[168]

2.5 Review of the literature

Clinical needs were the primary motivation for surgeons and anatomists seeking a better understanding of the vascular anatomy of the thigh. Even though, the findings of these earlier researchers[6-9] and others did not influence surgical practice at the time, they have ultimately provided the foundation of current flap surgery, understanding of underlying vascular anatomy, and paved the way for further vascular anatomical research. Recent studies[1-3,11,12,14-19] have elaborated on compensation mechanisms from vascular territories adjacent to the donor site following flap harvest. An expanded understanding of the 400 reliable perforating vessels provides versatile options for reconstructive surgery-[1] This has allowed donor site selection to move beyond the limitations of conventional choices in favour of options with reduced donor site morbidity.[16]

Earlier vascular anatomical studies[1-3,6-9,11,12,14-19] had described the vascular architecture of the thigh using dissection, two-dimensional angiography and a combination of both, which still did not allow for accurate assessment of perforators. Perforators were often sacrificed during dissection as a result of flattening the integument for imaging, and it was difficult to comprehensively document the vascular anatomy. Nevertheless, these illustrations were useful in estimating the horizontal territories of the cutaneous perforators (Figure 7 and 8). Further, limitations encountered in the study of these small perforators, inability to measure diameter and pedicle length using 2D angiographic images of flattened integument and reliance on dissection alone, have presented an incomplete picture of the regional vasculature.

Reports from clinicians and some anatomical research[69-168] are limited because they pertain to specific flaps and lack a general overview of the whole thigh region. The study

of scattered sites for specific flaps leaves unstudied gaps in between these discrete sites, and limits a comprehensive knowledge of the region, diminishing possibilities to harvest new flaps, modify or rescue flaps on adjacent perforators. This is especially relevant when an unusual vascular anatomy challenges flap elevation, which may in turn, damage the vascular pedicle. In depth knowledge of the whole thigh region will allow for a full exploration of possibilities, and maximize the utilization of the region for flap surgery. Clinical reports have placed less emphasis on certain flaps due mainly to surgical expediency, especially when the flap crosses a joint. This neglect has spawned a drought in research into these anatomical regions. In addition, conflicting debates regarding the vascular anatomy of certain flaps, necessitate the re-investigation of the vascular supply of the relevant donor sites.

Enhanced knowledge of vascular anatomy and more sophisticated methods to study the human integument provided a foundation for the use of perforator flaps. The innovation in, simplification and modification of, angiography methods[13,20,28,32] have aided the development of perforator flaps and improved insight into vascular anatomy.

The 3D digitized modeling of the arterial vascular anatomy, a novel field of research, therefore provides useful information for clinical implementation, preoperative simulation, and perforator flap design in the field of plastic and reconstructive surgery.[20] To date, there has been no published work that uses the modern 3D computerized modeling of the arterial vascular anatomy to provide a comprehensive description of the arterial vasculature of the thigh region. 3D capability ensures a more precise visualization of arterial anastomoses and orientation of local vascular territories. A thorough description of this microvascular

anatomy, using the best available technology would therefore provide the infrastructure for expanded use of perforator flaps in this region.

The quantitative data generated through the 3D modeling technique, such as number of perforators, diameter, pedicle length, the cutaneous angiosome surface, and the average perforasome can be subjected to statistical analysis making it possible, for example, to estimate the blood provided by each vascular territory, and hence, the reliability of perforator anatomy.

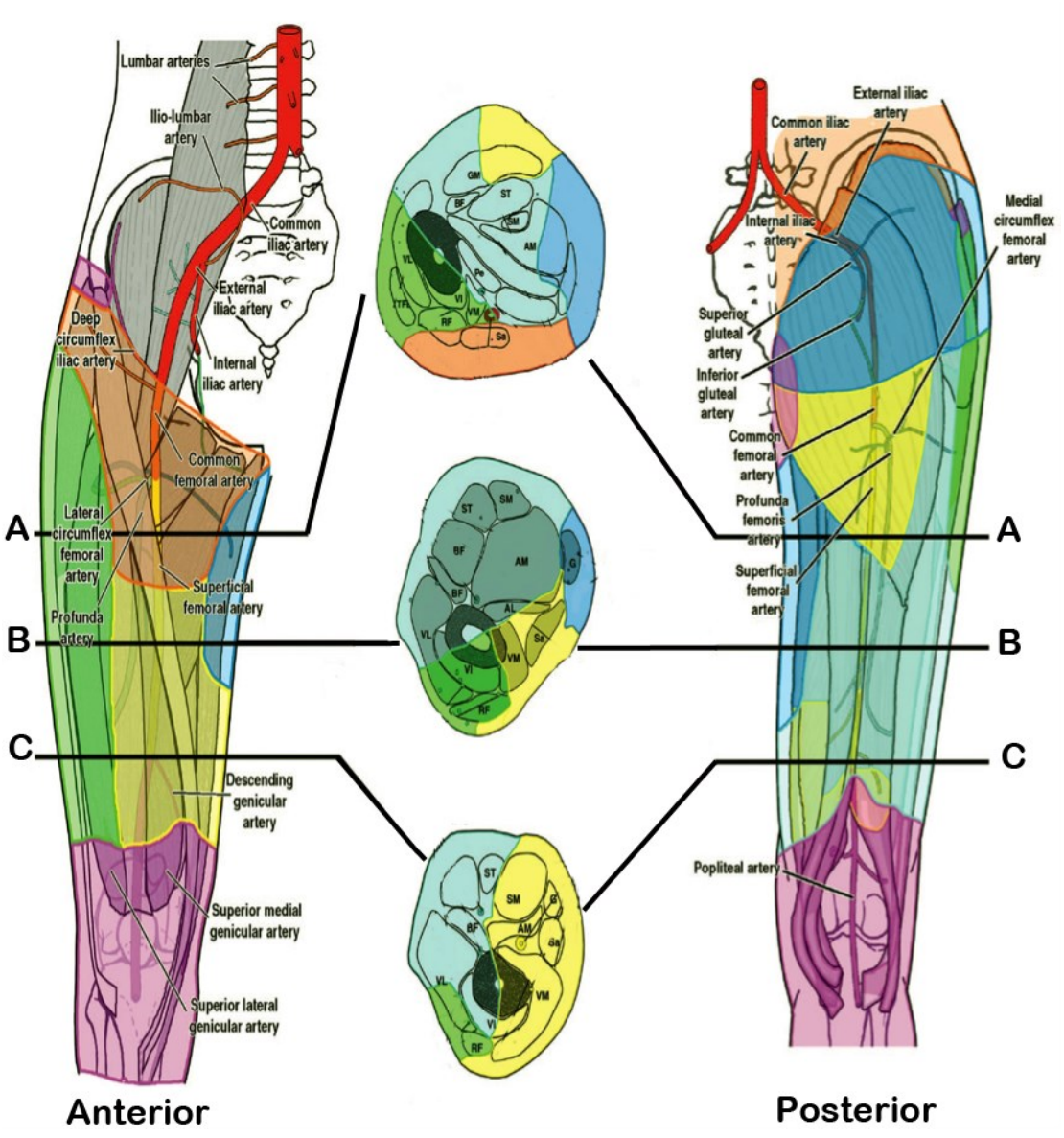

Figure 7: Angiosomes of the thigh.[3] Anterior (left) and posterior (right) views of the thigh with cross-sections (center) at three levels, viewed distally. Each color refers to a particular angiosome (orange) the common femoral artery, (green) the lateral circumlex femoral artery, (yellow in section A) inferior gluteal artery, (aqua) profunda femoral artery, (blue) adductor compartment and (yellow in sections B and C) superficial femoral artery. Note the angiosome territories and their borders in each case.[3] (Modified from Pan and Taylor[3])

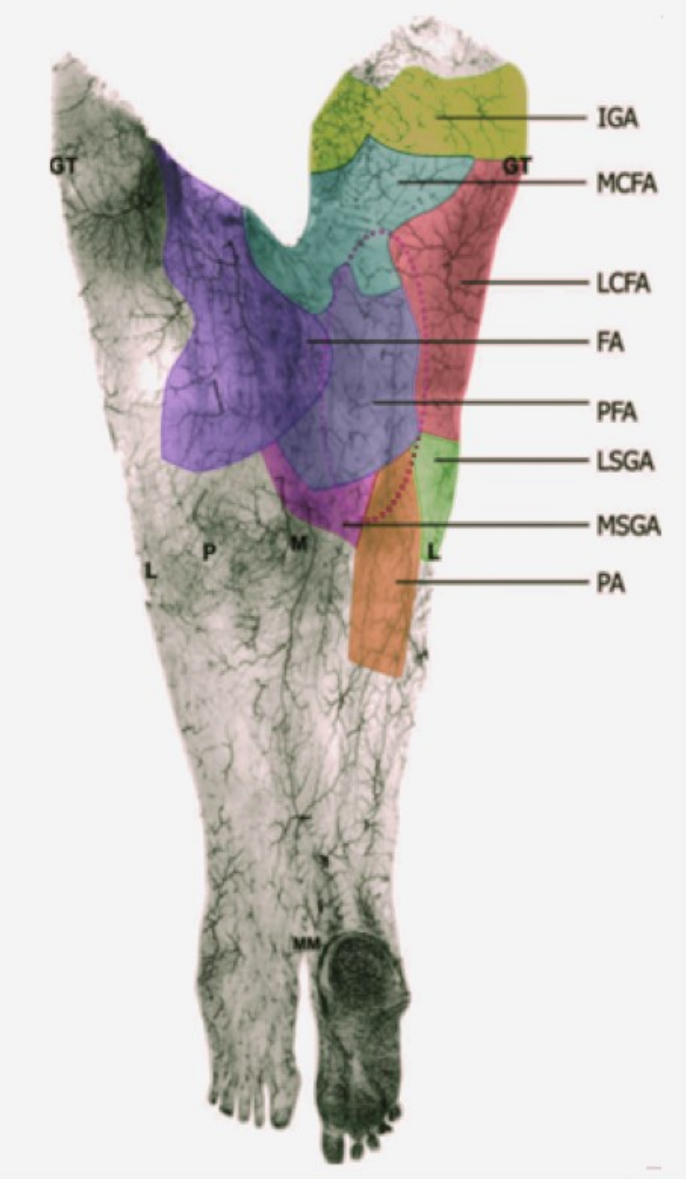

Figure 8: Angiogram of the left lower extremity integument of a human cadaver dissected with a lateral incision.[2] The angiogram shows various vascular territories of the posterior aspect of the thigh region. Vascular territories of inferior gluteal artery (IGA); lateral circumflex femoral artery (LCFA); lateral superior genicular artery (LSGA); medial circumflex femoral artery (MCFA); medial superior genicular artery (MSGA); popliteal artery (PA); profunda femoral artery (PFA); femoral artery (FA). (Modified from Ahmadzadeh et al.[2])

Table 6: Summary of the clinical applications of thigh flaps.

Sub-region	Flaps	Source vessel	Applications
AL	ALT	Inferior branch of the descending branch of the LCFA	Head and neck Upper and lower extremity Abdomen Breast
	TFL	Ascending branch of the LCFA	Abdomen Trochanteric decubitus ulcers Ischial pressure sores Breast Extremities Inguinal defects
	LSGAP	LSGA	Knee region
AM	AMT	SFA	Head and an neck Posttraumatic Foot
	MSGAP	MSGA	Burns; Popliteal fossa
PL	Lateral thigh	PFA - first branch	Ischial and trochanteric Head and an neck Extremities
	Lateral thigh	PFA - second branch	Ischial and trochanteric Head and an neck Extremities
	PFAP-4	PFA - fourth branch	Lower extremity defect
PM*n*	Gluteal thigh	D-IGA	Pelvic Gluteal region Breast
	Popliteo-posterior thigh	PA	Knee region
PM*l*	Medial groin	MCFA	Breast Femoral triangle wounds Perennial defects
	PAP/ Adductor	PFA - third branch	Breast Ischial pressure sores Lower extremity
	Acland	DGA (Saphenous) branch	Head and neck Popliteal fossa Ankle and foot

CHAPTER 3 OBJECTIVES AND HYPOTHESES

OBJECTIVES:

Overall Objective: *To comprehensively document the vascular anatomy of cutaneous perforators to the skin of the thigh region and show how this relates to surgical flap harvest*

***Specific Objectives*:**

1. To determine how many consistent, clinically important perforators (> 0.5 mm external diameter) occur in the thigh region, and what are their source vessels?
2. To describe these perforators' diameter, pedicle length, relevant angiosomes' surface area and average perforasome area, and to determine if a correlation exists between any of the characteristics that will demonstrate the reliability of their vascular territories?
3. To determine the consistency of the perforators' anatomy in order to facilitate the safe design of perforator flaps in the thigh region?
4. To determine the accuracy of virtual dissection versus physical dissection in the generation of quantitative data on the precise spatial orientation of the thigh vasculature, especially, the boundaries of the cutaneous territories of thigh angiosomes and the anastomoses between them?
5. To determine if safe flap design from the thigh's vascular territories can be simulated using the MIMICS 3D software?

HYPOTHESES:

Objective 1: To determine how many consistent, clinically important perforators (> 0.5 mm external diameter) occur in the thigh region, and what are their source vessels?

The clinical importance of perforators is dependent on the diameter at the point of emergence from the deep fascia. All perforators equal to or greater than 0.5 mm in diameter will be relevant for this study. Though, the improved reconstructive possibilities of super-microsurgery allows microvascular anastomosis of vessels of 0.3 to 0.8 mm diameter,[68] 0.5 mm diameter has been the clinically accepted cut off diameter for surgical anastomosis.[169] First the diameter of the perforators will be measured and the perforator identified by tracing to the source vessel on generated 3D models of the thigh vasculature. A table of the nine source vessels and the related perforators with their diameters will be constructed.

Clinical reports, 2D angiography and/or physical dissection have shown the thigh region to be suitable for flap harvest; however, these processes may underestimate the number of potential perforators by disrupting or overlooking other smaller but clinically relevant perforators. Three-dimensional spatial orientation of the thigh vasculature has the potential benefit of revealing more consistent and smaller perforator as it studies the vasculature without any physical dissection that may disrupt anatomical relationships.

Hypothesis 1
There are many additional consistent clinically important perforators from all vascular territories in the thigh region than currently reported in the literature.

Objective 2: To describe these perforators' diameter, pedicle length, relevant angiosomes' surface area and average perforasome area, and to determine if a correlation exists between any of the characteristics that will demonstrate the reliability of their vascular territories?

In order to establish a common set of quantifiable characteristics, the average number of perforators in each of the nine vascular territories, the average perforator diameter (at the point of emergence through the deep fascia), the average pedicle length (from the deep fascia to the source vessel), the average area perfused by each vascular territory (cutaneous angiosome area) will be calculated. These quantifiable characteristics and the relationship between them, if any, would be relevant in the prediction of flap size and flap survival in clinical applications.

Hypothesis 2
Perforators from vascular territories in the thigh region are related by a common set of quantifiable characteristics from which the reliability of the vascular territory and the related perforators can be ascertained.

Objective 3: To determine the consistency of the perforators' anatomy in order to facilitate the safe design of perforator flaps in the thigh region?

Detailed knowledge of the regional anatomy underpins the safe design of flaps which in turn, is facilitated by predictions regarding flap size that consequently lead to improved survival rate of the flap. In addition to the quantifiable characteristics regarding the arterial perforator anatomy, this study, will focus on, and discus any correlations between these characteristics, establishing how the correlations might predict the flap size to optimize safe flap design.

The perforator diameter is considered an important variable in effective flap surgery. Salmon's equilibrium law elaborated on the relationship between arteries supplying the same cutaneous region.[9] Essentially, the law states that if the cutaneous territory of one artery is large, the territory of corresponding arteries will be small.[9] Applied to angiosomes and perforators then, a pertinent point of inquiry would be to consider what factors might determine the expansion of cutaneous angiosomes or the perforasomes respectively.

An expanded perforasome has a high volume of blood supplied by a perforator. Volume of blood is dependent on the diameter and the cutaneous length of the perforator according to the flowing equation:

$$\text{Volume} = \pi\ (d^2/4)l \qquad \pi = 3.14., \quad \text{d: diameter,} \quad \text{l: cutaneous length}$$

If two vessels of the same length are compared, one with a small diameter, and the other with a larger diameter, the defining variable for volume of blood is the square of the diameter. At the same time with a larger diameter which delivers a larger volume of blood,

the flow rate *Q*, which is also dependent on vessel cross-sectional area and hence diameter makes perforator diameter a crucial variable in supplying expanded cutaneous territories.

$Q = vA$ *Q*: flow rate. v: velocity of flow A: area= π ($d^2/4$)

So, the expansion size of perforasome is highly dependent on the vessel diameter. Assuming that the number of perforators is variable from person to person, then the cumulative diameters (number of perforators x average diameter) of perforators become causal in determining that expansion of the cutaneous territories of a particular angiosome. This point of view is supported by a previous study based on whole body barium injection studies that correlated between vessel, diameter and cutaneous territory.[170] The correlation between the diameter, cumulative diameter and the surface areas of the angiosome and perforasome will be discussed in the study.

Regarding pedicled flaps, the perforator pedicle length is the pre-eminent variable, because a long pedicle increases the versatility of flap transposition. The average pedicle length of the perforators of each vascular territory will be calculated and overviewed.

Regarding flap size and the related survival rate, cutaneous arterial knowledge will be combined with the application of the safe flap design rules to predict the flap size in all of the thigh vascular territories.[14,15]

Hypothesis 3
Comprehensive arterial anatomical knowledge will facilitate safe flap design based on perforator arteries from all of the thigh's vascular territories.

Objective 4: To determine the accuracy of virtual dissection versus physical dissection in the generation of quantitative data on the precise spatial orientation of the thigh vasculature, especially, the boundaries of the cutaneous territories of thigh angiosomes and the anastomoses between them?

3D angiography obtained from a computed tomography (CT) scanner combined with MIMICS software creates a digitized, interactive, visual 3D model of the arterial vascular anatomy allows for spatially accurate depictions of the complex vascular anatomy of the area of interest, and facilitates data collection. In order to accurately evaluate virtual versus physical dissections, a comparison of number of perforators, diameter, pedicle length, and perforator course, using both methods will be established. This will provide an unambiguous vascular anatomy of the previously known flaps, alternate potential pedicles to rescue unsuccessful elevated flaps, and yield new donor sites.

In addition, the cutaneous territories of angiosomes and anastomoses between them will be delineated by the extent to which the branches of the associated perforators ramify before anastomosing with adjacent territories. The delineations will be based on angiographic criteria obtained from whole body barium injection studies.[170]

Hypothesis 4
Virtual dissection is superior to physical dissection in the display of the spatial orientation of the anatomy, and presents a more precise method for visualizing and measuring vascular anatomy.

Objective 5: To determine if safe flap design from the thigh's vascular territories can be simulated using the MIMICS 3D software?

3D angiography is often used to visualize the donor and recipient sites area as part of preoperative assessments. A major intention of this study is to combine both 3D angiography and MIMICS 3D software in order to enable the simulation of safe flap surgeries that could be used in future as preoperative assessment. This generated knowledge like flap size, length of pedicle (in case of pedicled flaps) and the compatibility of the anastomosed vessel (in case of free flaps) increase the options for safe surgery.

Hypothesis 5
MIMICS will allow simulation of safe flap design of flaps from all the vascular territories of the thigh, and present increased future options for safe flap surgery from this region.

CHAPTER 4 MATERIAL AND METHODS

This study was carried out on human cadavers, which were donated to the Human Body Donation Program. The research steps included cadaver procurement, cadaver preparation and systemic arterial injection of the cadavers using the modified lead oxide technique,[32] scanning using computed tomography (CT), reconstructions of 3D models of the arterial system and the perfused soft tissues, analysis of the 3D models including quantifying the number of perforators, diameter, pedicle length, angiosome and perforasome areas and quantitative data analysis. Results will be presented as means plus or minus the standard deviation.

4.1 Human Body donation Program and Research Ethics Board Approval

The cadavers were donated through the Human Body Donation Program of the Department of Medical Neurosciences, Dalhousie University. The study procedures were performed in accordance with Dalhousie University Ethical Guidelines. Full Ethics Approval was obtained from the Health Science Human Research Ethics Board of Dalhousie University.

4.2 Cadaver inspection, preparation and data collection

ISFISAD (Inspect, Scan, Flush, Inject, Scan, Analyze and Dissect) procedure

4.2.1 Cadaver inspection

The appropriate cadaver condition and subsequent preparation before injection determine the quality of 3D models that facilitate data collection and analysis. Exclusion criteria include: evidence of severe, extensive surgical scars, scars over the area of interest,

pressure sores, post mortem body degradation, evidence of skin metastasis or neoplasia, missing limbs, major joint fusion, disarticulation, prosthesis and anatomical landmark alteration. There were 15 thighs (10 male and 5 female) obtained from 10 fresh human cadavers (5 male and 5 female) studied. Due to unsuitable technical maneuvers or unobserved internal cadaveric conditions resulting in poor 3D information in some specimens, the other 5 thighs were excluded from data analysis. While data was collected from 15 thighs, in this thesis, the anatomical diagrams are from the right thigh of a female cadaver.

4.2.2 Cadaver preparation: scanning, flushing and injection

The steps for cadaver preparation and injection followed a specific protocol:

1. Pre-injection scanning of the whole cadaver using CT scanner aids in the reconstruction of soft tissue without the interference of radiopaque material.
2. Following the pre-injection scan, the arterial system was flushed using Foley catheters. The incisions to the femoral arteries were commenced as proximal as possible to ensure the integrity of the vascularity of the region. Foley catheters of appropriate sizes were inserted proximally and distally in the CFA via a longitudinal arteriotomy. The femoral vein was cannulated with a standard metallic embalming cannula that was large enough to accommodate the passage of large blood clots. A 40 ^{o}C solution of tap water and potassium acetate (0.9%) was injected through the CFA under continuous perfusion and at 140-170 kPa until the venous outflow was clear, after which, the lead oxide mixture was injected.

3. The cadavers were injected through the CFA with a mixture containing 100 g of lead oxide and 5 g of gelatin per 100 mL of water, for a total infusing volume dependent on the cadaver mass (approximately 20-30 ml/kg). The optimal injectate formula is listed in Table 7.
4. The injectate mixture was warmed to 40 °C, stirred and rapidly injected while checking for strong syringe backpressure as indication of injection completeness. During this step, pressure points were alleviated over bony prominences that may be otherwise under-injected by floating the cadaver in a warm water bath (40˚C), helping to increase the temperature of the integument, and the subsequent maintenance of the injectate mixture above its melting point during the injection. The lead oxide mixture was thus kept circulating in the vasculature without solidifying, and sedimentation within the suspension therefore prevented. Finally, the integument was rinsed to remove any deposits of lead oxide.

4.2.3 Data collection: scanning, 3D reconstructions and dissection

After the injection step, the cadavers, kept in the same posture as in the pre-injection scans, were scanned again using a CT scanner. The cadavers were refrigerated for 24 hours at 4 ºC to allow the injectate to solidify prior to dissection. The pre and post-injection CT scans were uploaded into MIMICS software to reconstruct 3D images of the arterial models. Dissection was then performed in order to test the hypothesis that the virtual dissection is superior to physical dissection in studying the vascular anatomy.

Table 7: Lead oxide preparation.[28]

Component	Amount
Lead Oxide ($Pb_3 O_4$)	100 g
Gelatin	5 g
Tap water (40-50 ˚C)	100 ml

4.3 Computed tomography (CT) scanning

All cadavers underwent 3D multi row detector computed tomography (Siemens Medical Solutions, Forchheim, Germany) before and after radiopaque mixture injection. It is crucial that 3D imaging modalities are used for anatomical research related to microsurgical applications because they produce adequate images of the entire course of each perforator. Two factors determined the quality of outcomes achieved - the injection procedure (including the cadaver condition and the perfusion degree) and the scanning quality (Figure 9).

Both pre and post-injection scans should be performed with the cadaver placed in the anatomic position. The pre-injection scanning aids in the reconstruction of soft tissue without the interference of radiopaque material. The post-injection scanning provides the desired vascular data required for 3D modeling and analysis of small perforating vessels. Removal of restrictive sheathing on the cadavers was necessary to prevent any alteration of the actual body shape, the orientation of the cutaneous vasculature and to provide realistic locations of anatomic structures. The cadaver should be clear from any metallic material to reduce the chance of creating scanning artifacts.

The scanning process produces slices at 0.6 mm intervals, generating over 500, 300 and 100 individual images of each specimen on transverse, sagittal and coronal planes respectively. These images are uploaded to a computer and collated by MIMICS software (Materialise, Leuven, Belgium). Choosing the correct scanner setting is integral to achieving the best quality images. The settings used in this study were recommended by experienced radiological technicians from Queen Elizabeth II Hospital in Halifax, Nova Scotia and are summarized in Table 8.

Scanning parameters

1. The radiographic contrast is controlled by KiloVoltage Peak (kVp) which is the maximum voltage applied through an X-ray tube. This value controls penetration of the X-ray beam, or the average wavelength of the photons, through various tissues in the body.
2. The radiographic density is controlled by milliampere seconds (mAs). Milliampere seconds correspond to the amount of energy used to produce a certain amount of radiation. This setting also plays an important role in determining X-ray penetration in the presence of different densities.
3. Slice Increments determine degree of overlap between successive images. If the increments are set to smaller values, the overlap between images increases.
4. Slice Thickness, a comparison between thick and thin slice imaging is listed in Table 9 and Figure 9.

Table 8**:** Computed tomography (CT) scanner settings for perforator artery three-dimensional (3D) analysis.

kVp	Width (pxl)	Height (pxl)	Pixel size (mm)	Slice increment (mm)	Slice thickness (mm)	mAs
120-130	512	512	0.4	0.5	0.6	74

Table 9: Comparison between thick and thin slice imaging.

Thick slice	Thin slice
Better low contrast	Poor low contrast resolution
Poor edge definition	Better edge definition
Poorer high contrast resolution	Better high contrast resolution
Partial volume artifacts	Less partial volume artifacts

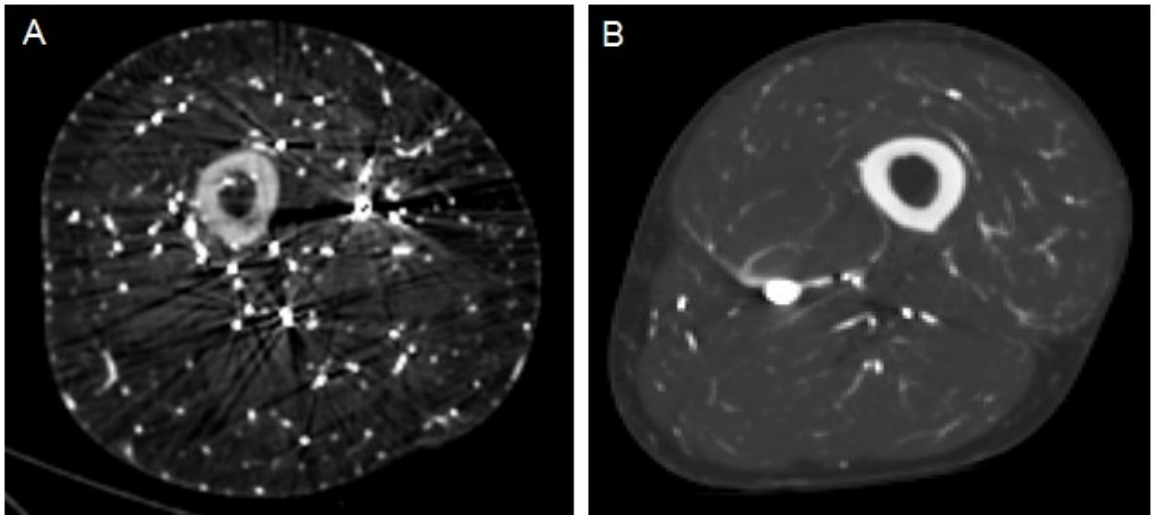

Figure 9 (A,B): Comparison between high (A) and low (B) quality scanning. The computed tomography (CT) scanner settings determine the quality of the scans and play a significant role in terms of the accuracy of the collected information.

4.4 Using MIMICS software in virtual dissection

MIMICS software interactively recognizes and collects CT scanner imported data in the Digital Imaging and Communications in Medicine (DICOM) format. *Thresholding* is a feature in MIMICS software that allows that isolation of tissues (e.g., bone, soft tissue, skin and vessels) called *masks,* according to their densities. Once an area of interest is isolated, it is rendered in 3D, and stereolithographic 3D models (STL) made. STL models can be visualized in 3D for design validation based on the anatomic geometry. Both data collection, analysis and simulation for surgical procedures using the software were then performed. 3D reconstructions of the vasculature were generated and viewed stereoscopically, allowing the demonstration of fine details including the course of arteries and their spatial relationship to surrounding structures. The data regarding the artery diameter, length, source vessel, areas and branches were also measured using the software.

Steps used to reconstruct and analyze stereolithographic 3D models

Mimics software processes CT scanner images in batches called *projects*. In this study each sample's scans were processed as an individual *project.*

1. 20 new *projects* were established, by importing CT scanner images of each thigh into MIMICS software in the DICOM format. MIMICS software organized, gathered, and previewed these images.
2. The integrity and sequence of the scans were verified.
3. MIMICS software's work panel provided reconstruction and editing functions to create a sharper rendition of *masks* of different anatomical structures. Different procedures were followed to reconstruct various structures with varying densities:

a) Reconstruction of vasculature

Large vessels and perforators

Large and principal vessels, abundantly filled with lead oxide, were reconstructed and isolated from post-injection CT angiograms by setting the *thresholding* of new *masks* to a high value (i.e.,: 2700-3071hu) according to Hounsfield Radio-density scale (Figure 10 + Table 10). The setting of the *thresholding* of the *mask* was manipulated to obtain the best visual image of the vasculature - the higher the *thresholding* was set, the more vascular density was displayed (Figure 11). Using higher *thresholding* allows for visualization of large vessels and some large perforators. Widening the *thresholding* allows for visualization of small perforators, and inherently includes bony structures in reconstruction (falling within the range of 1450-769 HU), creating a composite model of small perforating vessels and bony structures (Figure 11).

Fine peripheral vasculature

Detection of fine perforators in post-injection angiograms requires some technical knowledge, skill, and some patience, since the density of fine perforators tends to interfere with bony structures. Further editing and manipulation to remove unnecessary structures from the *mask* before reconstructing the object as a 3D image is often necessary. This step is desirable to obtain clean images for detailed examination of the vascular anatomy.

b) Reconstruction muscles and bones

Muscles and bones were easily reconstructed using the pre-injection scans and pre-determined *thresholding* values that were pre-determined by MIMICS software. These objects were exported as stereolithographic (STL) models and uploaded to the post-injection *project*. The location of the STL models is adjustable using X, Y and Z

coordinates on the post-injection *project* and was required to achieve accurate placement of these imported structures (Figure 12).

c) Editing of *masks*

The purpose of editing the *masks* is to clarify the course of source vessels. Editing can be coarse or fine:

Editing in 3D (Coarse editing)

Coarse editing of the *mask* in 3D view is a valuable function, because it permits interactive editing on *masks* through a temporary 3D rendition of the *mask* (Figure 13). The highlighted undesired tissues or any unrelated structures to the area of interest were removed directly from the original *mask* and subsequently, from the rendered 3D model.

Multi-slice editing (fine editing)

The multi-slice editing function is a more selective editing tool; it permits *mask* editing (deletion or *thresholding*) by highlighting the pixels in a specific part of the slice (Figure 14). The interpolation function permits dynamic editing, allowing the user to highlight pixels of several slices between two highlighted spots. The highlighting tool size is adjustable to fit the editing needs**.**

4. The edited *masks* were then generated into 3D models. Smoothing surfaces and triangle reductions, which are morphological modification options that MIMICS software provides to improve the quality of the rendered model, were used. Following 3D reconstruction, the vasculature was viewed stereoscopically.

5. After rendering the 3D models, measurement tools available within MIMICS software were used to analyze the models which were represented in life size scale. The diameter, direct distance, distance over surfaces, angles, area surfaces and volumes, in addition to advanced measurements such as density and ellipses can be quantified. MIMICS calculated the angiosome areas by using 3D models of the skin overlying the vascular territory of each source vessel. The area of each angiosome was calculated from reconstructions of the overlying cutaneous tissue.
6. Recording and developing videos and images to export from the *project* under study enables sharing morphological information. This provides a medium for the creation of educational videos useful for teaching of anatomy related to surgery. For enhanced simulation, these videos can also be viewed as 3D videos or as holograms.
7. Exporting and importing STL models is a MIMICS software feature that enables to convert the 3D objects into exchangeable STL format. This allows for transferring *objects* to another MIMICS *projects*. The purpose is to gather soft tissue structures such as bones, muscles and skin as discussed previously.
8. New 3D printing technology are used to print STL models, providing a physical anatomical sample.

4.5 Cadaver dissection

Physical dissection on 6 of the thighs was performed next, mainly to compare with the preliminary digitized outcomes. Confidence increased progressively in the initial hypothesis that 3D modeling (virtual dissection) outcomes were markedly superior to those of physical dissection.

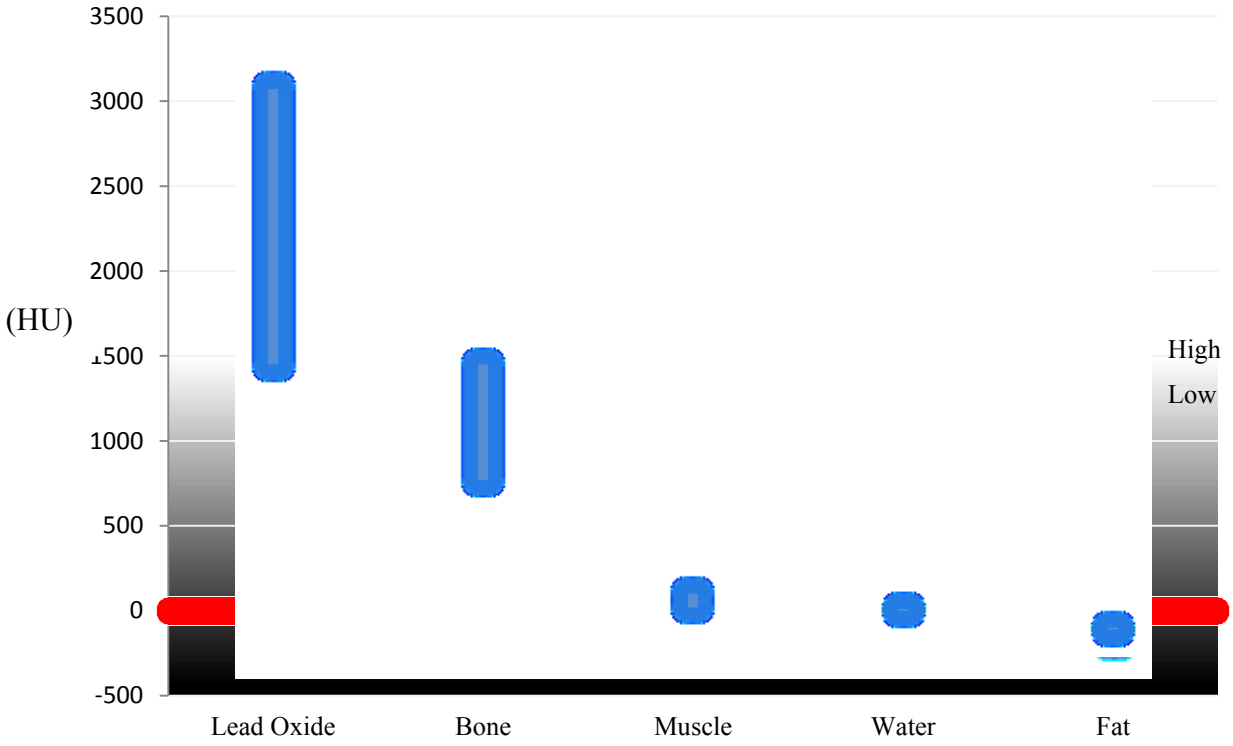

Figure 10: Hounsfield radiodensity scale. The scale shows the mean range of the radiodensity of different substances.

Table 10: The mean range of the radiodensity of different substances, associated with Figure 10.

Substance	**Radiodensity (HU)**
Lead Oxide	3071-1450
Bone	1450-769
Muscle	100-20
Water	0
Fat	-100
Air	-1024

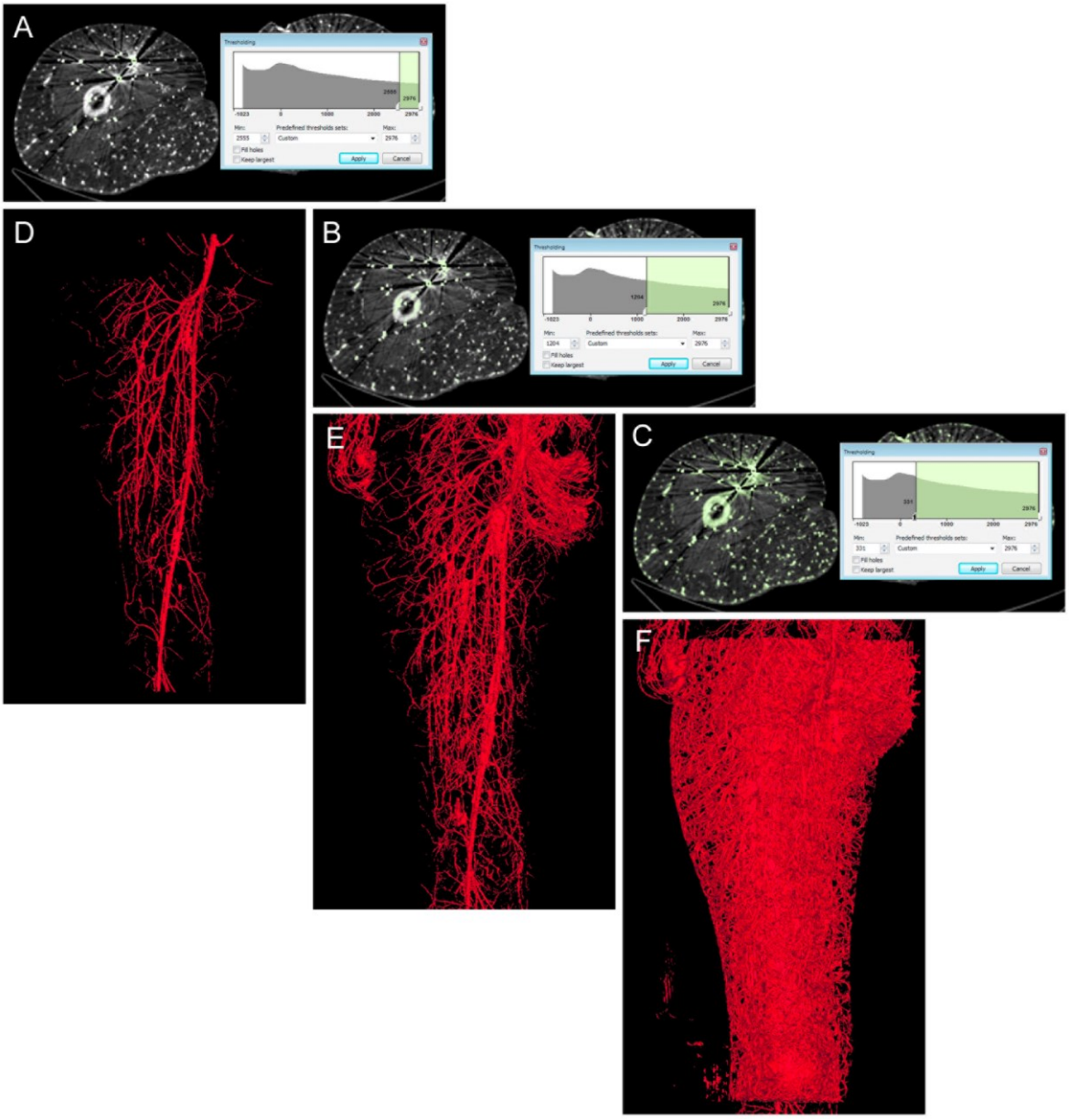

Figure 11 (A-F): Relationship between *masks* and three-dimensional (3D) data.
A new *mask* is being generated using post-injection scan with three different *thresholding* intervals (A-C). In 10A and D, the *thresholding* interval is adjusted to a high value, which is useful to reconstruct large vessels and some large perforators. In 10B and E, the *thresholding* interval was expanded. The radiodensities of bones and small perforators are similar in post-injection computed tomography (CT) scans. Parts of the femur were detected within the *thresholding*, and hence, the associated three-dimensional model. In 10C and F, the more expanded *thresholding* interval helps to detect small perforators and give the orientation of the cutaneous arterial anatomy.

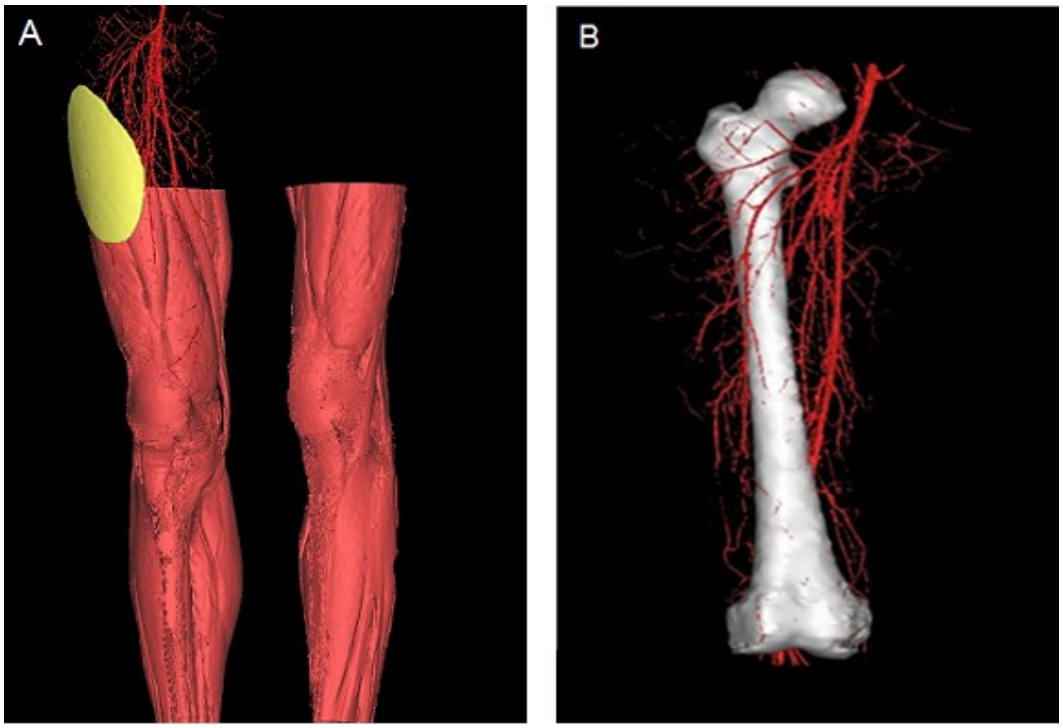

Figure 12 (A,B): Reconstructions from pre-injection scans. Muscles, skin - an anterolateral thigh (ALT) perforator flap is shown - (11A), bones (11B) and other soft tissues can be reconstructed from the pre-injection scans and imported in transferable format (STL) to post-injection *projects*. The main objective of the pre-injection scans is to reduce the interference caused by lead oxide after the injection.

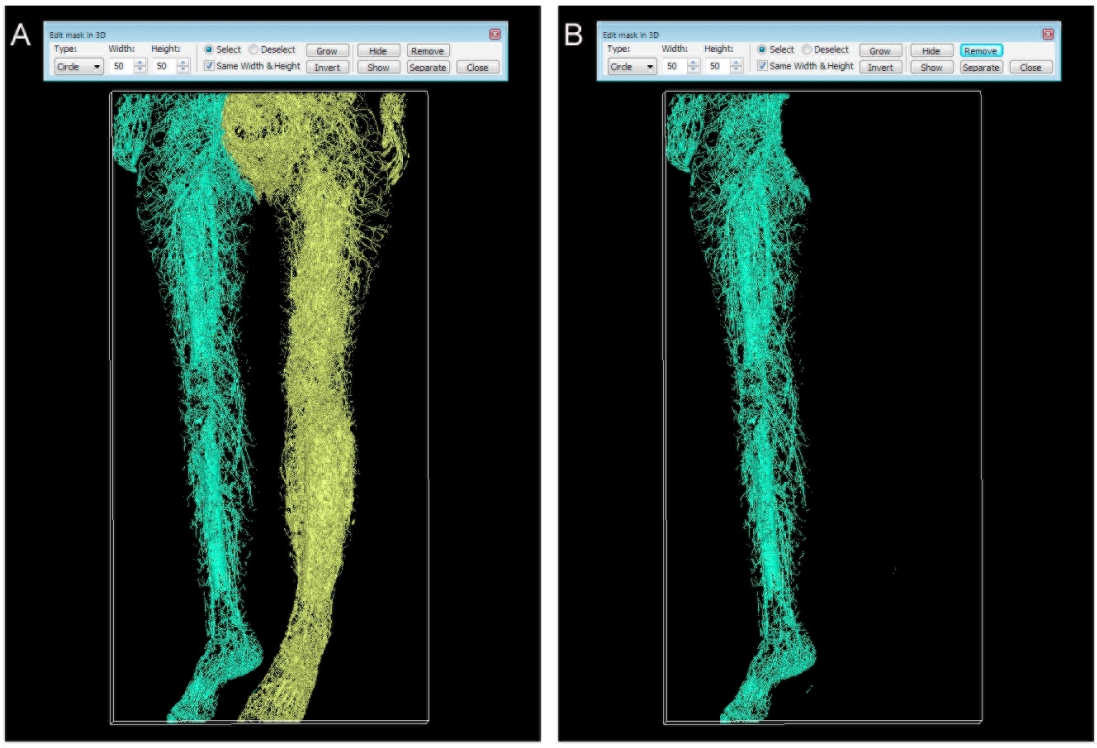

Figure 13 (A,B): Interactive three-dimensional (3D) *mask* editing. The three-dimensional (3D) editing, "coarse editing", enables the highlighting (12A) and omitting (12B) of unwanted structures on a temporary 3D model. The omitted areas will then be deleted from the original *mask* directly. This gives the ability to manipulate and rotate the region that is being edited.

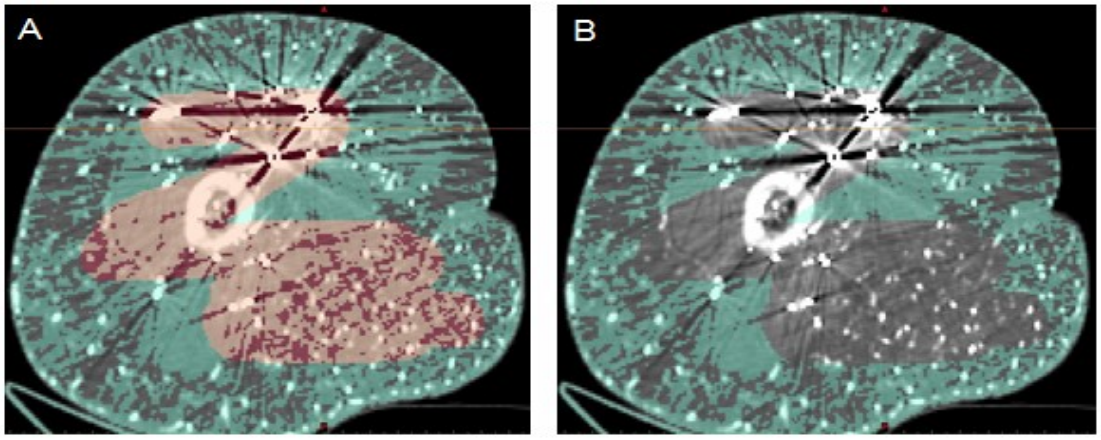

Figure 14 (A,B): Precise multi-slice *mask* editing. The multi-slice editing "fine editing", enables the highlighting (13A) and omitting (13B) of unwanted structures on transverse slices of the edited *mask*.

CHAPTER 5 RESULTS

Using the modified lead oxide gelatin injection method, 3D angiography and MIMICS software, thorough anatomical models of the arterial anatomy of the thigh region were obtained. This study investigated the thigh as it extends distally from the inguinal ligament line anteriorly, and posteriorly from the gluteal fold to a horizontal line along the superior pole of the patella (Figure 15). Based on these interactive digitalized models, measurements and analysis were undertaken (Figure 16). A mixture of musculocutaneous and septocutaneous perforators originate from nine main source arteries, which are all branches of the CFA supplying the integument of this region. Large perforators are prevalent in the SFA, MCFA and LCFA territories. The posterior thigh has large, distinct perforators, the majority of which come from the PFA. Based on the analysis of (n=15) thighs obtained from 10 cadavers, an average of 88 ± 16 arterial perforators supply the integument of each thigh.

The results are presented based on the source vessels and the related perforators; Table 11 summarizes the results of the thigh region and provides a detailed analysis of the number, diameter, pedicle length and area of the perforators for each source artery (cutaneous angiosome area). Then, the thigh was divided for descriptive purposes into five sub-regions, two anteriorly and three posteriorly. Perforators supplying the overlying skin of each sub-region will be presented.

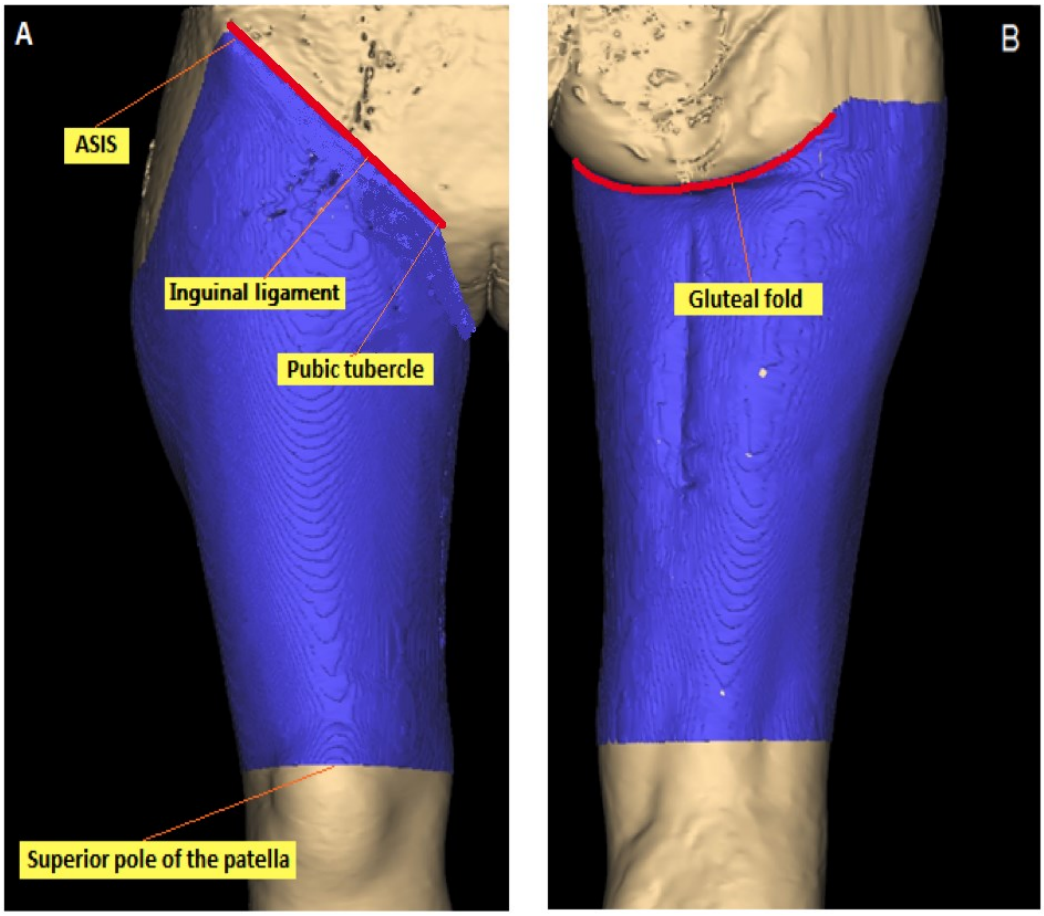

Figure 15 (A,B): Boundaries of the thigh region. Anterior (15A), and Posterior (15B) views of a 3D model of the right thigh of a female cadaver identify the boundaries of the thigh region. The thigh region extends distally from the inguinal ligament line anteriorly, and posteriorly from the gluteal fold to a horizontal line along the superior pole of the patella.

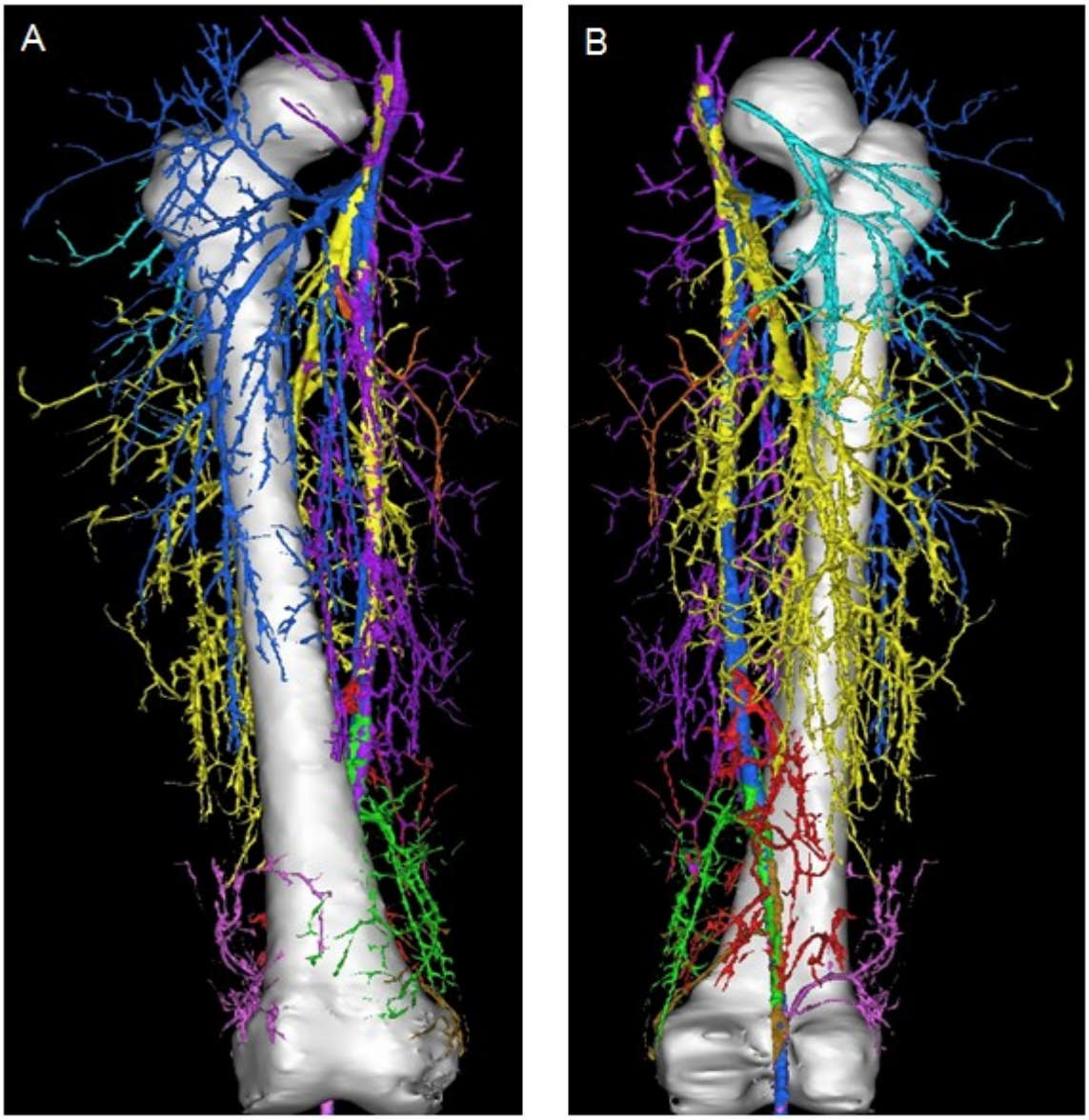

Figure 16 (A-D): Three-dimensional (3D) models of the arterial vasculature of the thigh. Anterior (16A) and Posterior (16B) views of three-dimensional (3D) models of the arterial vasculature of the right thigh of a female cadaver injected with lead oxide and gelatin solution, and scanned using computed tomography (CT) scanner. Vascular territories of descending genicular artery (green); descending branch of the inferior gluteal artery (light blue); lateral circumflex femoral artery (dark blue); lateral superior genicular artery (pink); medial circumflex femoral artery (orange); medial superior genicular artery (brown); popliteal artery (red); profunda femoral artery (yellow); superficial femoral artery (purple). This 3D Figure shows the relationship between the vascular territories of the arteries supplying the thigh region.

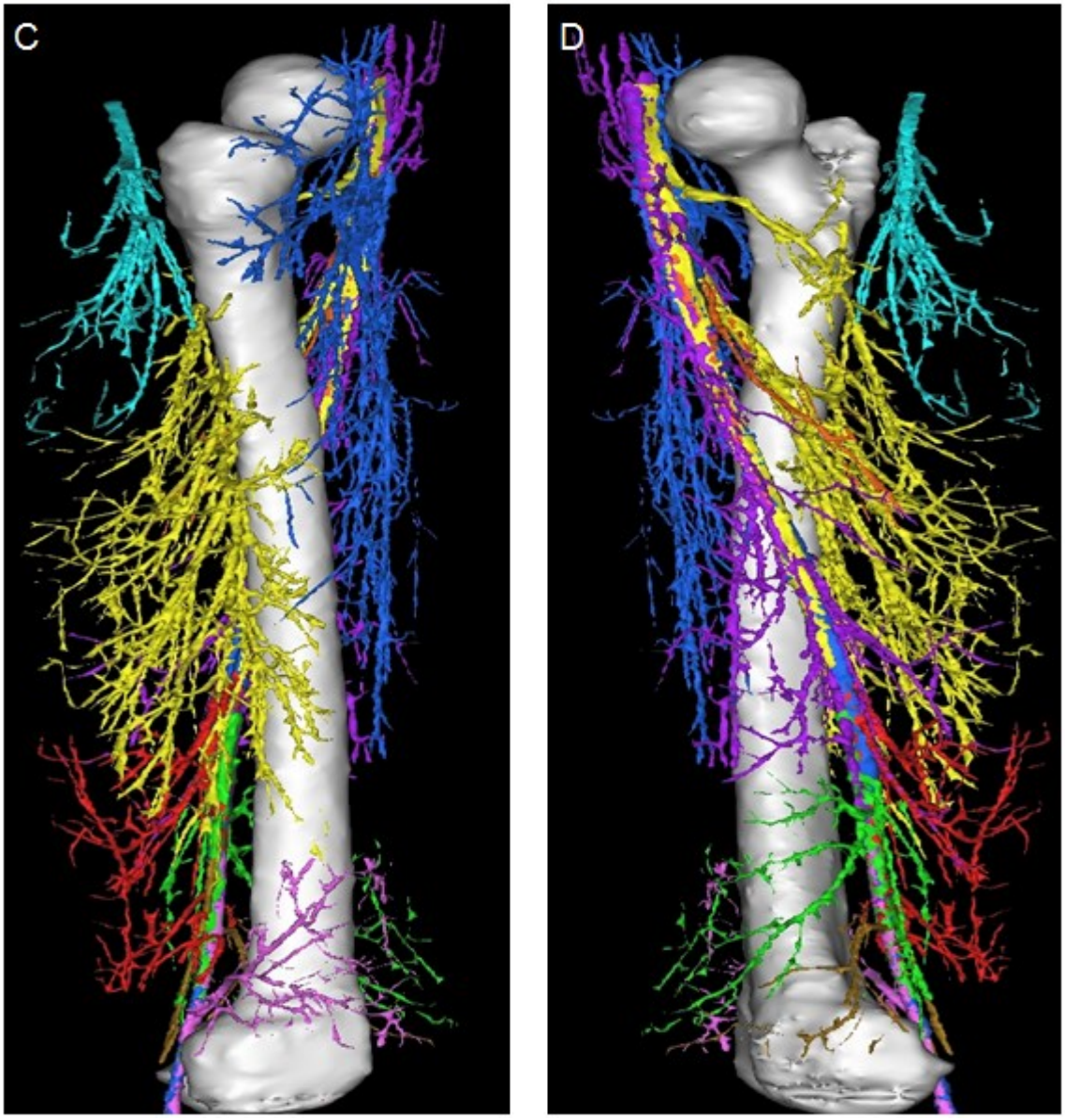

Figures 16C and 16D show the Lateral (C) and Medial (D) views of three-dimensional (3D) models of the arterial vasculature of the right thigh of a female cadaver injected with lead oxide and gelatin solution, and scanned using computed tomography (CT) scanner. Vascular territories of descending genicular artery (green); descending branch of the inferior gluteal artery (light blue); lateral circumflex femoral artery (dark blue); lateral superior genicular artery (pink); medial circumflex femoral artery (orange); medial superior genicular artery (brown); popliteal artery (red); profunda femoral artery (yellow); superficial femoral artery (purple). These 3D Figures show the relationship between the vascular territories of the arteries supplying the thigh region.

Table 11: Summary of measured quantitative data for the cutaneous vascular territories of the thigh region (n=15).

Angiosome	Number of perforator	Diameter (mm)	Pedicle length (mm)	Angiosome area (cm^2)
D-IGA	3.3 ± 2.6	0.8 ± 0.3	116 ± 50	45 ± 37
SFA	20 ± 9	0.8 ± 0.3	69 ± 31	350 ± 137
PFA	21 ± 9	1 ± 0.5	120 ± 42	375 ± 81
MCAF	4 ± 2	1 ± 0.4	93 ± 38	48 ± 27
LCFA	11 ± 4	1 ± 0.7	99 ± 61	271 ± 76
DGA	8 ± 4	0.8 ± 0.2	76 ± 42	97 ± 38
PA	8 ± 3	1.0 ± 0.7	83 ± 33	99 ± 27
LSGA	5 ± 3	0.9 ± 0.3	66 ± 38	60 ± 29
MSGA	3 ± 2.5	0.7 ± 0.2	88 ± 46	31 ± 17

All data are means plus or minus the standard deviation for the number, diameter, length and surface areas perfused in the angiosome, in thighs (n=15) obtained from 10 cadavers. This data was obtained from three-dimensional (3D) models produced from human cadavers using 3D angiography. Abbreviation of angiosomes; descending genicular artery (DGA); descending branch inferior gluteal artery (D-IGA); lateral circumflex femoral artery (LCFA); lateral superior genicular artery (LSGA); medial circumflex femoral artery (MCFA); medial superior genicular artery (MSGA); popliteal artery (PA); profunda femoral artery (PFA); superficial femoral artery (SFA).

5.1 Descending branch of inferior gluteal artery (D-IGA)

The inferior gluteal artery emerges from the anterior division of the internal iliac artery and enters the gluteal region from the greater sciatic foramen adjacent to the lower border of the piriformis and medial sciatic nerve. The D-IGA (Figure 17), divides into medial and lateral branches, with a descending third branch accompanying the posterior cutaneous nerve of the thigh, and descending into the posterior thigh to supply the skin below the gluteal fold.

In this study (n=15), the D-IGA territory in the proximal, posterior thigh anastomoses laterally with the first branch of PFA, and medially with the deep and cutaneous territories of the MCFA. The average cutaneous area perfused by the D-IGA was 45 ± 37 cm^2, representing 3% of the total thigh surface area, perfused by an average of 3.3 ± 2.6 perforators with pedicle length 116 ± 50 mm from the descending branch of the inferior gluteal artery. Their appropriate average diameter 0.8 ± 0.3 mm would allow the anastomosis with recipient vessels, and provide a reliable arterial supply of flaps harvested below the gluteal fold.

5.2 Superficial femoral artery (SFA)

The external iliac artery becomes the CFA as it enters the femoral triangle. At the superior aspect of the femoral triangle, the vessel gives off the PFA branch and before entering the adductor canal (Hunter's canal) at the inferior apex of the triangle. From there, as the SFA, it courses deep to the sartorius muscle and passes inferomedially through the adductor hiatus where it becomes the PA (Figure 18). The SFA supplies the majority of the medial and AM thigh.

In this study (n=15), the SFA supplies an average cutaneous area of 350 ± 137 cm^2 in the medial and AM thigh, constituting 26% of the thigh region (Figure 19). An average of 20 ± 9 perforators were found with 0.8 ± 0.3 mm in diameter and 69 ± 31mm as an average pedicle length. Septocutaneous perforators in the medial thigh, and mostly musculocutaneous perforators in the AM thigh, provide reliable arterial supply of many flaps in the two sub-regions.

5.3 Profunda femoral artery (PFA)

The trunk of the PFA begins as it emerges from the posteromedial (PM*l*) and sometimes PL aspect of the CFA in the femoral triangle and terminates as a fourth perforating branch. In this study, the PFA has a deep inferomedial course and supplies the majority of the posterior thigh. Out of the 15 samples studied, 13 of them had four main branches, and 5 branches in the other 2 samples, supplying majority of the muscles of the posterior thigh, overlying subcutaneous fat and skin. The first and second branches of PFA anastomose with the descending branch of the inferior gluteal artery and run alongside the posterior femoral cutaneous nerve on the posterior aspect of the main trunk.

The cutaneous area supplied by PFA is 375 ± 81 cm^2 (n=15), equivalent to 27% of the thigh region, through long pedicles with an average length of 120 ± 42 mm, large average diameter of 1 ± 0.5 mm, and composed mostly of 21 ± 9 septocutaneous perforators (Figure 20). From an anatomical point of view flaps could be based on perforators from all four branches. Perforators from the first branch were consistently found inferior and lateral to the gluteal fold. The second and third did not show consistency in the bifurcation pattern from the PF main trunk. From observation in the study, the

second branch supplies the area under the first perforator, while the third branch perforates the PM*l* thigh sub-region to supply the overlying subcutaneous areas. The fourth and final branch provides perforators to the distal portion of the PL thigh.

5.4 Medial circumflex femoral artery (MCFA)

The MCFA branches from the PFA near its origin in the CFA and descends inferomedially. Its branches exhibit considerable anatomic variation, with MCFA branches sometimes emanating as independent trunks from the SFA.

In this study (n=15), 1 ± 0.4 mm was the average diameter of the MCFA perforators, with an average quantity of 4 ± 2, and an average pedicle length of 48 ± 27 mm. the MCFA perforators course mostly through the gracilis muscle to supply the medial superior thigh and the overlying skin (Figure 21). Perforators of the MCFA are the main arterial supply to the skin and subcutaneous fat overlying the superior portions of the gracilis muscle and PM*l* thigh. The average cutaneous territory supplied by this vessel (n=15) is 93 ± 38 cm^2, which is 4% of the integument surface of the thigh region.

5.5 Lateral circumflex femoral artery (LCFA)

The lateral branch off the PFA trunk is the LCFA. The LCFA usually branches into three; ascending, descending and transverse. In this study, the branching patterns of the LCFA (Figure 22) and its three main branches appeared to be a matter of anatomic variation - LCFA branches sometimes arose as independent trunks from the SFA. All three of these arteries give perforators to supply the integument overlying the AL thigh and

trochanteric sub-regions. The ascending branch supplies the skin overlying the TFL muscle with large diameter consistent perforators; the descending branch has medial and lateral branches; the lateral branch is the main supply of the skin overlying the vastus lateralis muscle. In this study, the majority of perforators were from the descending branch.

Superiorly, arterial territories of the ascending branch anastomose with inferior gluteal artery territories and first branch of the PFA lateral territories. The descending branch anastomose over the iliotibial tract with the first and second branches from the PFA laterally. Medially, perforators from the medial branch of the descending LCFA anastomose with perforators from the SFA over the midline of anterior thigh. Distally, the descending branch vascular territories anastomose with ascending territories of the LSGA.

In this study, the integument of the AL thigh and trochanteric sub-regions is supplied by approximately 11 ± 4 perforators (n=15) with an average diameter of 1 ± 0.7 mm and pedicle length 99 ± 61 mm. This vessel supplies a large cutaneous territory 271 ± 76 cm^2 over the distal posterior aspect of the thigh, representing 20% of the integument surface area of the thigh region.

5.6 Descending genicular artery (DGA)

The DGA originates from the medial aspect of the SFA before it passes through the adductor hiatus to become the PA. Out of the 15 samples studied, the DGA in two thighs originated from the PA, i.e., after the SFA had passed through the adductor hiatus. The vessel divides into three branches: the musculoarticular, osteoarticular and the saphenous branches. The musculoarticular branch runs anteriorly to supply the distal part of the vastus medialis, sartorius muscles and the overlying skin through small diameter adjacent

perforators. The saphenous (Figure 23) branch emerges from the main trunk after it bifurcates off the SFA between the vastus medialis and adductor magnus and runs superficially alongside the saphenous nerve and vein, supplying the medial aspect of the knee. The osteoarticular branch emerges from the saphenous branch, and runs medially to the medial femoral epicondyle, and then anteromedially, anastomosing with the MSGA. The saphenous branch provides reliable perforators with long pedicles for flaps as documented in the literature.

In this study (n=15), the location of the DGA allows for this vessel territory to anastomose with adjacent territories: superiorly with the SFA, anteriorly with the LSGA, and posteriorly with the PFA and the PA. The DGA provides an average of 8 ± 4 perforators with an average diameter of 0.8 ± 0.2 mm that supply an average of 97 ± 38 cm^2 of the integument and subcutaneous fat overlying the medial and distal parts of the AM thigh, representing 7% of the integument surface of the thigh. The average pedicle length was 76 ± 42 mm.

5.7 Popliteal artery (PA)

As the main arterial supply of the leg and foot, the PA is the distal continuation of the SFA as it passes through the adductor hiatus of the adductor magnus muscle. In all 15 sample studied, the PA (Figure 24) provides several consistent perforators that ascend from the popliteal fossa and anastomose with PFA perforators to contribute in supplying the inferior posteromedian (PM*n*) thigh. In 2 cases, this vessel clearly demonstrated Salmon's equilibrium law;[9] the PA perforators anastomosed in the PL thigh with perforators from the corresponding PFA to supply the overlying subcutaneous fat and integument. Also in the

PM*l* thigh sub-region, PA perforators anastomosed with perforators from the SFA to supply the subcutaneous fat and the overlying skin of this sub-region. In this study (n=15), the PA supplies approximately 7% of the thigh integument (average 99 ± 27 cm^2) with 8 ± 3 perforators. The average diameter for these perforators is 1 ± 0.7 mm and the average pedicle length is 83 ± 33 mm.

5.8 Lateral superior genicular artery (LSGA)

The LSGA (Figure 25), originating from the lateral aspect of the PA, runs over the lateral epicondyle to supply the superolateral aspect of the patella. The location of this vessel allows for the superficial anastomoses between many adjacent vascular territories: superiorly with the inferior branch of the LCFA, inferiorly with other genicular arteries and posteriorly with the PFA.

In this study (n=15), the area supplied by the LSGA perforators (5 ± 3 in number) to the lateral side of the superopatellar area is approximately 60 ± 29 cm^2, which is 4% of the thigh integument surface area. The average diameter of these perforators is 0.9 ± 0.3 mm and the average pedicle length is 66 ± 38 mm.

5.9 Medial superior genicular artery (MSGA)

Out of the 15 samples studied, in 14 samples, the MSGA (Figure 26) emerges from the medial aspect of the PA. In 1 sample however, it emerged from the DGA. The MSGA constitutes the smallest vascular territory that nourishes a limited area over the

superomedial aspect of the superopatellar integument in addition to the DGA. It also anastomoses with osteoaricular and musculoaricular over the medial femoral epicondyle.

The MSGA has 3 ± 2.5 (n=15) perforators with an average of 0.7 ± 0.2 mm diameter, and supplies a small area of 31 ± 17 cm^2 representing 4% of the integument surface area of the thigh region. The average length of these perforators was 88 ± 46 mm.

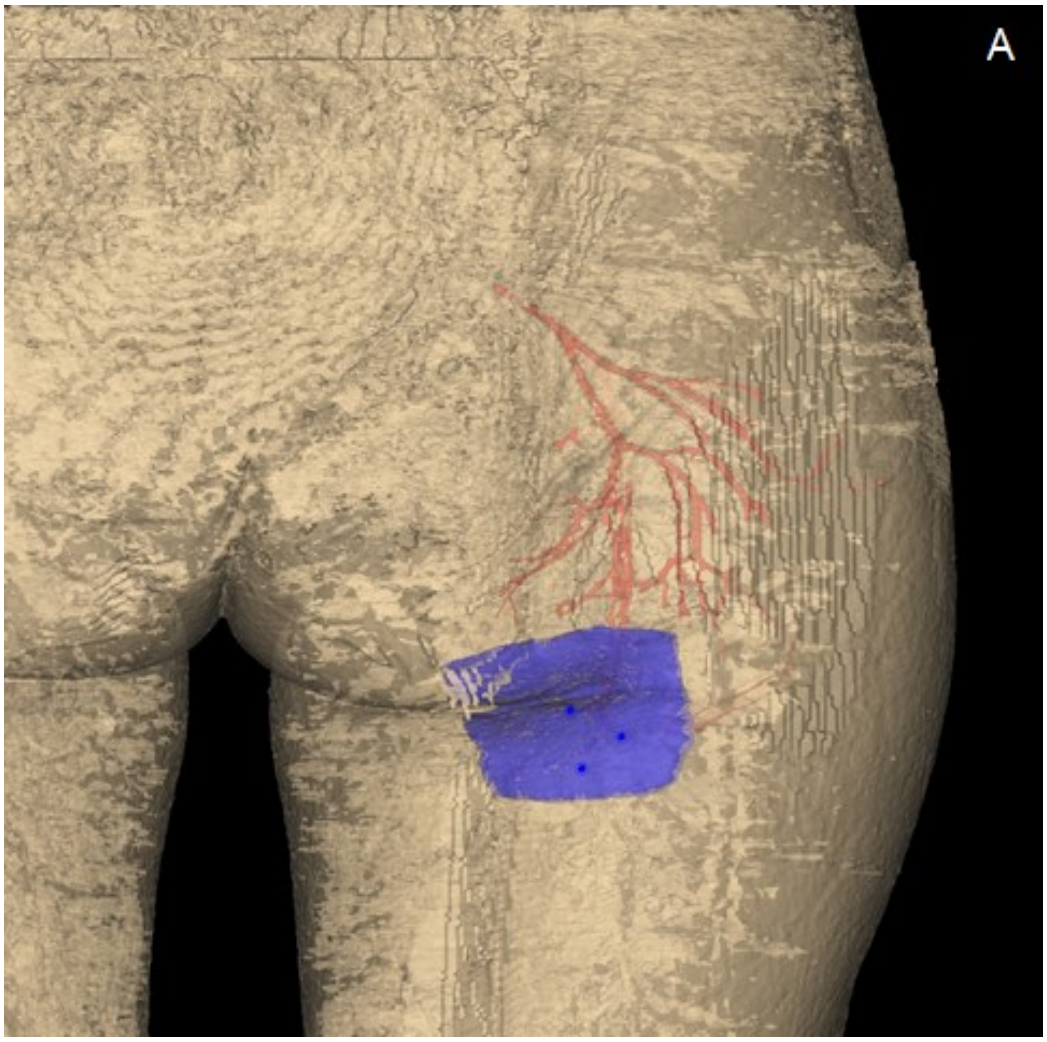

Figure 17 (A,B): Three-dimensional model (3D) of the descnding branch of the inferior gluteal artery (D-IGA). Figure 17A shows the posterior view of a three-dimensional (3D) model of the descending branch of the inferior gluteal artery (D-IGA) in the posterior thigh sub-region of the right thigh of a female cadaver injected with lead oxide and gelatin solution, and scanned using computed tomography (CT) scanner. The area perfused by the D-IGA vascular territory and relevant perforators (blue dots) are shown. Other soft tissues were omitted from the Figure to clarify the course of the D-IGA, the relevant branches and perforators.

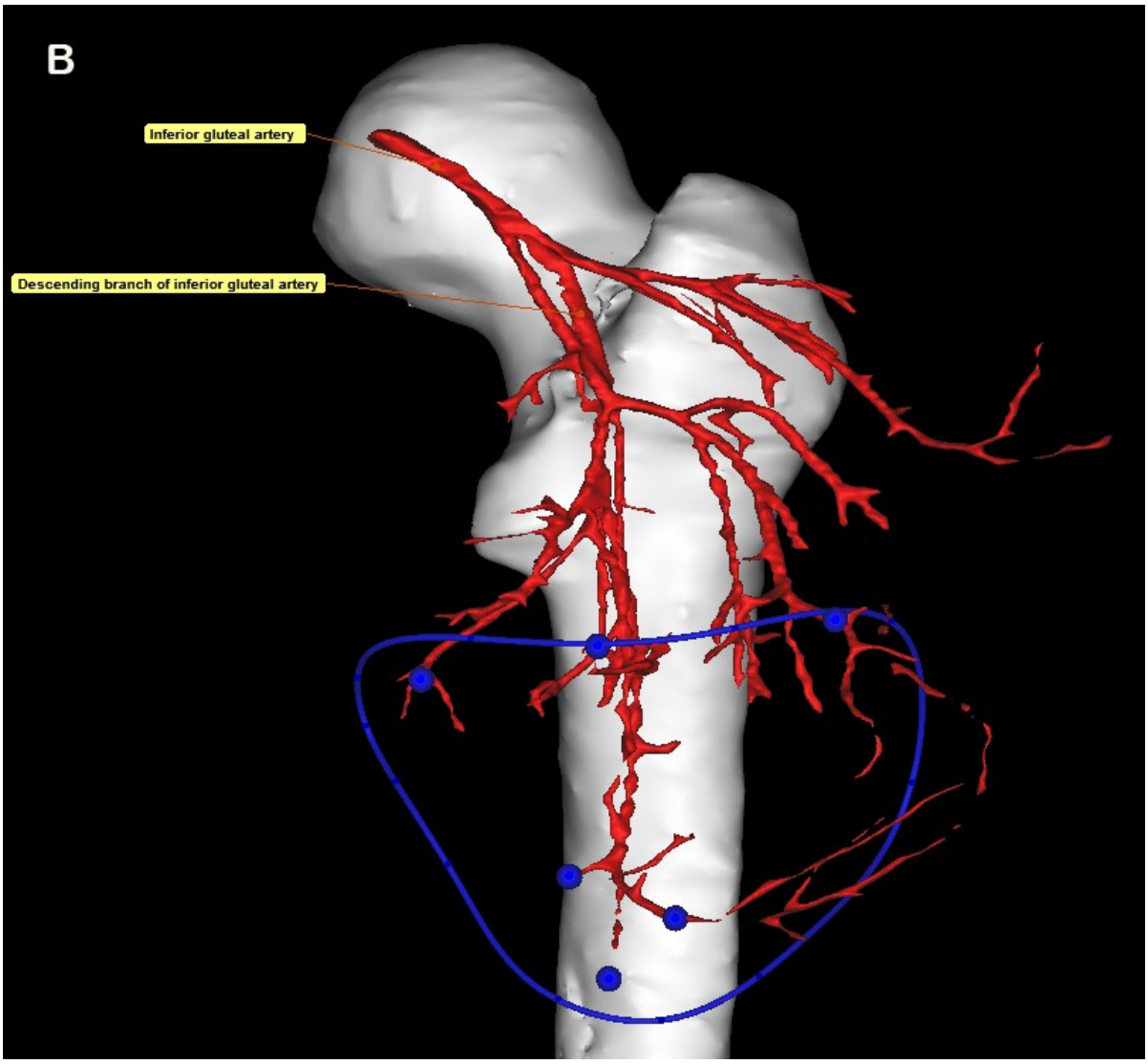

Figure 17B shows the posterior view of a three-dimensional (3D) model of the descending branch of the inferior gluteal artery (D-IGA) in the posterior thigh sub-region of the right thigh of a female cadaver injected with lead oxide and gelatin solution, and scanned using computed tomography (CT) scanner. The D-IGA vascular territory and relevant perforators (blue dots) are shown. Other soft tissues were omitted from the Figure to clarify the course of the D-IGA, the relevant branches and perforators.

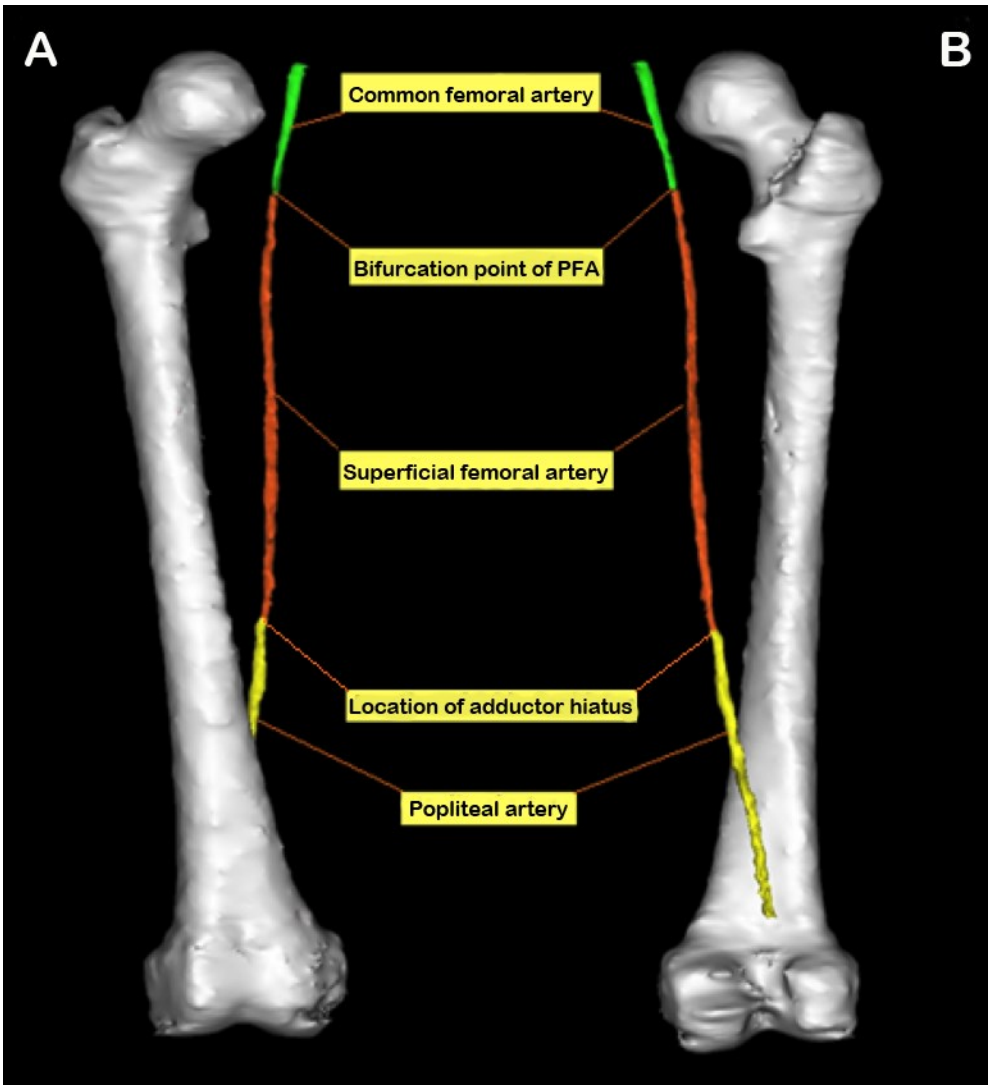

Figure 18 (A,B): The course of the common femoral artery (CFA), superficial femoral artery (SFA) and popliteal artery (PA). The Figures 18A anterior and 18B posterior views of three-dimensional (3D) models show the course of the common femoral artery (green), superficial femoral artery (orange) and popliteal artery (yellow). (from the right thigh of a female cadaver).

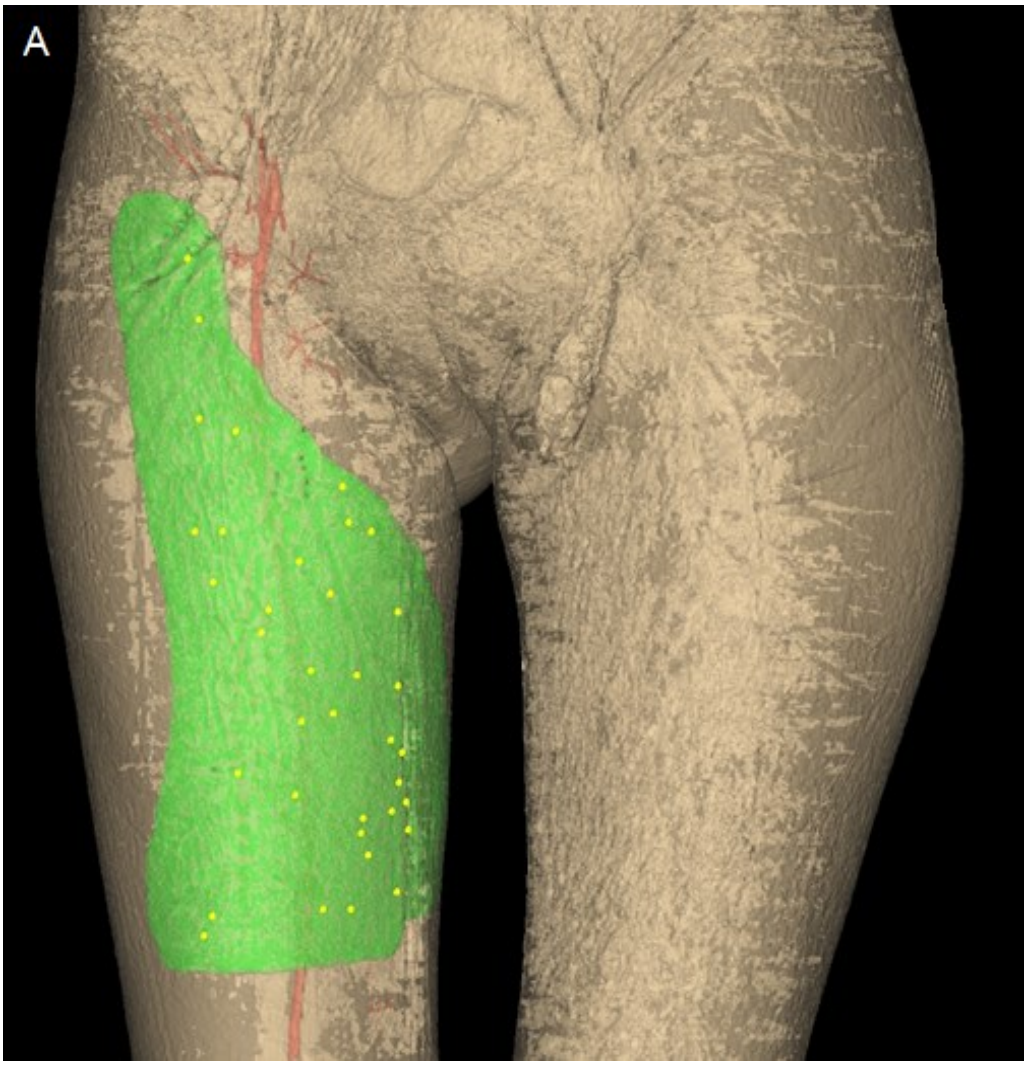

Figure 19 (A,B): Three-dimensional (3D) model of the superficial femoral artery (SFA). Figure 19A shows the anteromedial view of a three-dimensional (3D) model of the superficial femoral artery (SFA) in the anteromedial (AM) and medial thigh sub-regions of the right thigh of a female cadaver injected with lead oxide and gelatin solution, and scanned using computed tomography (CT) scanner. The area perfused by SFA vascular territory and relevant perforators (yellow dots) are shown. Other soft tissues were omitted from the Figure to clarify the course of the SFA, the relevant branches and perforators.

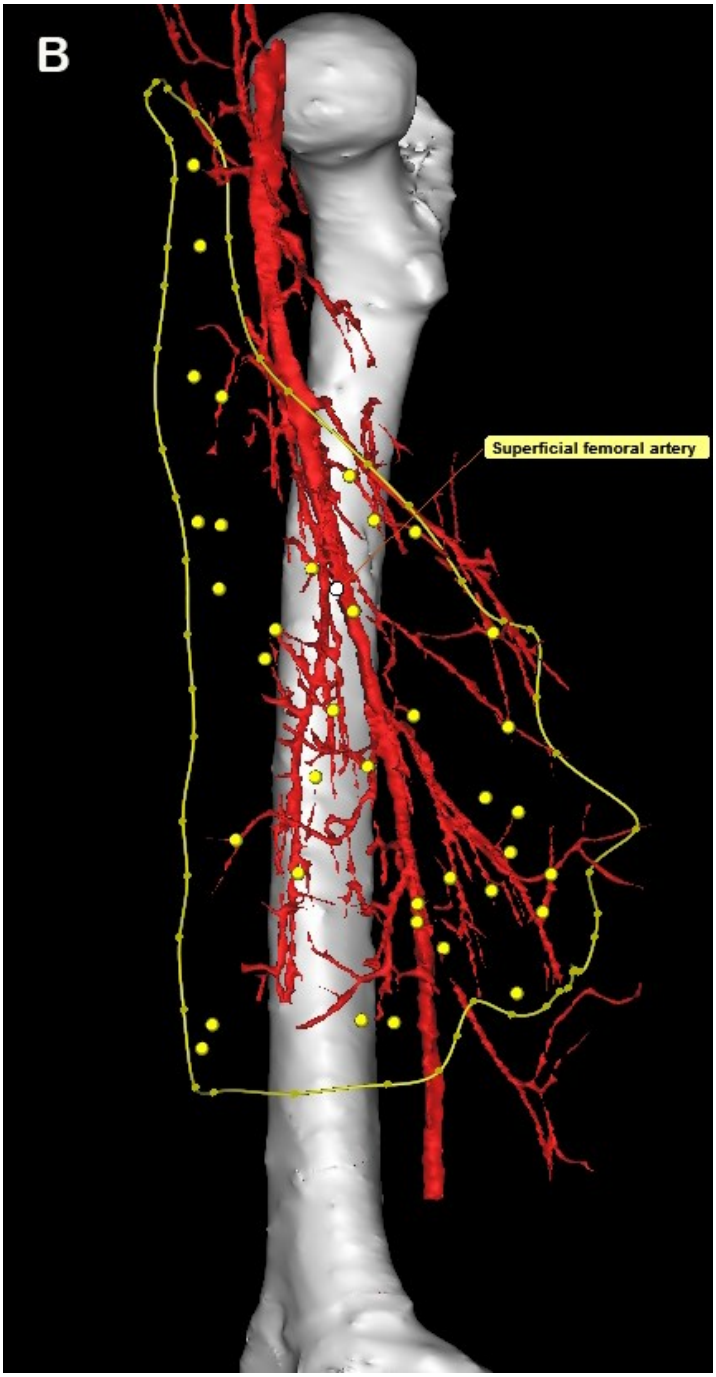

Figure 19B shows the medial view of a three-dimensional (3D) model of the superficial femoral artery (SFA) in the anteromedial (AM) and medial thigh sub-regions of the right thigh of a female cadaver injected with lead oxide and gelatin solution, and scanned using computed tomography (CT) scanner. The SFA vascular territory and relevant perforators (yellow dots) are shown. Other soft tissues were omitted from the Figure to clarify the course of the SFA, the relevant branches and perforators.

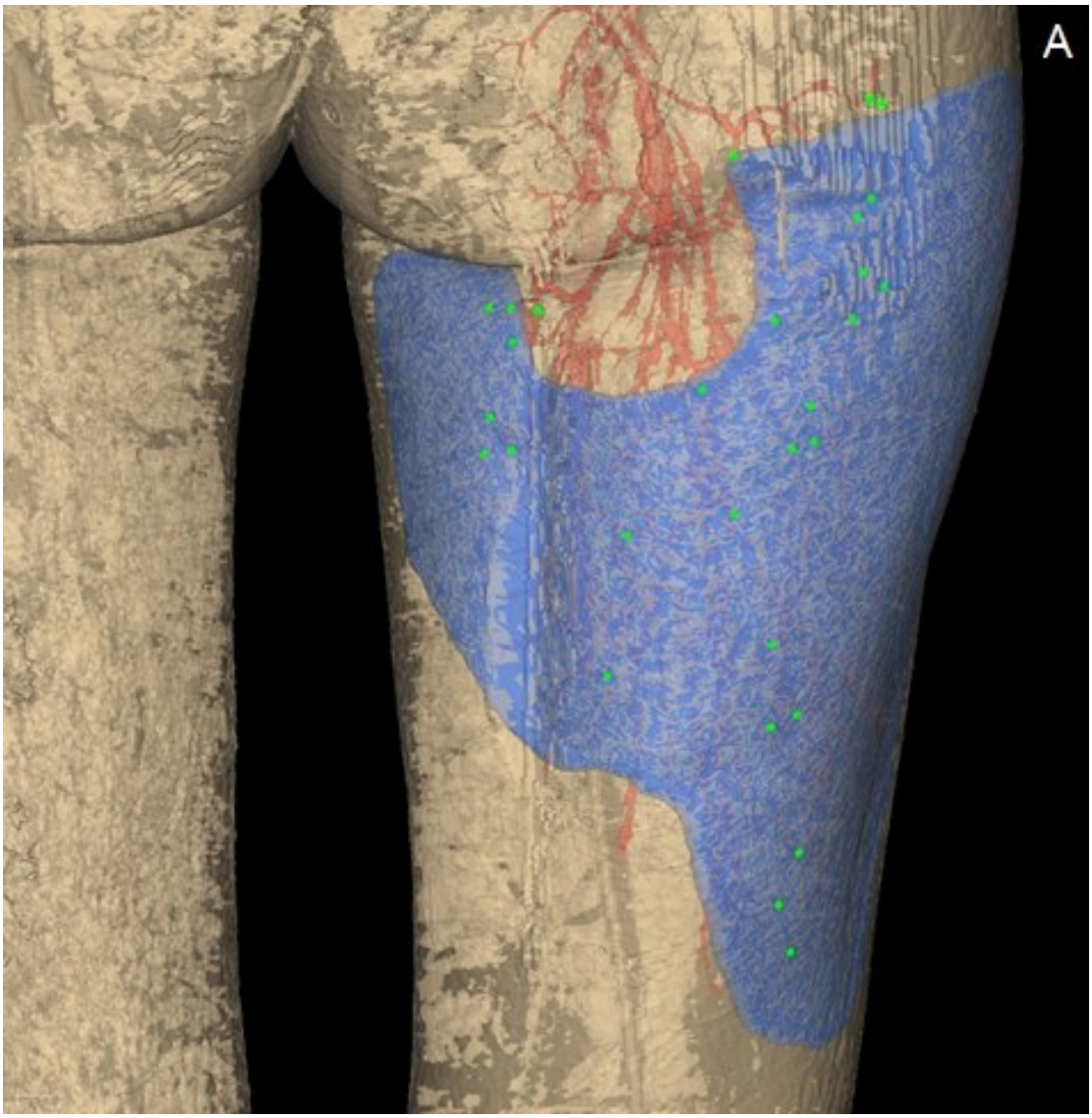

Figure 20 (A,B): Three-dimensional (3D) model of the profunda femoral artery (PFA). Figure 20A shows the posterior view of a three-dimensioal (3D) model of the profunda femoral artery (PFA) in the posterior thigh sub-region of the right thigh of a female cadaver injected with lead oxide and gelatin solution, and scanned using computed tomography (CT) scanner. The area perfused by PFA vascular territory and relevant perforators (green dots) are shown. Other soft tissues were omitted from the Figure to clarify the course of the PFA, the relevant branches and perforators.

Figure 20B: In this Figure the posterior view of a three-dimensional (3D) model of the profunda femoral artery (PFA) in the posterior thigh sub-region of the right thigh of a female cadaver injected with lead oxide and gelatin solution, and scanned using computed tomography (CT) scanner. The PFA vascular territory and relevant perforators (green dots) are shown. Other soft tissues were omitted from the Figure to clarify the course of the PFA, the relevant branches and perforators.

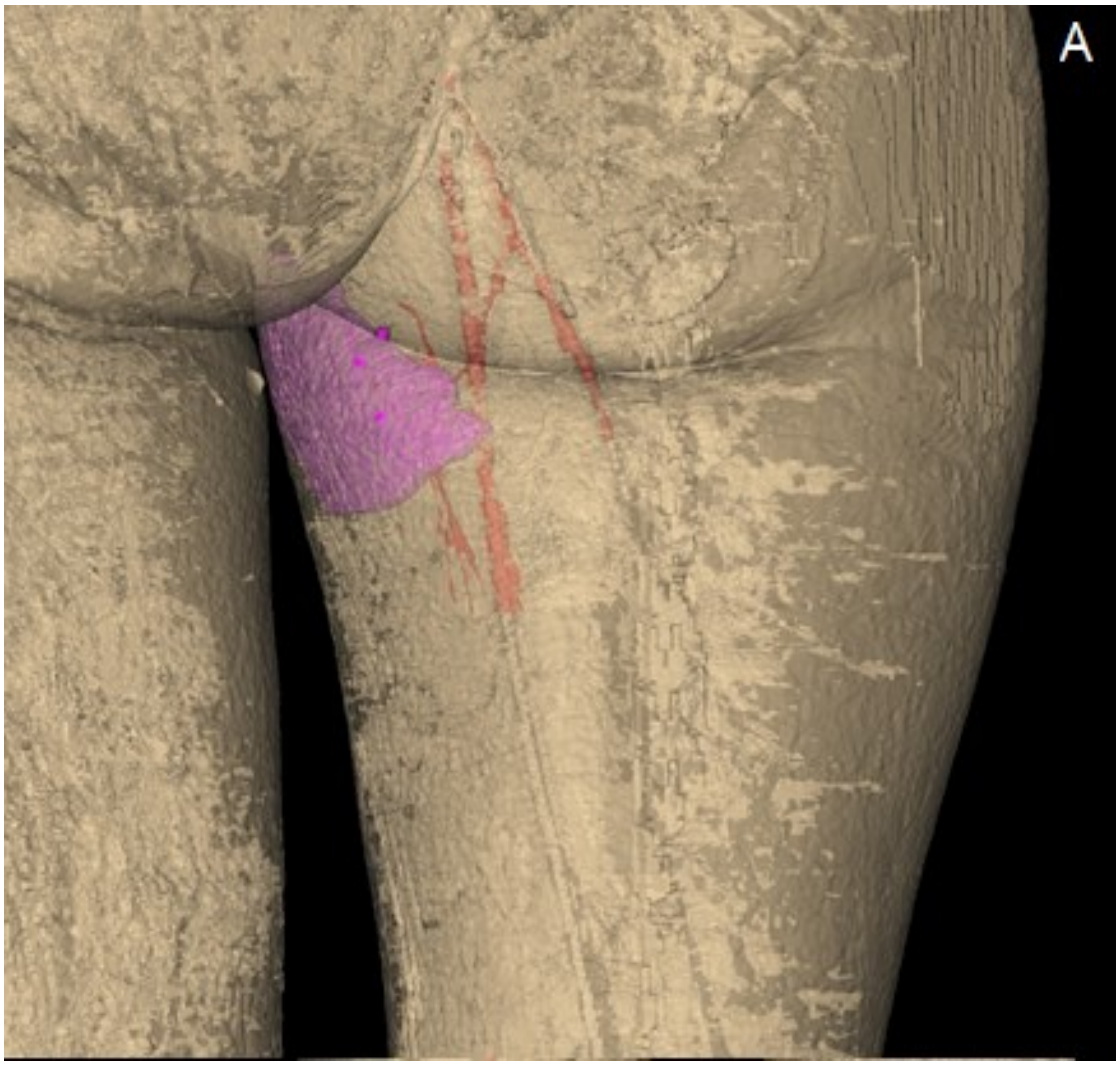

Figure 21 (A-C): Three-dimensionl (3D) model of the medial circumflex femoral artery (MCFA). Posteromedial (PM*l*) view (21A) of a three-dimensional (3D) model of the medial circumflex femoral artery (MCFA) in the medial thigh sub-region of the right thigh of a female cadaver injected with lead oxide and gelatin solution, and scanned using computed tomography (CT) scanner. The area perfused by MCFA vascular territory and relevant perforators (pink dots) are shown. Other soft tissues were omitted from the Figure to clarify the course of the MCFA, the relevant branches and perforators.

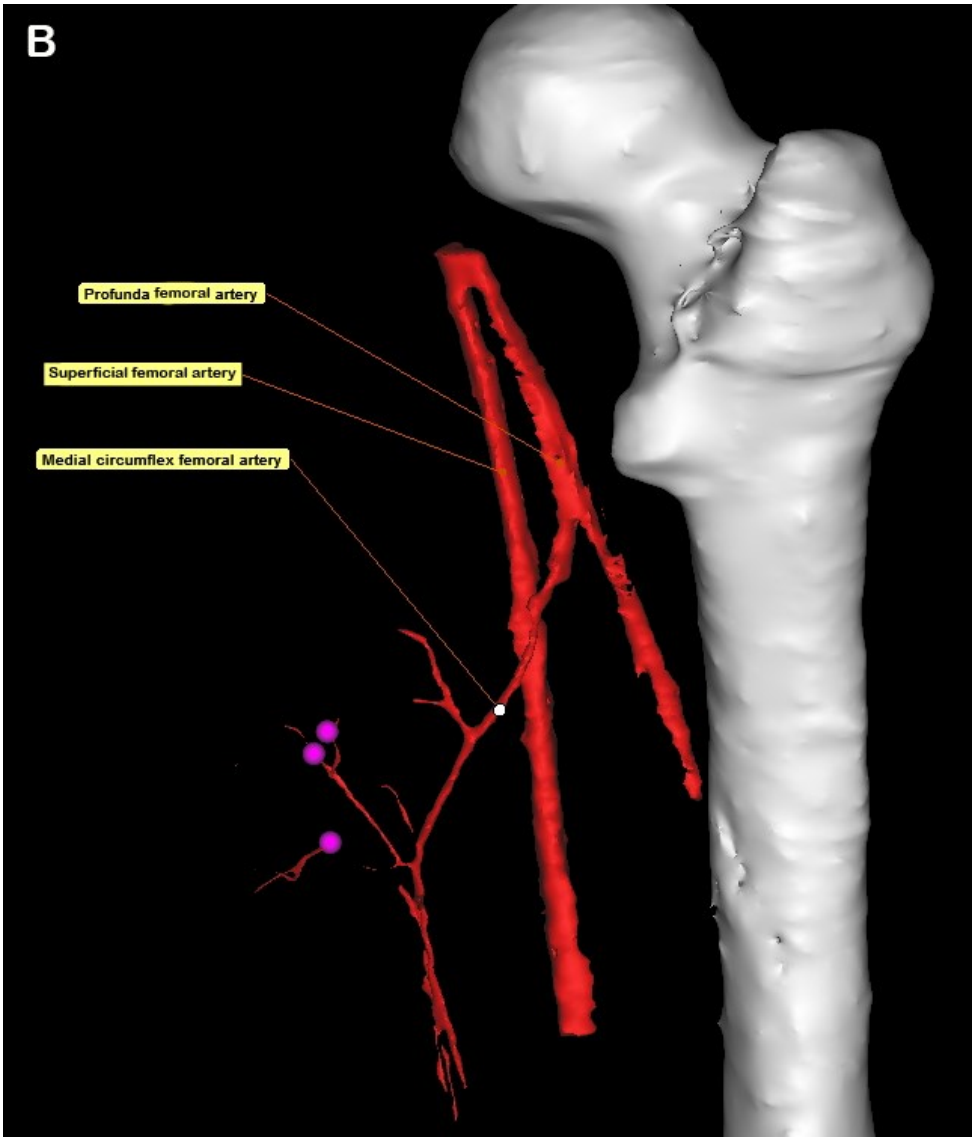

Figure 21B shows the posterior view of a three-dimensional (3D) model of the medial circumflex femoral artery (MCFA) in the medial thigh sub-region of the right thigh of a female cadaver injected with lead oxide and gelatin solution, and scanned using computed tomography (CT) scanner. The MCFA vascular territory and relevant perforators (pink dots) are shown. Other soft tissues were omitted from the Figure to clarify the course of the MCFA, the relevant branches and perforators.

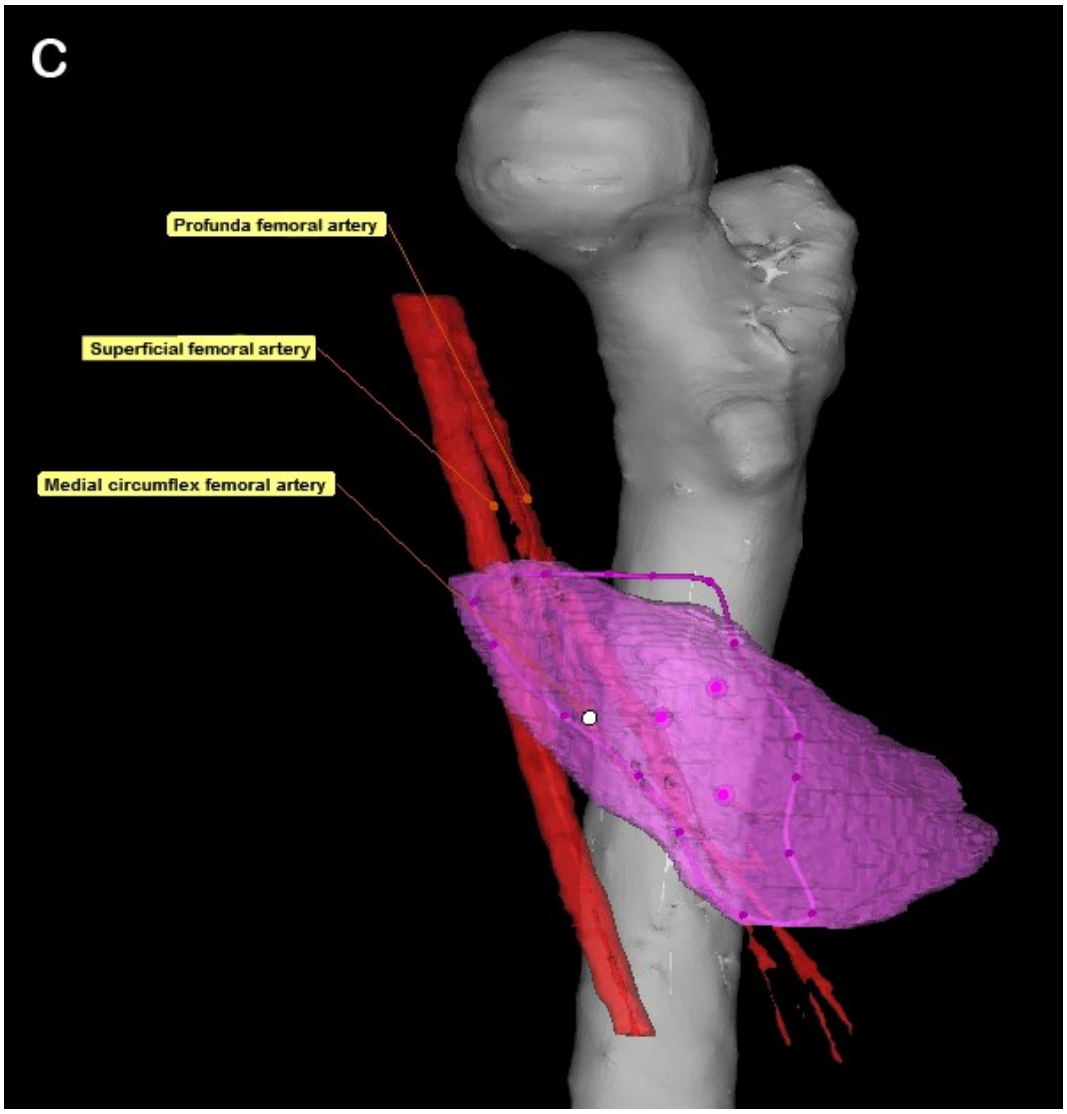

Figure 21C shows the medial view of a three-dimensional (3D) model of the medial circumflex femoral artery (MCFA) in the medial thigh sub-region of the right thigh of a female cadaver injected with lead oxide and gelatin solution and, scanned using computed tomography (CT) scanner. The area perfused by MCFA vascular territory and relevant perforators (pink dots) are shown. Other soft tissues were omitted from the Figure to clarify the course of the MCFA, the relevant branches and perforators.

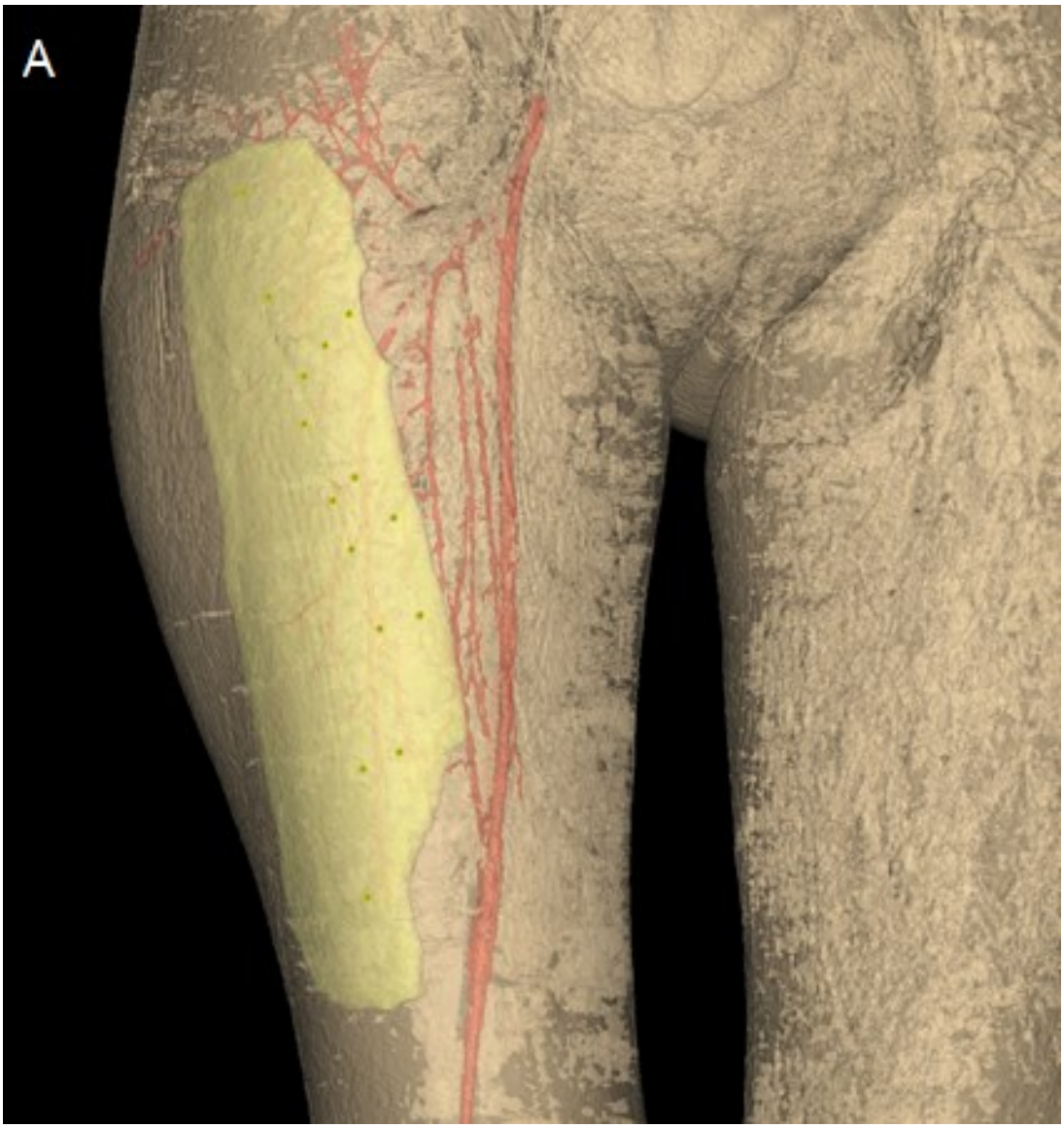

Figure 22 (A,B): Three-dimensional (3D) model of the lateral circumflex femoral artery (LCFA). Anterior view (22A) of a three-dimensional (3D) model of the lateral circumflex femoral artery (LCFA) in the anterolateral (AL) thigh and trochanteric sub-regions of the right thigh of a female cadaver injected with lead oxide and gelatin solution, and scanned using computed tomography (CT) scanner. The area perfused by the LCFA vascular territory and relevant perforators (dark yellow dots) are shown. Other soft tissues were omitted from the Figure to clarify the course of the LCFA, the relevant branches and perforators.

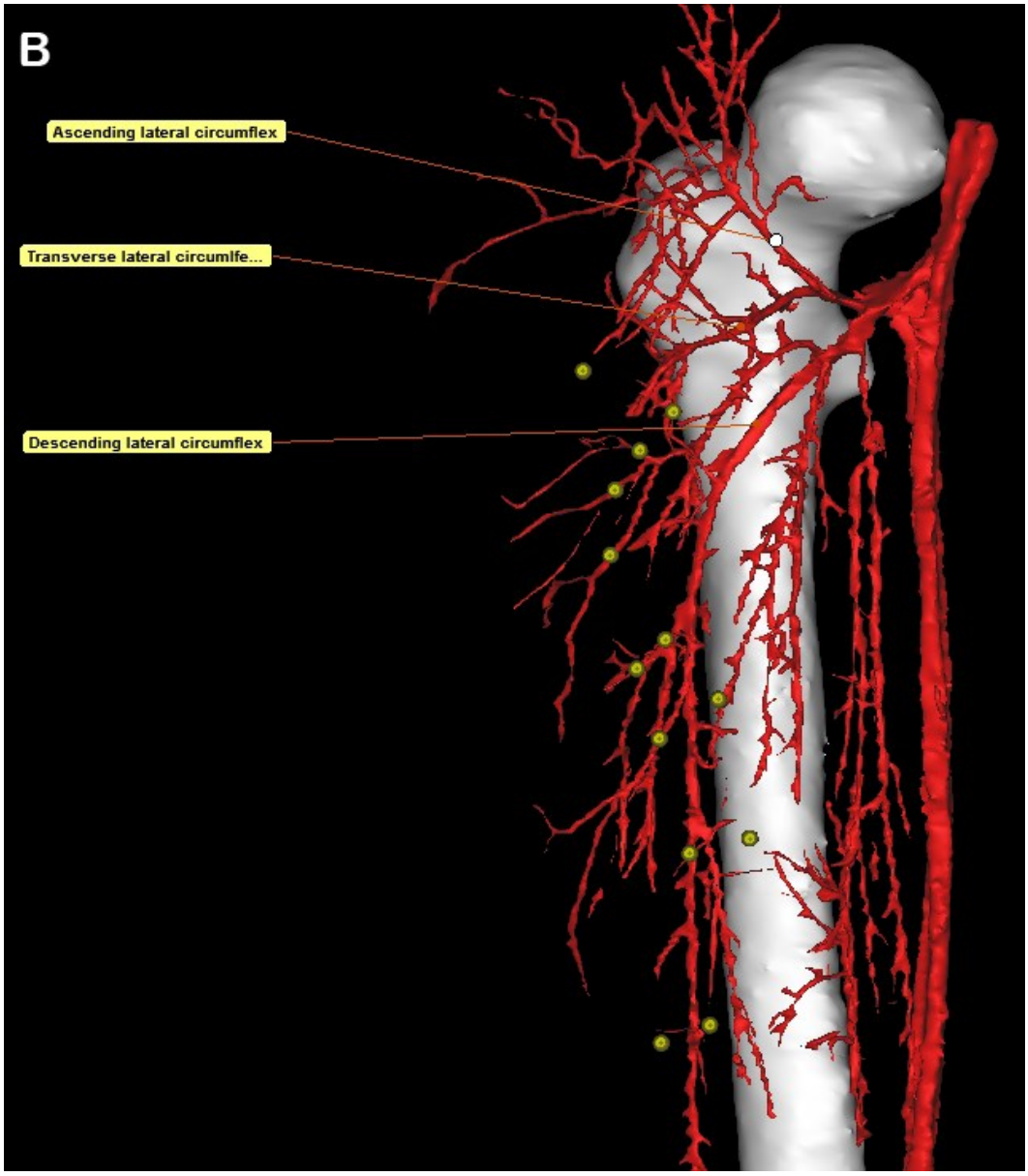

Figure 22B shows the anterior view of a three-dimensional (3D) model of the lateral circumflex femoral artery (LCFA) in the anterolateral (AL) thigh and trochanteric sub-regions of the right thigh of a female cadaver injected with lead oxide and gelatin solution, and, scanned using CT scanner. The LCFA vascular territory and relevant perforators (dark yellow dots) are shown. Other soft tissues were omitted from the Figure to clarify the course of the LCFA, the relevant branches and perforators.

Figure 23 (A,B): Three-dimensional (3D) model of the descending genicular artery (DGA). Figure 23A shows the anteromedial (AM) view of a three-dimensional (3D) model of the descending genicular artery (DGA) in the anteromedial (AM) and medial thigh sub-regions of the right thigh of a female cadaver injected with lead oxide and gelatin solution, and scanned using computed tomography (CT) scanner. The area perfused by DGA vascular territory and relevant perforators (green dots) are shown. Other soft tissues were omitted from the Figure to clarify the course of the DGA, the relevant branches and perforators.

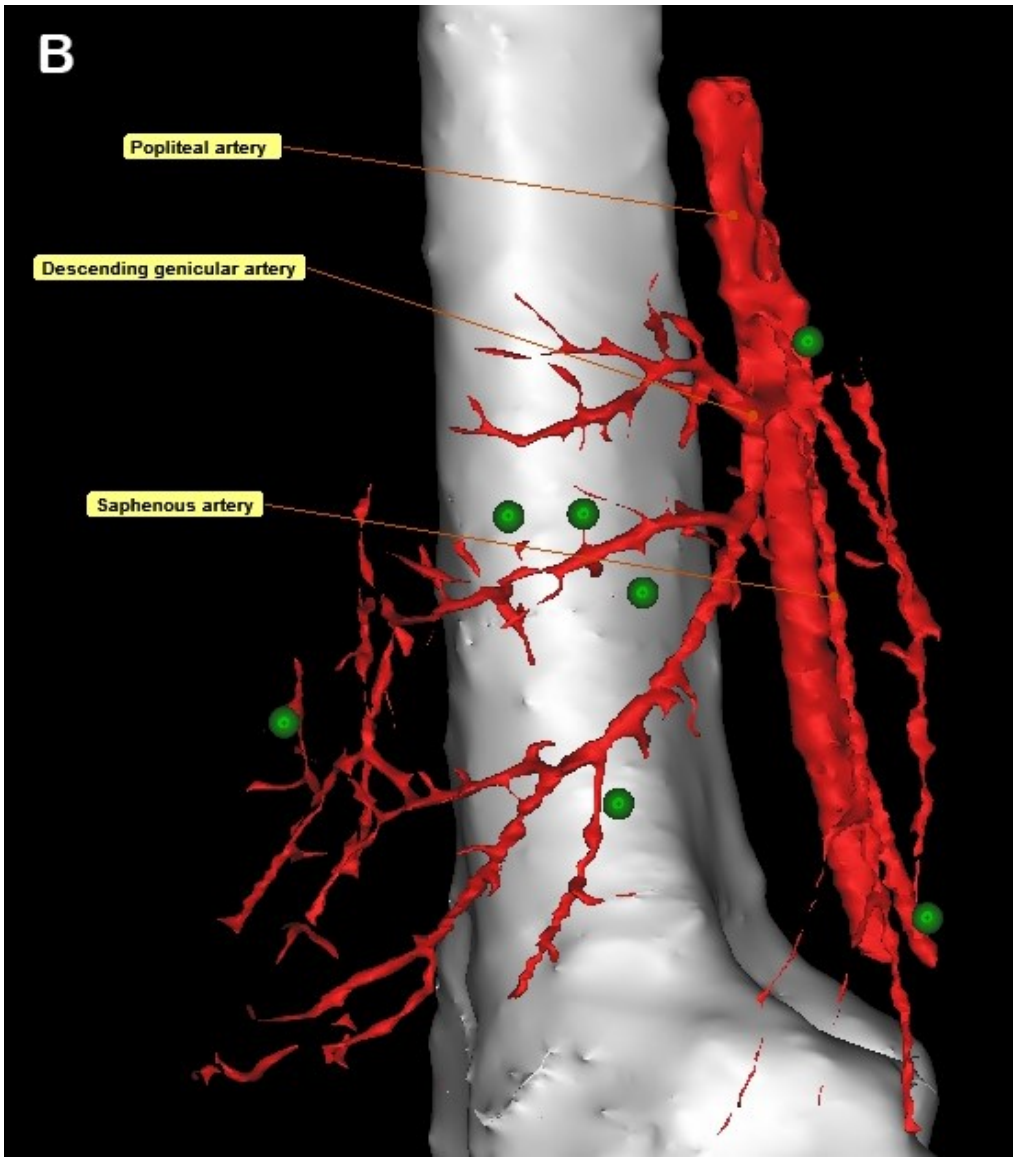

Figure 23B shows the medial view of a three-dimensional (3D) model of the descending genicular artery (DGA) in the anteromedial (AM) and medial thigh sub-regions of the right thigh of a female cadaver injected with lead oxide and gelatin solution, and scanned using computed tomography (CT) scanner. The DGA vascular territory and relevant perforators (green dots) are shown. Other soft tissues were omitted from the Figure to clarify the course of the DGA, the relevant branches and perforators.

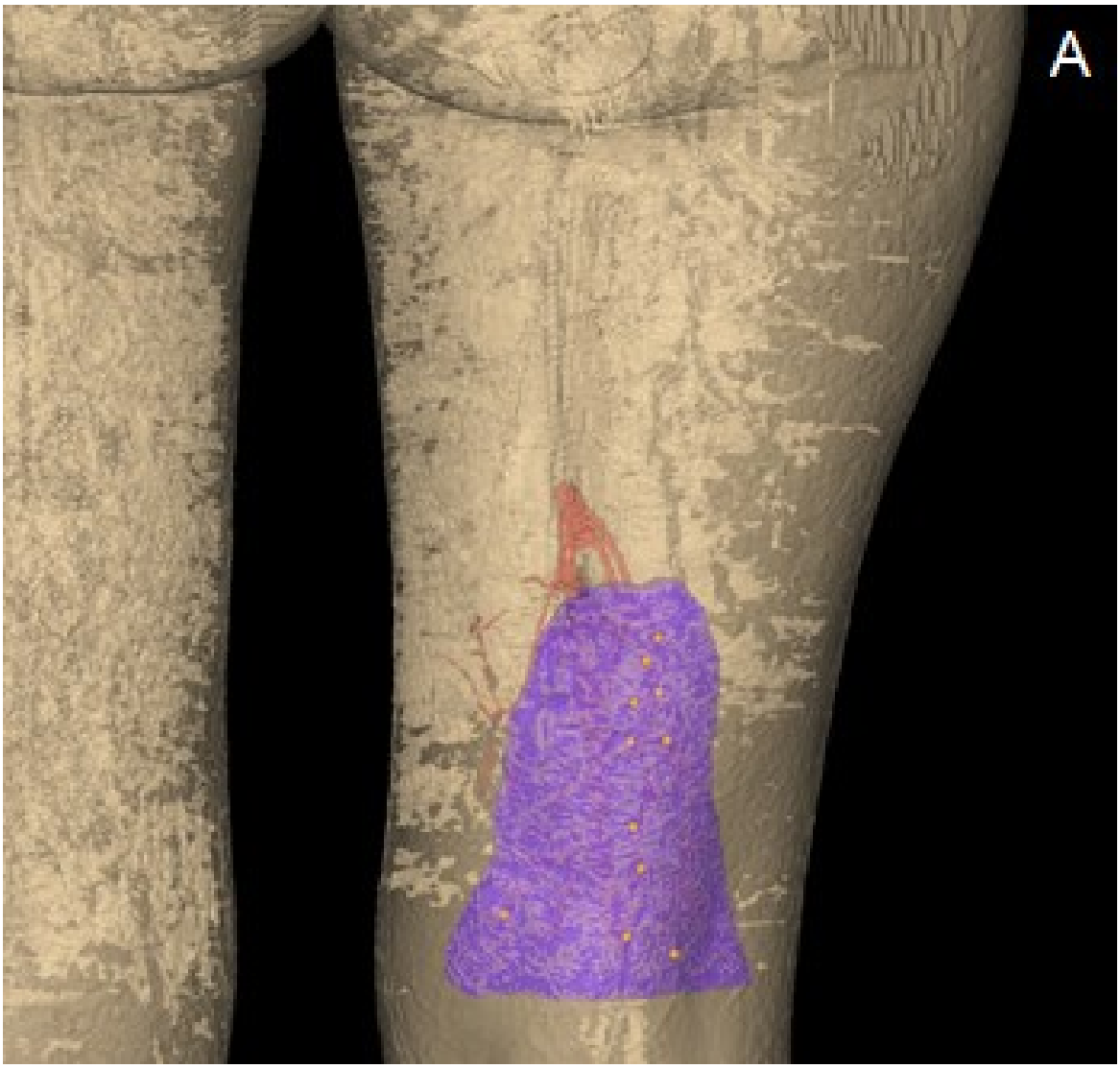

Figure 24 (A,B): Three-dimensional (3D) model of the popliteal artery (PA). Figure 24A shows the posterior view of a three-dimensional (3D) model of the popliteal artery (PA) in the posterior thigh sub-region of the right thigh of a female cadaver injected with lead oxide and gelatin solution, and scanned using computed tomography (CT) scanner. The area perfused by the PA vascular territory and relevant perforators (orange dots) are shown. Other soft tissues were omitted from the Figure to clarify the course of the PA, the relevant branches and perforators.

Figure 24B shows the medial view of a three-dimensional (3D) model of the popliteal artery (PA) in the posterior thigh sub-region of the right thigh of a female cadaver injected with lead oxide and gelatin solution, and scanned using computed tomography (CT) scanner. The PA vascular territory and relevant perforators (orange dots) are shown. Other soft tissues were omitted from the Figure to clarify the course of the PA, the relevant branches and perforators.

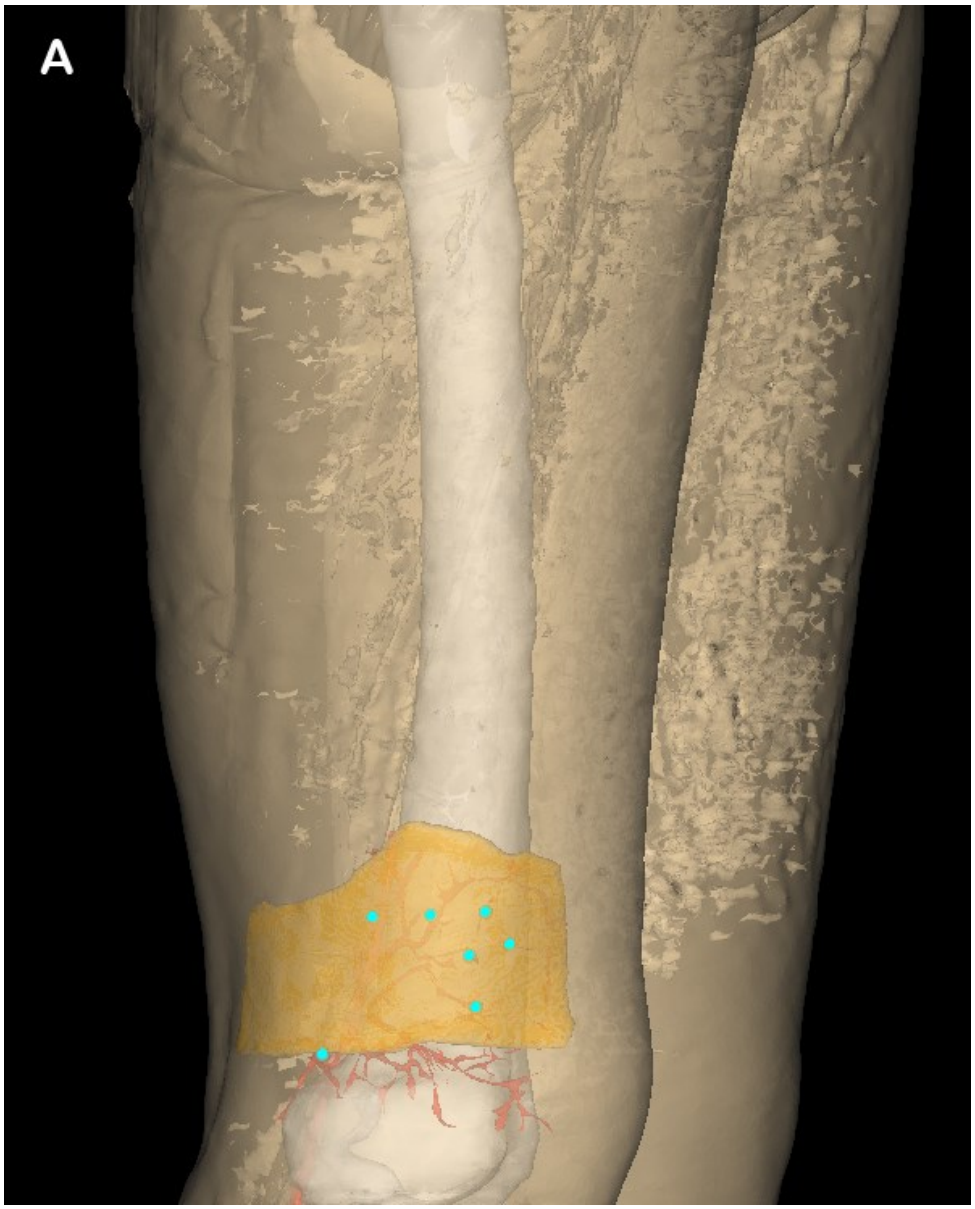

Figure 25 (A-C): Three-dimensional (3D) model of the lateral superior genicular artery (LSGA). Figure 25A shows the lateral view of a three-dimensional (3D) model of the lateral superior genicular artery (LSGA) in the anterolateral (AL) thigh sub-region of the right thigh of a female cadaver injected with lead oxide and gelatin solution, and scanned using computed tomography (CT) scanner. The area perfused by LSGA vascular territory and relevant perforators (light blue dots) are shown. Other soft tissues were omitted from the Figure to clarify the course of the LSGA, the relevant branches and perforators.

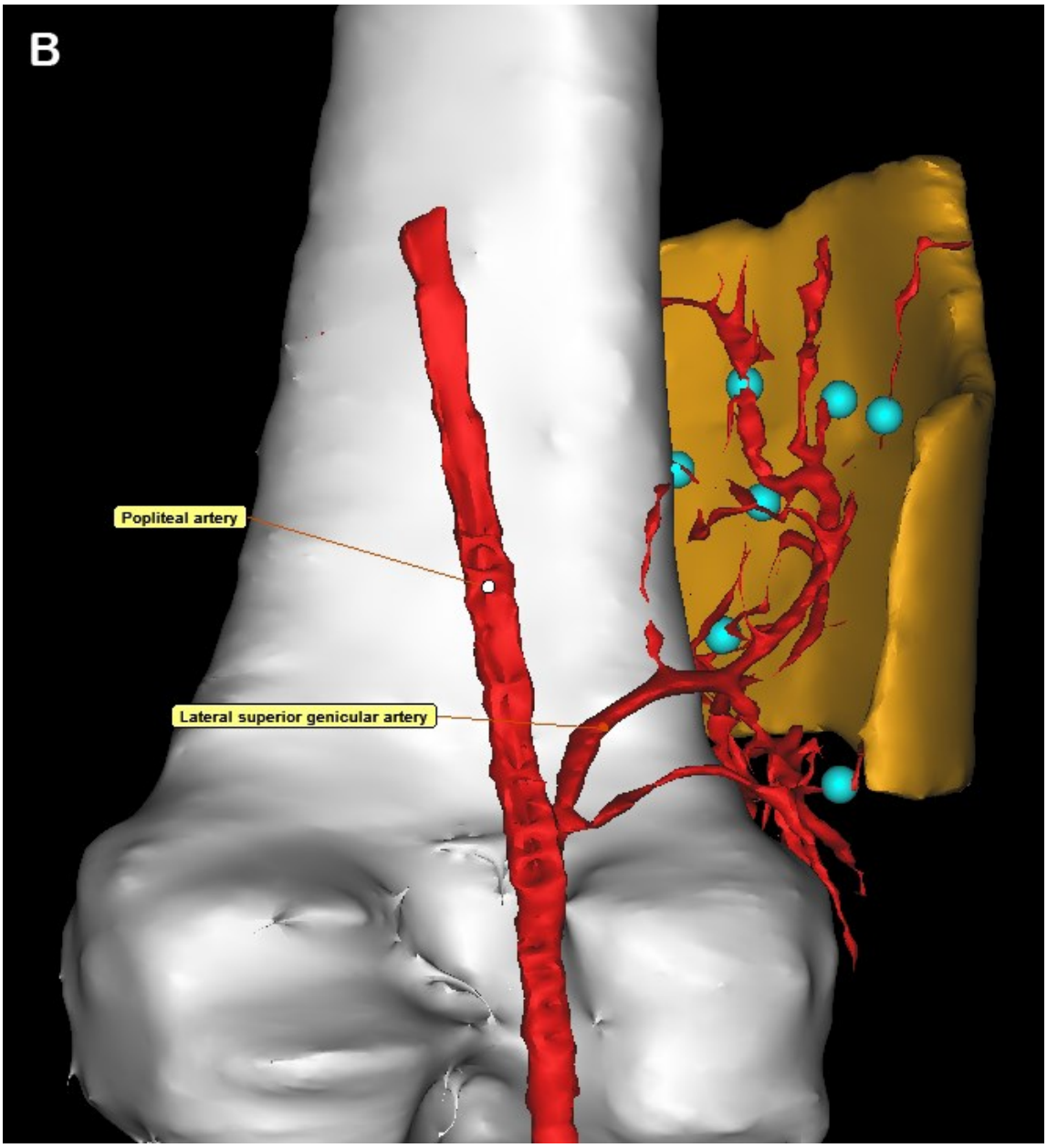

Figure 25B shows the posterior view of a three-dimensional (3D) model of the lateral superior genicular artery (LSGA) in the anterolateral (AL) thigh sub-region of the right thigh of a female cadaver injected with lead oxide and gelatin solution, and scanned using computed tomography (CT) scanner. The area perfused by LSGA vascular territory and relevant perforators (light blue dots) are shown. Other soft tissues were omitted from the Figure to clarify the course of the LSGA, the relevant branches and perforators.

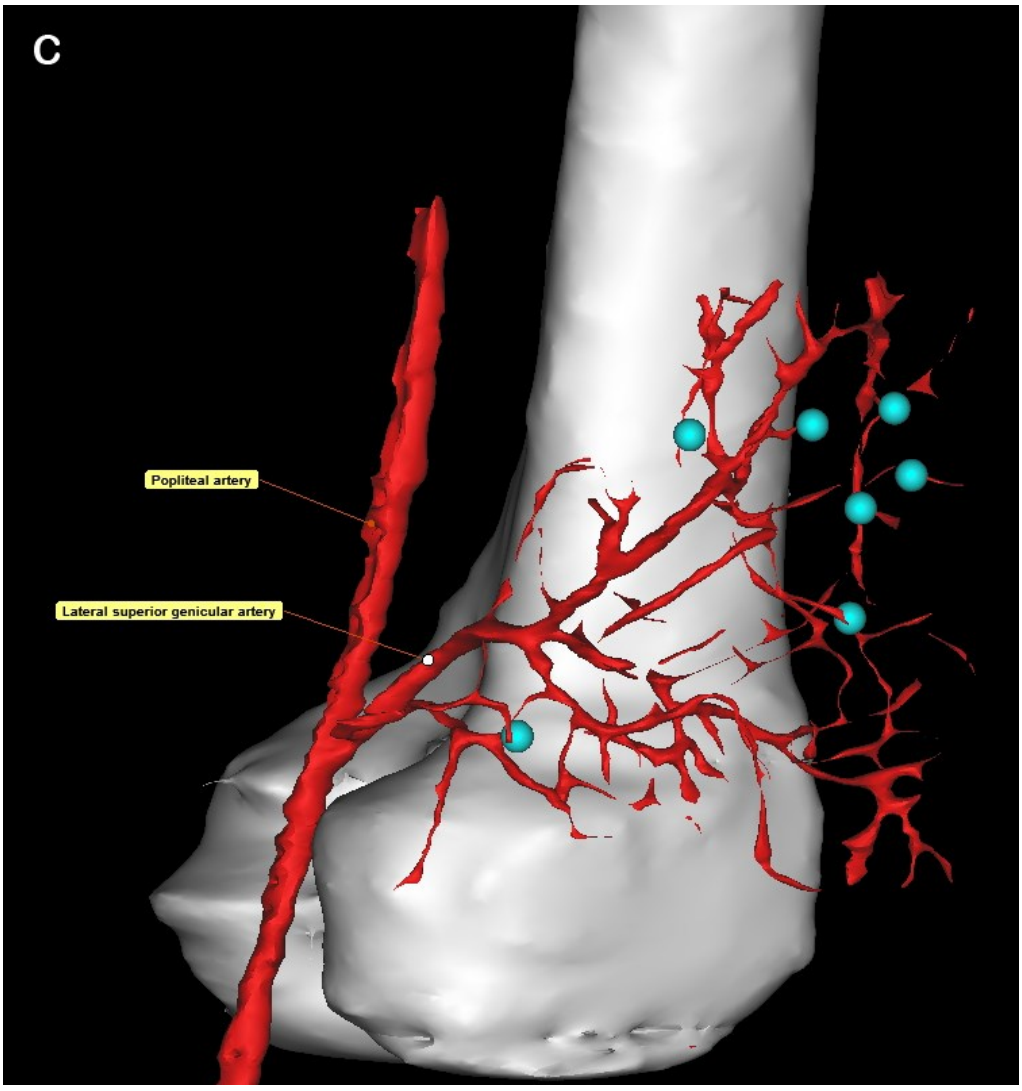

Figure 25C shows the posterolateral (PL) view of a three-dimensional (3D) model of the lateral superior genicular artery (LSGA) in the anterolateral (AL) thigh sub-region of the right thigh of a female cadaver injected with lead oxide and gelatin solution, and scanned using computed tomography (CT) scanner. The LSGA vascular territory and relevant perforators (light blue dots) are shown. Other soft tissues were omitted from the Figure to clarify the course of the LSGA, the relevant branches and perforators.

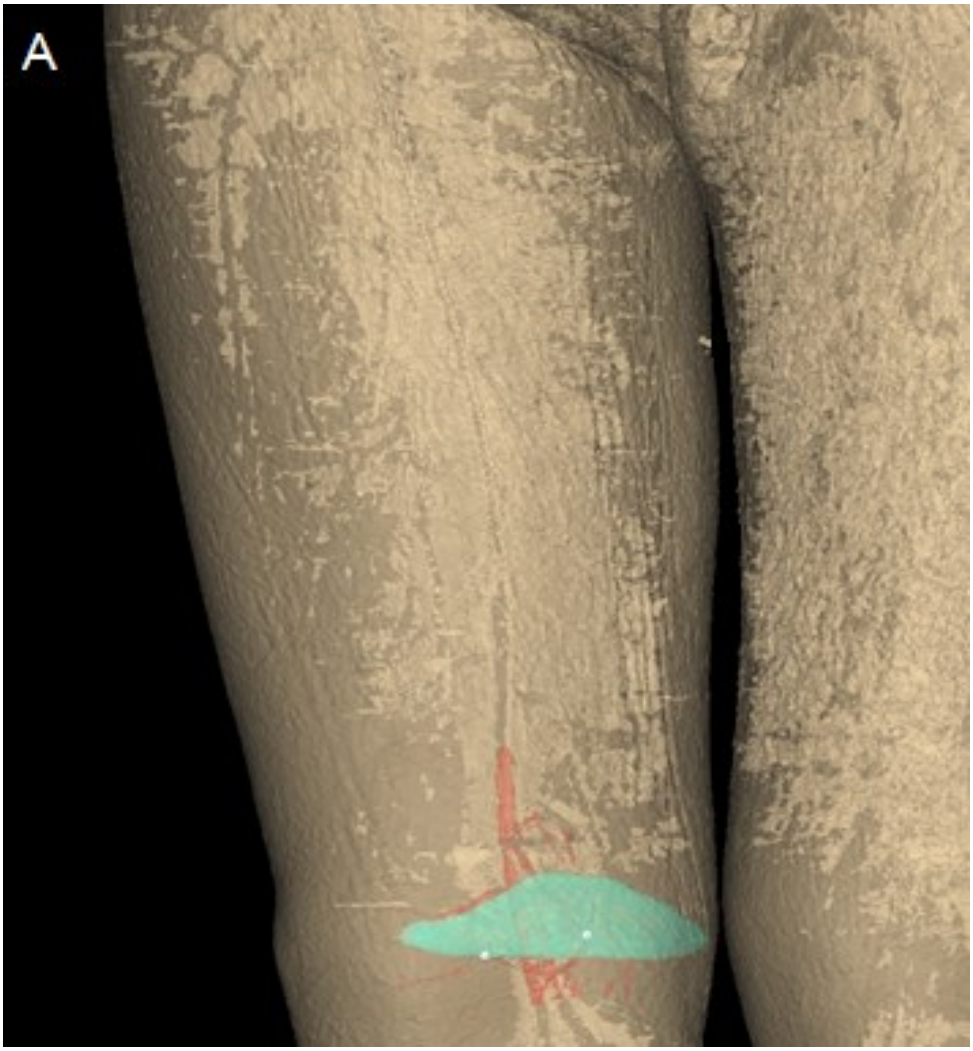

Figure 26 (A-D): Three-dimensional (3D) model of the medial superior genicular artery (MSGA). Figure 26A shows the anteromedial view of a three-dimensional (3D) model of the medial superior genicular artery (MSGA) in the anteromedial (AM) and medial thigh sub-regions of the right thigh of a female cadaver injected with lead oxide and gelatin solution, and scanned using computed tomography (CT) scanner. The area perfused by the MSGA vascular territory and relevant perforators (white dots) are shown. Other soft tissues were omitted from the Figure to clarify the course of the MSGA, the relevant branches and perforators.

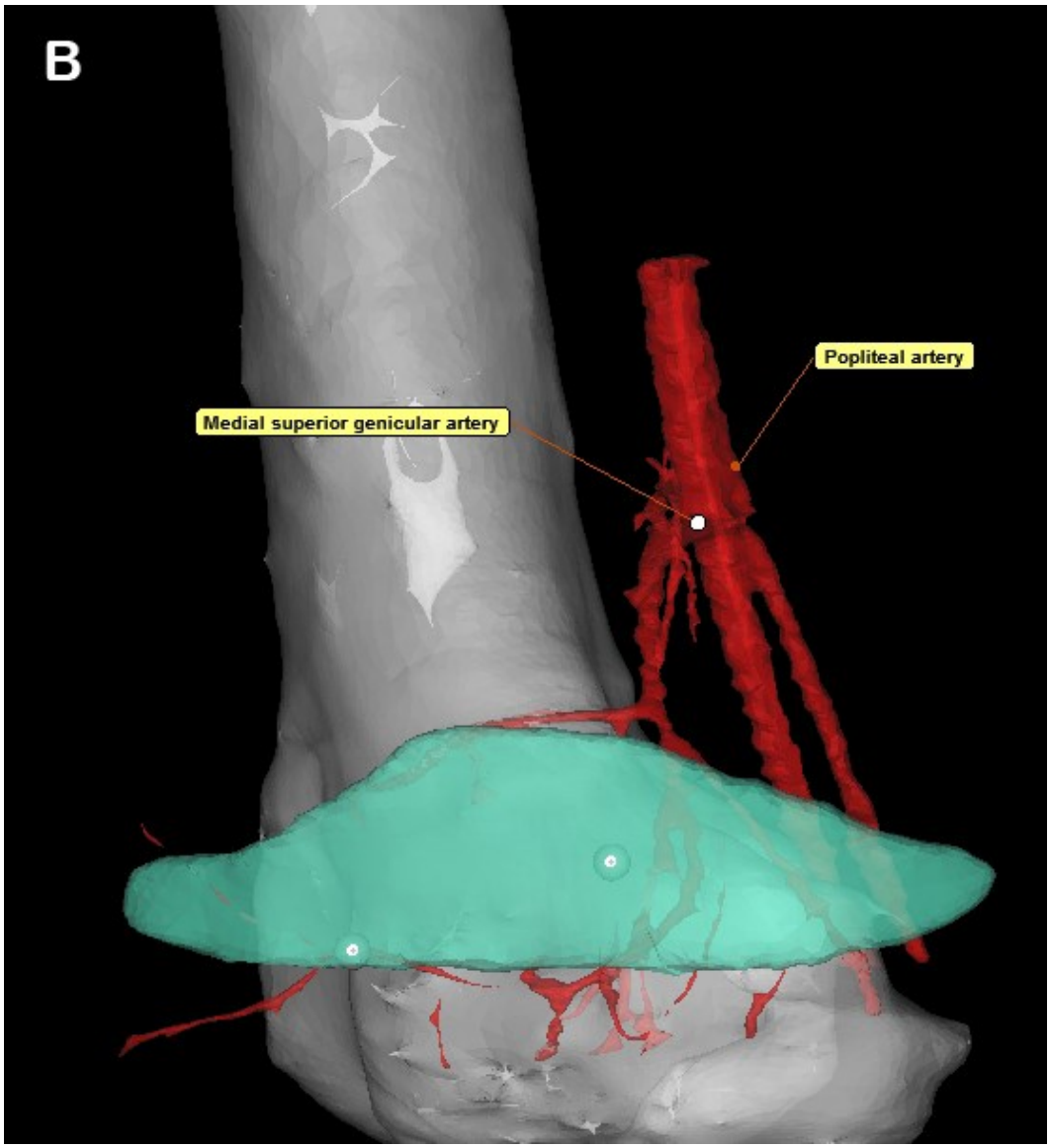

Figure 26B shows the medial view of a three-dimensional (3D) model of the medial superior genicular artery (MSGA) in the anteromedial (AM) and medial thigh sub-regions of the right thigh of a female cadaver injected with lead oxide and gelatin solution, and scanned using computed tomography (CT) scanner. The area perfused by the MSGA vascular territory and relevant perforators (white dots) are shown. Other soft tissues were omitted from the Figure to clarify the course of the MSGA, the relevant branches and perforators.

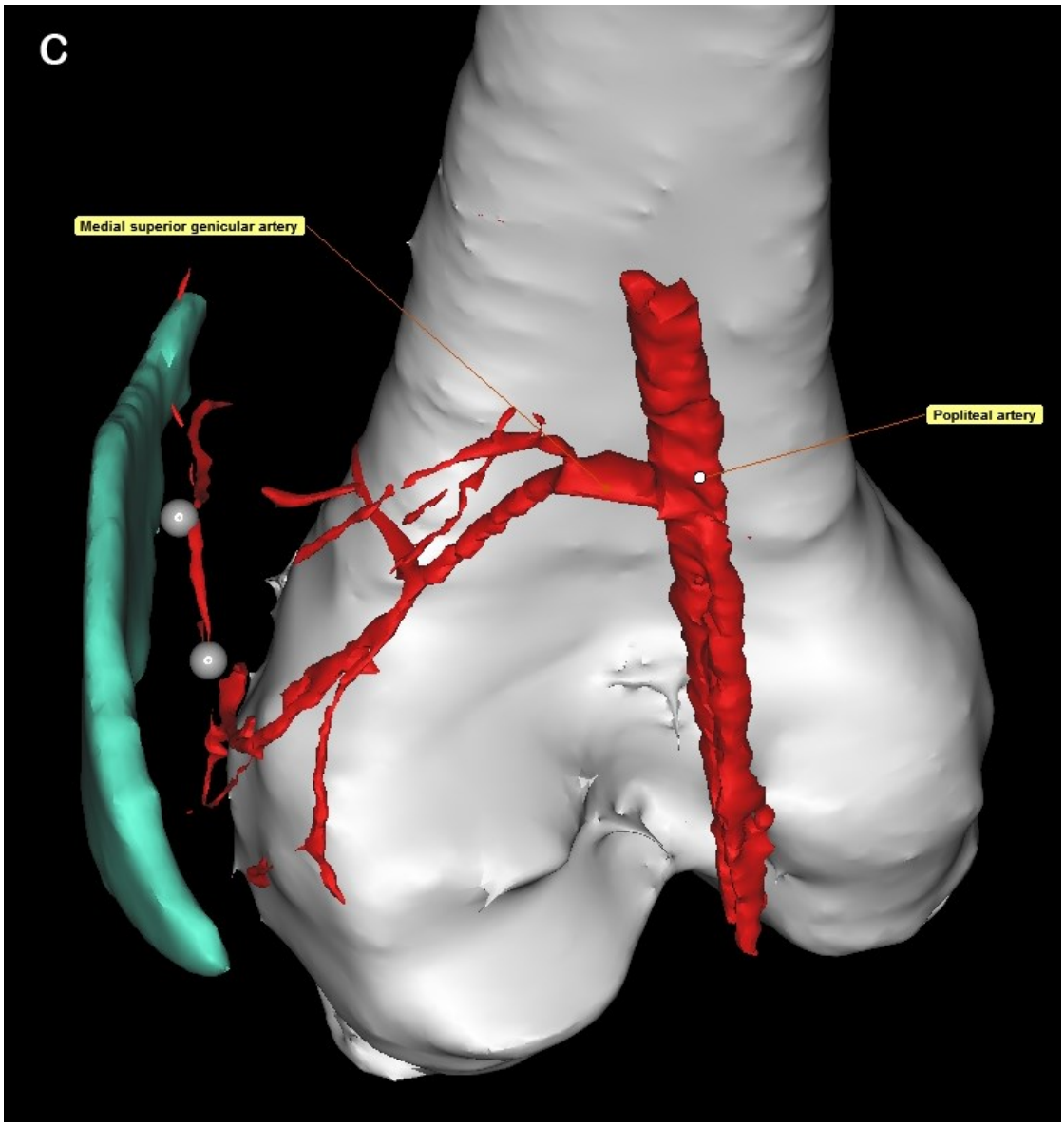

Figure 26C shows the inferioposterior view of a three-dimensional (3D) model of the medial superior genicular artery (MSGA) in the anteromedial (AM) and medial thigh sub-regions of the right thigh of a female cadaver injected with lead oxide and gelatin solution, and scanned using computed tomography (CT) scanner. The area perfused by MSGA vascular territory and relevant perforators (white dots) are shown. Other soft tissues were omitted from the Figure to clarify the course of the MSGA, the relevant branches and perforators.

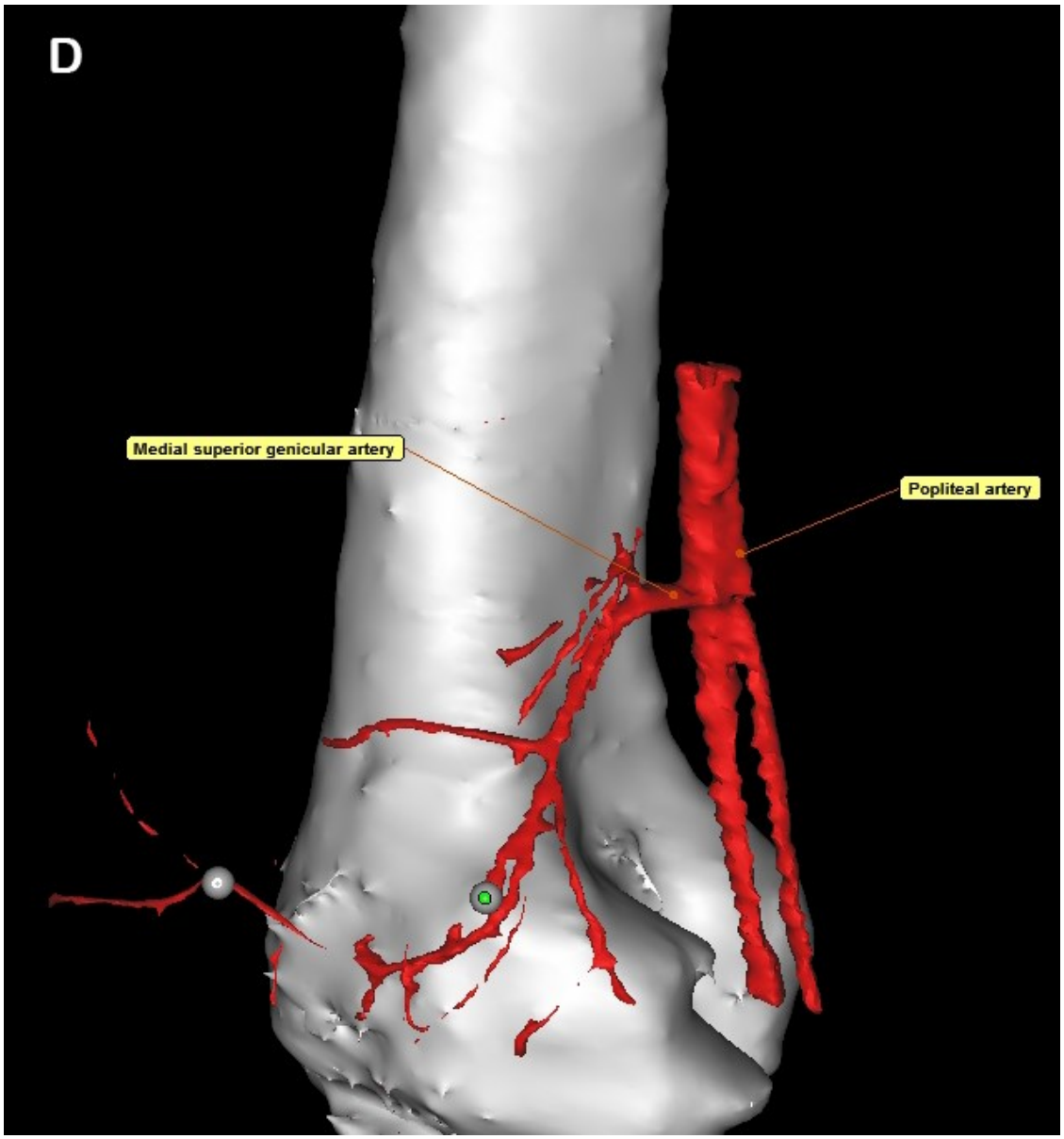

Figure 26D shows the posteromedial (PM*l*) view of a three-dimensional (3D) model of the medial superior genicular artery (MSGA) in the anteromedial (AM) and medial thigh sub-regions of the right thigh of a female cadaver injected with lead oxide and gelatin solution, and scanned using computed tomography (CT) scanner. The MSGA vascular territory and relevant perforators (white dots) are shown. Other soft tissues were omitted from the Figure to clarify the course of the MSGA, the relevant branches and perforators.

CHAPTER 6 DISCUSSION

6.1 Review of main findings

6.1.1 Consistent, clinically important perforators exist from all source vessels in the thigh region

The integument of the thigh region is supplied by mixture of perforators from nine vascular territories (D-IGA, SFA, PFA, MCFA, LCFA, PA, DGA, LSGA and MSGA) with 88 ± 16 (n=15) perforators perfusing an average thigh skin surface area of 1376 cm^2. These numbers are higher than what has been reported in previous studies[1-3,16] precisely because 3D spatial orientation of the thigh vasculature revealed more consistent perforators than studies utilizing 2D angiography and/or dissection, which often sacrificed, or were oblivious to other perforators in the region.

The study was performed on 15 thighs - 10 male and 5 female - obtained from 10 fresh human cadavers (5 male and 5 female). Though not a specific objective of this study, the analysis included a visual comparison of the vascular architecture of male and female samples. In this study no obvious differences were observed regarding the branching pattern, location of source vessels or angiosomes location between the male and female.

Two source vessels SFA and the PFA with an average of 44 perforators (n=15) account for 25% and 24% respectively of all perforators in the thigh region. A third source vessel the LCFA accounts for 13% of perforators in the region making PFA, SFA and the LCFA supplying an average total of 62% of perforators in the thigh (Figure 27).

With regard to area, the majority of the thigh integument is perfused by PFA, SFA and LCFA covering 27%, 26% and 20% respectively (Figure 28). The ratio of percent perforators to percent area perfused in the thigh is 1:0.9 (Table12).

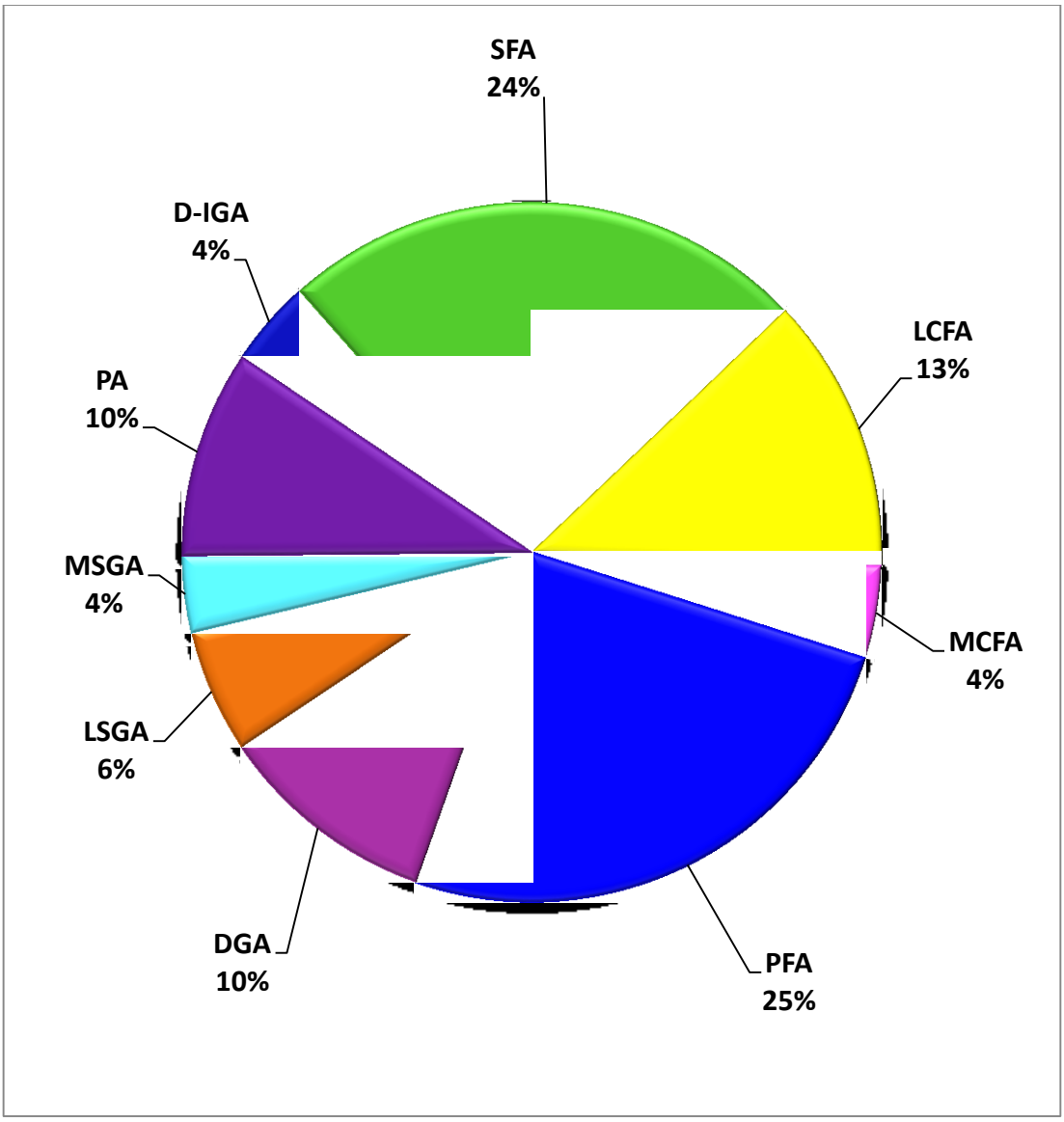

Figure 27: Composition of perforators in the thigh according to the source vessel (n=15). The descending genicular artery (DGA); descending branch of the inferior gluteal artery (D-IGA); lateral circumflex femoral artery (LCFA); lateral superior genicular artery (LSGA); medial circumflex femoral artery (MCFA); medial superior genicular artery (MSGA); popliteal artery (PA); profunda femoral artery (PFA); superficial femoral artery (SFA).

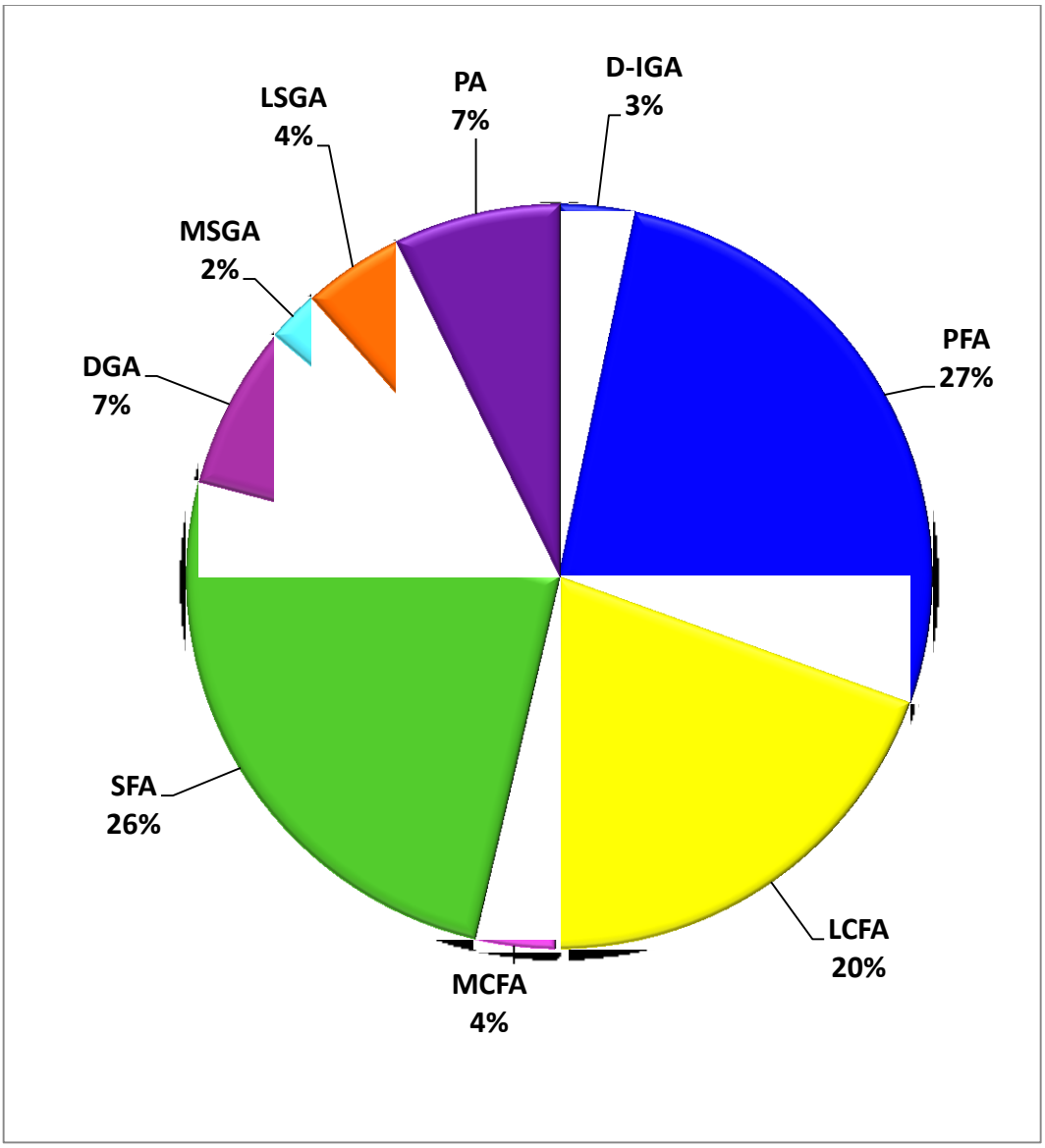

Figure 28: Area perfused by the various source vessels (cutaneous angiosomes area) in the thigh (n=15). The descending genicular artery (DGA); descending branch of the inferior gluteal artery (D-IGA); lateral circumflex femoral artery (LCFA); lateral superior genicular artery (LSGA); medial circumflex femoral artery (MCFA); medial superior genicular artery (MSGA); popliteal artery (PA); profunda femoral artery (PFA); superficial femoral artery (SFA).

Table 12: The ratio of percent perforators to percent area perfused in the thigh (n=15).

Source artery	Perforators % (P)	Perfused Surface area % (SA)	Ratio of (P:SA)
D-IGA	4	3	1:0.75
SFA	24	26	1:1.08
PFA	25	27	1:1.08
MCFA	4	4	1:1
LCFA	13	20	1:1.54
DGA	10	7	1:0.7
PA	10	7	1:0.7
LSGA	6	4	1:0.67
MSGA	4	2	1:0.5
Average		1:0.9	

The descending genicular artery (DGA); descending branch of the inferior gluteal artery (D-IGA); lateral circumflex femoral artery (LCFA); lateral superior genicular artery (LSGA); medial circumflex femoral artery (MCFA); medial superior genicular artery (MSGA); popliteal artery (PA); profunda femoral artery (PFA); superficial femoral artery (SFA).

6.1.2 Correlations between the number of perforators, perforator diameter, and angiosome cutaneous area

Having established a set of quantifiable characteristics, other pertinent characteristics were calculated in order to determine correlations between these characteristics. The quotient of the average cutaneous areas supplied by each angiosome and the number of associated perforators yields the average perforasome areas (Table 13). According to the calculated average perforasome area of all angiosomes (n=15), the LCFA (24.6 cm^2), PFA (17.9 cm^2) and SFA (17.5 cm^2) emerged with the largest perforasomes, providing perforators oriented with low enough distribution density to yield large sized perforasomes compared to other angiosomes with average area ranging from (10.3-13.6 cm^2). By plotting area perfused against the number of perforators on a line of best-fit scatter plot (Figure 29), a positive slope revealed a proportional relationship between the number of perforators and the perfused cutaneous angiosome area. The slope of this plot (19.54 cm^2) represents the average perforasome area.

The cumulative diameter was obtained as a product of the average number of perforator and average diameter (Table 13). By dividing each average cutaneous area of angiosomes by the cumulative diameters of the relevant perforators, average areas perfused per mm perforator diameter were obtained. According to the calculated average area perfused per mm perforator diameter of all source vessels (n=15), the LCFA (24.6 cm^2), SFA (21.9 cm^2), PFA (17.9 cm^2) and D-IGA (17.3 cm^2) emerged as supplying the largest areas per mm perforator diameter, by providing perforators oriented with low enough distribution density to yield large sized territories compared to other angiosomes with average area ranging from (12-15.2 cm^2). By plotting area perfused against the cumulative

diameter of perforators on a line of best-fit scatter plot (Figure 30), a positive slope revealed a proportional relationship between the cumulative diameter of perforators and the perfused cutaneous angiosome area. The slope of this plot (20.74 cm^2) represents the average area perfused per mm perforator diameter.

No correlations have been established regarding pedicle length and other measured or calculated characteristics, but discussion of the usefulness of the pedicle length regarding pedicled flaps is discussed in the next section. Overview of average pedicle length of the perforators of the thigh vascular territories is presented in Figure 31.

Table 13: Summary of measured and calculated quantitative data for the cutaneous vascular territories of the thigh region (n=15).

Angios-ome	Mean number of perforator (P)	Mean diameter (mm) (D)	Cumulative Diameter (PxD)	Mean Pedicle length (mm)	Mean Angiosome area (cm^2) (K)	Mean Perforat-some area (cm^2) (K/P)	Mean Area Perfused by cumulative diameter (K/(PxD))
D-IGA	3.3 ± 2.6	0.8 ± 0.3	2.6	116 ± 50	45 ± 37	13.6	17.3
SFA	20 ± 9	0.8 ± 0.3	16	69 ± 31	350 ± 137	17.5	21.9
PFA	21 ± 9	1 ± 0.5	21	120 ± 42	375 ± 81	17.9	17.9
MCAF	4 ± 2	1 ± 0.4	4	93 ± 38	48 ± 27	12	12
LCFA	11 ± 4	1 ± 0.7	11	99 ± 61	271 ± 76	24.6	24.6
DGA	8 ± 4	0.8 ± 0.2	6.4	76 ± 42	97 ± 38	12.1	15.2
PA	8 ± 3	1.0 ± 0.7	8	83 ± 33	99 ± 27	12.4	12.4
LSGA	5 ± 3	0.9 ± 0.3	4.5	66 ± 38	60 ± 29	12	13.3
MSGA	3 ± 2.5	0.7 ± 0.2	2.1	88 ± 46	31 ± 17	10.3	14.8

Abbreviation of angiosomes; the descending genicular artery (DGA); descending branch of the inferior gluteal artery (D-IGA); lateral circumflex femoral artery (LCFA); lateral superior genicular artery (LSGA); medial circumflex femoral artery (MCFA); medial superior genicular artery (MSGA); popliteal artery (PA); profunda femoral artery (PFA); superficial femoral artery (SFA).

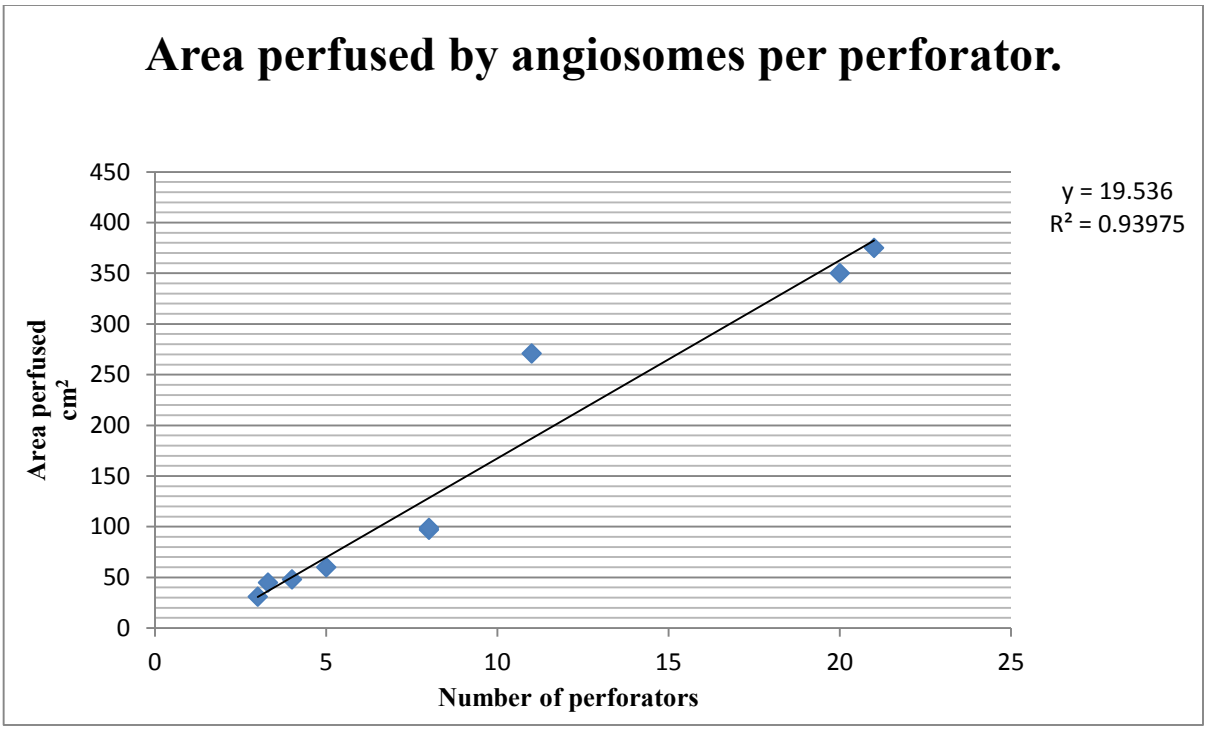

Figure 29: Relationship between the number of perforators and the perfused cutaneous angiosome area (n=15). The positive slope shows a proportional relationship between the number of perforators and the perfused cutaneous angiosome area. The slope value (19.54 cm2) represents the average perforasome area in the thigh region.

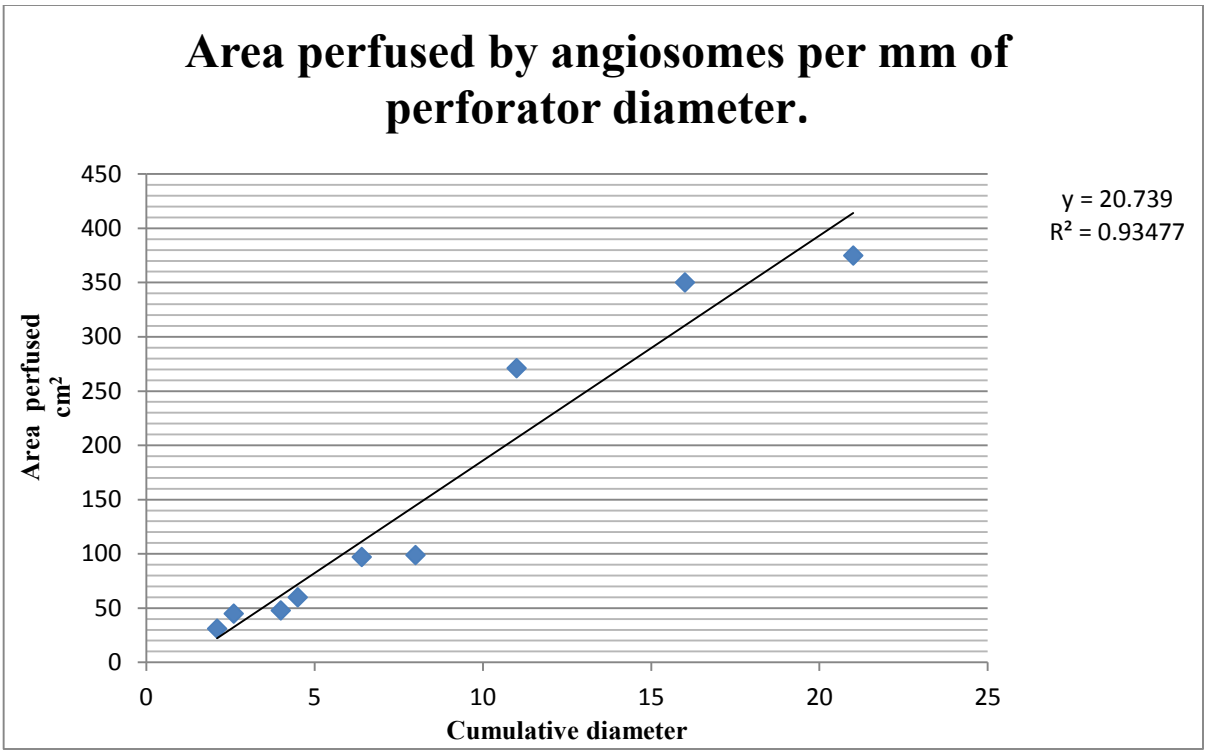

Figure 30: Relationship between the cumulative diameter of perforators and the perfused cutaneous angiosome area (n=15). The positive slope shows a proportional relationship between the cumulative diameter of perforators and the perfused cutaneous angiosome area. The slope value (20.74 cm2) represents the average area perfused per mm perforator diameter in the thigh region.

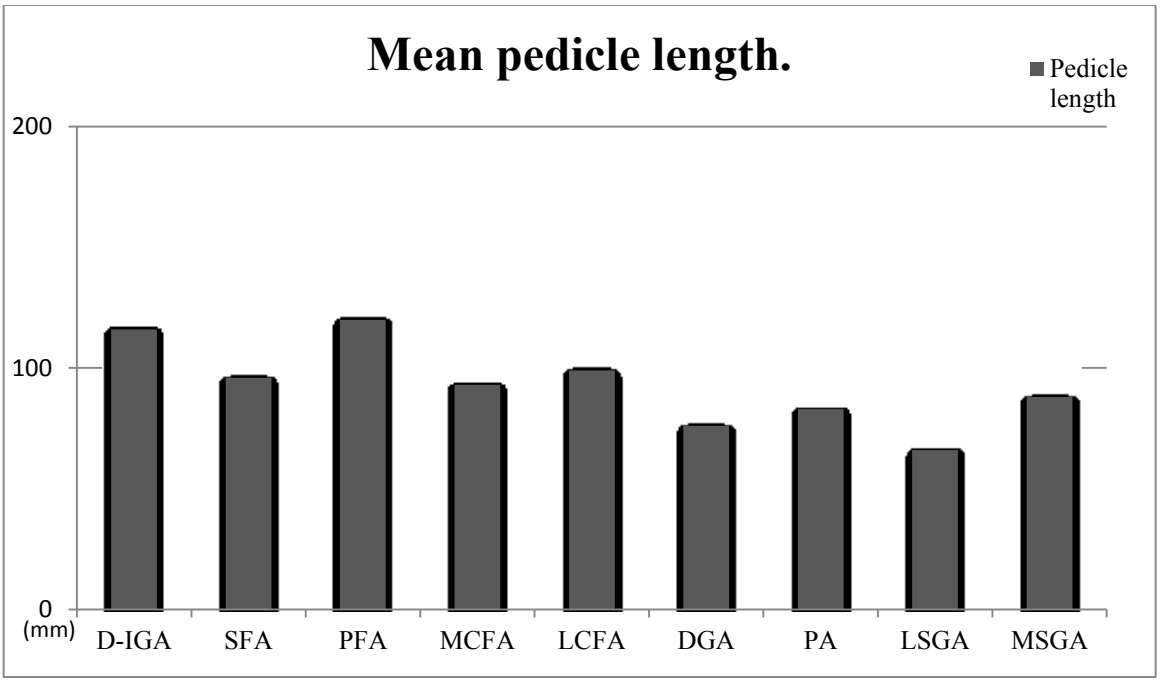

Figure 31: Mean pedicle length of the thigh perforators according to the source vessel (n=15). The descending genicular artery (DGA); descending branch of the inferior gluteal artery (D-IGA); lateral circumflex femoral artery (LCFA); lateral superior genicular artery (LSGA); medial circumflex femoral artery (MCFA); medial superior genicular artery (MSGA); popliteal artery (PA); profunda femoral artery (PFA); superficial femoral artery (SFA).

6.1.3 Predictions about the perforators' reliability, and facilitation of the safe design of perforator flaps in the thigh region

Reliability of perforator anatomy was established by certain quantifiable characteristics and establishing correlations that can be used in the prediction of flap selection and flap size. The purpose is to improve flap survival, attenuate the morbidity of the donor site. Virtual dissection has enabled the establishment of a correlation on the one hand, and the safe design of perforator flaps on the other.

The LCFA (24.6 cm^2), PFA (17.9 cm^2) and SFA (17.5 cm^2) are the largest perforasome (n=15), providing perforators oriented with low enough distribution density to yield large sized perforasome compared to other angiosomes with average area ranging from (10.3-13.6 cm^2). The LCFA (24.6 cm^2), SFA (21.9 cm^2), PFA (17.9 cm^2) and D-IGA (17.3 cm^2) supply the largest areas per mm perforator diameter, by providing perforators oriented with low enough distribution density to yield large sized territories compared to other angiosomes with average area ranging from (12-15.2 cm^2).

Cormack and Lamberty[170] argue that "for practical purposes, knowledge of the size of anatomical territories is of no value in determining the maximum dimensions of a flap". This statement is quite problematic given that studies by Taylor et al.[14] and Morris and Taylor[15] propose that the easy and safe harvest of the primary zone of a perforasome along with capturing the adjacent perforasome from the neighboring source vessels. This necessitates a comprehensive knowledge of perforator spatial architecture. However, Cormack and Lamberty agree that "the dimensions of anatomical areas of supply may have relevance in defining minimum dimensions for skin islands carried on muscles".[170]

Knowledge of pedicle length, the pre-eminent variable in pedicled flaps, enhances the versatility of flap positioning. The longest pedicle lengths of thigh perforators were found in proximal vascular territories.

6.1.4 Superiority of virtual dissection over physical dissection: simulation of safe flap design

Challenges encountered in physical dissection on fresh cadavers include difficulty of manipulation of the thigh region during the dissection. The cadavers often needed to be repositioned to expose different sub-region of the thigh. Other challenges encountered in physical dissection are the time and cadaver deterioration factors. The duration of cadaver usefulness is limited by the onset of deterioration, giving limited time for dissection and documentation of results. Post-dissection cremation of the cadavers makes it impossible to re-evaluate the results if and when needed. Magnification tools were also necessary for tedious dissection of perforators. In contrast, data accessibility gained by the ability of MIMICS to simulate separation and storage body parts while maintaining the spatial orientation in different files enables easy visualization, dissection and analysis of areas of interest.

Since knowledge of perforator anatomy of the thigh integument is fundamental to flap surgery, the present study has attempted to add to the current state of knowledge through a re-evaluation of the arterial anatomy of thigh region and the relevant flaps. MIMICS provides a precise 3D visualization of the arterial anatomy of certain flaps and has provided a clear determination of potential donor sites that have been neglected in the literature and clinical practice. The following is a discussion of the arterial anatomy and

simulated “safe” flap harvest of thigh perforator flaps (the prediction of the size and design of the simulated flaps were based on detailed understanding of the cutaneous vascular anatomy with implementation of safe design rules[14,15]), and observations regarding the anastomoses between the cutaneous territories of the thigh angiosomes in the five anatomical sub-regions: anteromedial (AM) thigh, anterolateral (AL) thigh and trochanteric, posterolateral (PL) thigh, posteromedian (PM*n*) thigh, and posteromedial (PM*l*) and medial thigh.

Anterior thigh

6.1.5 Anterolateral (AL) thigh sub-region

The AL thigh sub-region is roughly defined from the anterior midline to the posterior border of the iliotibial tract. The mid portion of the AL thigh sub-region has a history of providing reliable perforators originating from the inferior branch of the descending branch of the LCFA. Potential flaps in this sub-region are shown in Figure 32.

Observations from this study (n=15) confirmed that the overlying skin of the AL thigh is supplied by LCFA and LSGA, and also showed the sub-region to be mainly perfused by perforators from the ascending, descending and transverse branches of the LCFA. This study observed that the ascending LCFA constantly provides cutaneous perforators through the TFL muscle to supply the overlying skin. The mid portion of the AL thigh originating from the inferior branch of the descending branch of the LCFA is supplied mostly by musculocutaneous perforators. Perforators perfusing the proximal thigh were found to be predominantly musculocutaneous. Multiple and variant in diameter,

perforators from the LSGA anastomose with terminal territories of the descending LCFA to supply the distal third of the ALT.

The anterolateral thigh perforator flap

Although this flap has a highly variable arterial anatomy[83-92] regarding fine details such as perforator location and course, the main reliable pedicle of this flap comes from the LCFA. The majority of perforators supplying the area were musculocutaneous [76,78,82,93,89] with a higher incidence of septocutaneous to proximal areas.[80]

Observations from this study (n=15) showed that the 99 ± 61 mm tortuous muscular or musculoseptocutaneous course (as Lakhiani et al.[85] have described) of the potential perforator of this flap emerged close to the intramuscular septum. This unpredictable course may be responsible for the challenges in the harvest of this flap[89,90,92] distracting from the popularity of the ALT flap (Figure 32).[171] However, it is well known that this a very reliable flap donor site in experienced hands.[82]

The anterolateral thigh perforator flap: The bailout perforator artery

Unusual vascular anatomy may challenge flap elevation and risk damage to the vascular pedicle.[90] Recommendations for salvage include elevation of adjacent flaps such as AMT flap, TFL flap, contralateral thigh flap, or use of a *freestyle* technique.[83,104,89,91] The ability to produce chimeric flaps to reconstruct complicated composite resections [61,101,103,172,173] has popularized the use of the ALT.

In this study (n=15), the area supplied by the LCFA was assessed for consistency of proximal perforators that could be utilized to salvage the ALT flap if the main perforator was damaged or not present during the flap elevation. At least one perforator was found emerging at the area of interest in all samples, with an average of 2.9 ± 1.8 perforators per

thigh. Mean pedicle length was 111 ± 20 mm. Average diameter at deep fascia was 1.1 ± 0.3 mm. The vessel course of the perforator was mostly musculocutaneous (90%). Perforators from the ascending (25%), oblique branch (32%) or descending branch (43%) of the LCFA in all cases. The 'bail out branch' was most commonly supplied by the ascending branch of the LCFA, an oblique branch with origin in the transverse branch of the LCFA, or a descending branch with origin in the LCFA.

The TFL perforator flap

Clinical applications of the TFL flap have made slow progress, due to anatomic anomalies of the perforators to this donor site[72] and contradictory descriptions of the of the vascular anatomy of this flap. The anatomical descriptions of the vascular anatomy of this flap have been confusing. Earlier, Hill et al.,[105] and more recently, Lin et al.,[125] described the transverse branch of the LCFA as the source artery. Other publications[126,111] indicated that the ascending branch is the source vessel. This study however, observed that the ascending LCFA constantly provides cutaneous perforators through the TFL muscle to supply the overlying skin (Figure 32).

The LSGA perforator flap

Observations from this study (n=15) showed that the distal third of the AL sub-region is supplied by multiple perforators with variant diameters that emerge from the LSGA and anastomose with terminal cutaneous territories of the descending LCFA. This part of the present study was geared towards the confirmation of the current knowledge of the vascular anatomy of this flap. Laitung's[127] cadaveric study of the anatomy of the lower PL thigh flap showed the blood supply to this flap to be provided by perforators from either the PA or the LSGA. With regard to Laitung's documentation of the use of LSGA

perforators to design lower PL thigh flaps, this study (n=15) observed the location of the LSGA perforators to persist within the distal third of the AL thigh, and ascending to anastomose proximally with the LCFA. The study also observed that the lower PL thigh is perfused by the PA, and more often by perforators from the fourth branch of the PFA.

As an added advantage to the proximal ascent of the cutaneous territories of the LSGA perforators, the design of flaps based on these perforators can be extended to include the anastomosed distal territory of the descending branch of the LCFA. Curiously, this donor site with reliable perforators of suitable diameter has been infrequently used in reconstruction of soft-tissue defects around the knee, or for free flaps, despite the excellent aesthetic outcomes.

Observations regarding the cutaneous territories and their orientation that could facilitate flap design in this sub-region

All the cutaneous territories of the LCFA three branches have a lateral orientation, and anastomose with each other within the proximal two-thirds of this sub-region. Laterally, the cutaneous territory of the LCFA anastomoses with the cutaneous territory of the PFA, and distally, with the cutaneous territories of the LSGA. The LSGA cutaneous territory is oriented superoanteriorly, and anastomoses with the cutaneous territory of the DGA over the anterior midline of the thigh.

The cutaneous territory of the medial descending branch of the LCFA anastomoses with the cutaneous territory of the CFA superiorly, with the cutaneous territory of the SFA in the middle and with the cutaneous territory of the DGA, inferiorly.

6.1.6 Anteromedial (AM) thigh sub-region

The AM thigh sub-region is roughly defined from the anterior midline of the thigh to the midline of gracilis muscle. The arterial anatomy of the overlying skin of the AM thigh comprises several vascular territories from different source vessels. Potential flaps in this sub-region are shown in Figure 33.

Observations from this study showed the sub-region to be mainly perfused by the SFA. Musculocutaneous perforators from the SFA, and less frequently from CFA, in the proximal areas, provide 55% of the blood supplied to the integument overlying the proximal two thirds of this sub-region while 45% was supplied by septocutaneous perforators. These perforators have relatively long superficial pedicle lengths (69 ± 31 mm); their cutaneous territories are oriented inferiorly to their point of emergence from the deep fascia. The distal third of this sub-region is supplied mainly by perforators from the musculoarticular branch of the DGA with a few contributing perforators from the MSGA.

The Anteromedial thigh flap or superficial femoral perforator flap

This study observed that musculocutaneous perforators are the main blood supply if the flap is designed within the borders of the proximal AM thigh. When the flap design proceeds towards the different boundaries of this sub-region, however, there is a likelihood of different source vessels providing perforators:

1. If the flap design proceeds laterally toward the anterior midline of the thigh then there is the probability of the incidence of septocutaneous perforators from the medial branch of the LCFA, because the area over the midline is perfused by LCFA vascular territory and hence would be a different flap (described by Song et al.).[70]

2. If the flap design proceeds medially toward the mid line of the gracilis muscle, the incidence of septocutaneous perforators from the SFA (inferiorly) or musculocutaneous perforators from the MCFA (superiorly) is likely.
3. If the flap design proceeds proximally, the incidence of short perforators from the CFA is likely.

These findings correspond with the documentation of back up musculocutaneous perforators[70] through the gracilis and sartorius muscles and the revision of the vascular anatomy to this flap,[132] which revealed that the main perforators are large cutaneous arteries branching off a muscular branch of the SFA supplying the sartorius and gracilis muscles. Initial arterial anatomic knowledge of this flap had described the pedicle as a septocutaneous perforator of an innominate[70] or the medial[136] branch of the descending LCFA. This point of view has persisted even until recently,[135] when it was recognized that the main perforator for this flap (AMT) was septocutaneous and could be identified at the medial border of the rectus femoris with the sartorius muscles intersection.

The medial superior genicular artery perforator flap

Observations from this study showed that the distal third of the AM thigh sub-region is supplied mainly by perforators from the musculoarticular branch of the DGA with a few contributing perforators from the MSGA, the smallest vascular territory in the thigh. Surprisingly, no perforator flaps based on the musculoarticular branch of the DGA perforators have been documented in the literature, a fact that may be attributed to the challenging course of the perforators which makes dissection through muscle, and flap harvesting difficult, However those few MSGA perforators documented in the literature in 1990 are suitable to base flaps on, and have been used to cover knee defects in flap

surgery.[137] This flap has not been studied or utilized extensively, possibly due to the reluctance of surgeons in clinical practice to harvest flaps which cross articular areas or which are based on small inconsistent perforators.

Observations that could facilitate flap design in this sub-region regarding the cutaneous territories and their orientation

The SFA cutaneous territory anastomoses superiorly with the cutaneous territories of the CFA, and superomedially, with MCFA territories. Posterior to the posterior border of the mid portion of the gracilis muscle, the SFA cutaneous territory anastomoses with the cutaneous territory of the third branch of the PFA. Inferiorly, the cutaneous territory of the SFA anastomose with the cutaneous territory of the DGA, which anastomoses anteriorly with the cutaneous territory of the medial branch of the descending LCFA and the cutaneous territory of the LSGA over the mid line of the thigh. Inferiorly the cutaneous territory of the DGA anastomoses with the cutaneous territory of the MSGA, posteriorly with both the cutaneous territories of the third PFA and inferior to the DGA-PFA anastomosis, with the cutaneous territory of the PA.

Posterior thigh

The posterior thigh sub-region is defined from the posterior border of the iliotibial tract to the midline of the gracilis muscle. This study (n=15) confirmed earlier findings that the PFA supplies the majority of the posterior thigh muscles and overlying skin. However, the current descriptions of the perforators of the PFA are based on clinical landmarks of discrete perforators. These descriptions do not provide a clear picture of the arterial anatomy of the perforators used for flap elevation. It was observed in this study that

becomes problematic to simply reference the perforators as first lateral, first medial, second lateral, second medial or third lateral. A thorough anatomical description of this vessel's branches, the relevant perforator orientations and the perfused areas are missing from the current literature.

Many confusing descriptive terms have been used to name posterior thigh flaps as a result of the complexity of the regional anatomy.[2] This complexity can be attributed to the presence of the different branches of the PFA and their variable branching patterns. This study however, confirmed the presence of perforators with large diameters and suitable pedicle lengths for vascular anastomoses from this source vessel in the posterior thigh sub-region, making it an attractive area for flap surgery.

Prior to this study, the most comprehensive description of the anatomical landmarks used to facilitate flap dissection of the lateral PFA perforators in the PL thigh was by Ahmadzadeh et al.[2] who proposed an approach to locate the PFA perforator arteries along an oblique line extending from the ischium to the lateral femoral condyle. Further anatomical and clinical investigations to locate and better understand the PFA anatomy within the posterior thigh have been carried out.[166,165]

The findings from the posterior thigh region demonstrate that the use of this 3D angiography technique and digital modeling and analysis are superior to dissection, and enable accurate tracing of musculocutaneous perforators to their source vessels, which had been challenging using dissection. In this discussion, the PFA perforators have been grouped according to their source branch and the supplied areas: first, second, third and fourth branches. Despite the variations in the branching pattern and the number of

perforators provided, the cutaneous vascular territories of the PFA were constant for all 15 samples.

6.1.7 Posterolateral (PL) thigh sub-region

The clinical uses of PFA perforators within the PL thigh have been documented in the literature; Maruyama et al.[161] reported the use of the "first perforator" of the PFA. Ramirez et al.[160] documented a flap based on a perforator from the "first deep femoral perforating vessel". Baek[69] and Song et al.[70] designed free flaps from this sub-region based on what they called the "third perforator" of the PFA. The use of the terminal fourth branch of the PFA for lower limb reconstruction has also been documented.[162]

Observations from this study (n=15) confirmed that the PL thigh is completely supplied by perforators of the PFA (Figure 34). Well defined, large diameter septocutaneous perforators from the first branch of the PFA supply the proximal third of this sub-region. Within the middle third of the PL thigh sub-region, perforators from the second branch of the PFA were frequently observed. The distal third of this sub-region was perfused by perforators from the fourth branch of the PFA. Regarding the documentation of Baek[69] and Song et al.[70] of the use of perforators of the third branch of the PFA to design free flaps, this study observed the location of the fourth branch of PFA perforators to persist within the distal third of the PL thigh, and the perforators documented actually originated from the fourth branch of the PFA.

Observations regarding the cutaneous territories and their orientation that could facilitate flap design in this sub-region

While the cutaneous territories of the first, second and fourth lateral branches of the PFA anastomose with each other, the cutaneous territories of the perforators of the first and second branches have transverse major lateral and minor medial orientations. The perforators of the first and second branches anastomose with the cutaneous territory of the LCFA laterally. All the lateral anastomosis of the cutaneous territory of the PFA and LCFA branches are over the iliotibial tract. Medially, the cutaneous territory of the first branch of the PFA anastomoses with the cutaneous territory of the D-IGA, while the cutaneous territory of the second and third branches of the PFA anastomose with each other. The cutaneous territory of the fourth branch anastomoses with the cutaneous territory of the LSGA laterally, and with the cutaneous territory of the PA medially.

6.1.8 Posteromedian (PM*n*) thigh sub-region

Flaps from the proximal and middle portions of this sub-region have been variously named. The area below the gluteal fold is known for providing flaps based on the PFA or the D-IGA; terms such as gluteal flap, inferior gluteal musculocutaneous[157] posterior thigh flap musculocutaneous flap[167,155] and more recently, profunda femoral perforator flap (PAP)[164] have been used to describe these flaps. The middle portion of this sub-region has been reliable for flap harvest based on the PFA; Angrigiani et al.[163] described what they called the "adductor flap" elevated on a musculocutaneous perforator from the "first medial branch" of the PFA. The distal third of this sub-region has no great clinical history; Maruyama and Iwahira described a technique using a popliteo-posterior thigh fasciocutaneous island flap to repair skin defects around the knee.[167] The first, second and

fourth branches of PFA are oriented laterally unlike the third branch that is oriented medially. Potential flaps in this sub-region are shown in Figure 35.

Observations from this study confirmed that the blood supply of the integument overlying the proximal third of PM*n* sub-region is provided by perforators of the D-IGA with contributions from the perforators of the third branch PFA below the gluteal fold. The area below the gluteal crease therefore provides reliable perforators for flap surgery from both the D-IGA and PFA, leaving the resulting donor site scar hidden in the gluteal fold. The middle third of the PM*n* sub-region is supplied completely by perforators of the third branch of the PFA, clarifying that the origin of the perforator of the adductor flap[163] is the third branch of PFA. Large diameter perforators of the PA, emerging and ascending from the popliteal fossa within the distal PM*n* sub-region, anastomose with the PFA septocutaneous perforators to supply the distal third of the PM*n* sub-region. These PA perforators are suitable for basing potential new free perforator flaps.

Observations regarding the cutaneous territories and their orientation that could facilitate flap design in this sub-region

Continuing from the lower buttock, the cutaneous territory of the D-IGA, at the area below the gluteal crease, anastomoses laterally with the cutaneous territory of the first branch of the PFA, and medially, with the cutaneous territory of the MCFA. As the cutaneous territory of the third branch of the PFA perfuses the majority of the middle of the sub-region, it anastomoses laterally with the cutaneous territory of the second branch of the PFA, superomedially with the cutaneous territory of the MCFA and medially and infero-medially with the cutaneous territory of the SFA.

The superiorly oriented cutaneous territory of the ascending perforators of the PA, anastomose laterally with the cutaneous territory of the fourth branch of the PFA. Superiorly, it anastomoses with the third branch of the PFA, superomedially with the cutaneous territory of the SFA and infero-medially, with the cutaneous territory of the DGA.

6.1.9 Posteromedial (PM*l*) and medial thigh sub-regions

Observations from this study indicate that the blood supply to this area is provided by the MCFA, SFA, PFA, DGA and PA. The superior areas of the PM*l* and medial thigh sub-regions are supplied by musculocutaneous perforators from the MCFA and the third branch of the PFA through the gracilis and adductor magnus muscles respectively. Within the middle third of the PM*l* and medial thigh sub-regions, septocutaneous perforators, and less frequently, musculocutaneous perforators from the SFA, with contributions of perforators from the third branch of the PFA supply the overlying skin. Perforators from the third branch of the PFA, and from the PA, supply the skin over the distal PM*l* thigh. Perforators with long pedicle length from the DGA are the main supply to cutaneous tissues of the distal portion of the medial thigh. Potential flaps in this sub-region are shown in Figure 36.

MCFA perforator flap or gracilis muscle perforator flap in the medial thigh

This flap has been widely known as dependent on a musculocutaneous perforator since it was initially utilized by Orticochea,[144] and McCraw et al.[147] In 1987, Wang et al. elevated this flap on a septocutaneous perforators.[146] More recently, Hallock used a musculocutaneous perforator to redesign this flap for femoral triangle wound closure.[152]

This study (n=15) observed the MCFA perforators to be predominantly musculocutaneous through the superior portion gracilis muscle. When the flap design proceeds towards the different boundaries of this sub-region, however, there is a likelihood of different source vessels providing perforators:

1. If the flap design proceeds anteriorly beyond the anterior border of the gracilis then there is the probability of the incidence of perforators from the SFA.
2. If the flap design proceeds posteriorly beyond the posterior border of the gracilis muscle, the incidence of perforators from the third branch of PFA is likely.
3. If the flap design proceeds distally, the incidence of perforators from a muscular branch of the SFA is likely.
4. Continuing from the perineum, the cutaneous territories of the internal pudendal artery supply the area over the upper medial boundary of the thigh. If the design of the MCFA perforator flap proceeds proximally or superoposteriorly, then the incidence of perforators from the internal pudendal artery (Singapore flap)[174] is likely.

The DGA; the saphenous artery (Acland) perforator flap in the distal medial thigh

The study confirmed the advantages of using the medial area of the knee as a potential donor site, which include: limited subcutaneous fat, a consistent perforator and distinct sensory nerve supply.

Observations regarding the cutaneous territories and their orientation that could facilitate flap design in this sub-region

Knowledge of the arterial anatomy of the gracilis muscle is key to understanding the cutaneous arterial anatomy of the medial thigh. The skin overlying the proximal, mid

and distal portions of the gracilis muscle is completely supplied by perforators of the MCFA, SFA and DGA, respectively.

The cutaneous territories of musculocutaneous perforators from the MCFA (through the gracilis muscle) and of the third branch of the PFA (through adductor magnus) are all oriented transversely, and anastomose to supply the skin in the superior area of the PM*l* thigh.

The cutaneous territories of musculocutaneous perforators through the gracilis muscle of the MCFA, and septocutaneous perforators of the SFA, both with a posteroinferior orientation, anastomose and supply the middle portion of the PM*l* and medial thigh. Over the distal PM*l* thigh, the cutaneous territories of the DGA and PA anastomose with each other.

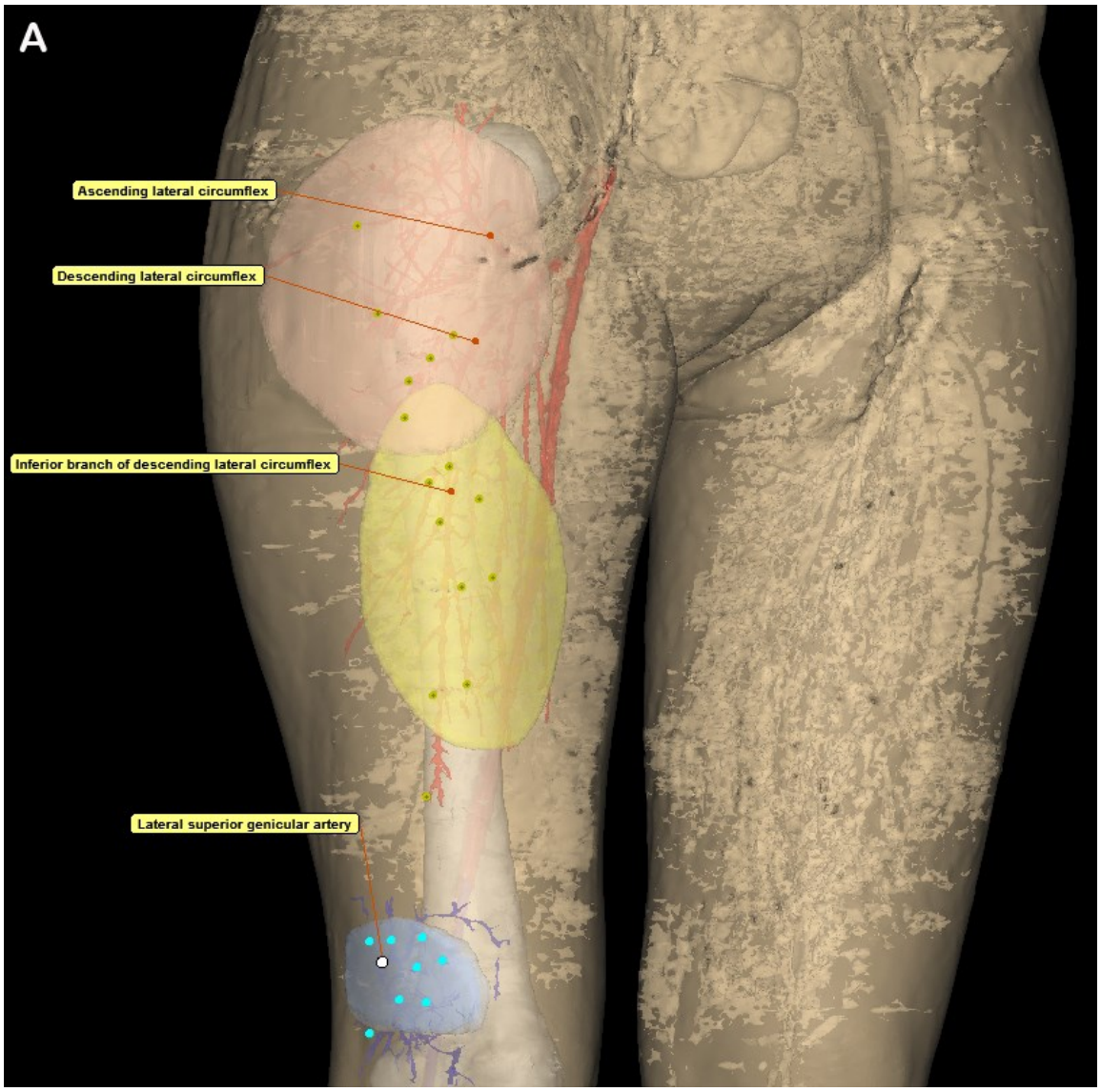

Figure 32 (A-E): Three-dimensional (3D) reconstructions of potential flaps in the anterolateral (AL) thigh sub-region. Figure 32A: the Figure shows three perforator flaps, reconstructed within the anterolateral (AL) thigh sub-region. The peach color flap is a tensor fascia lata (TFL) flap designed on a perforator of the ascending branch of the lateral circumflex femoral artery (LCFA). Other potential perforators from this source vessel are indicated with yellow-green dots .The yellow flap is an anterolateral thigh flap (ALT) designed on a perforator of the inferior branch of the descending LCFA. Other potential perforators from this source vessel are indicated with yellow-green dots. Note the perforators located within the intersection of the TFL and ALT flaps, of the transverse branch of the LCFA, can be used as bail out perforators for the ALT flap. The light blue flap is a lateral superior genicular artery (LSGA) perforator flap designed on a perforator of the LSGA. Other potential perforators from the LSGA are indicated with light blue dots.

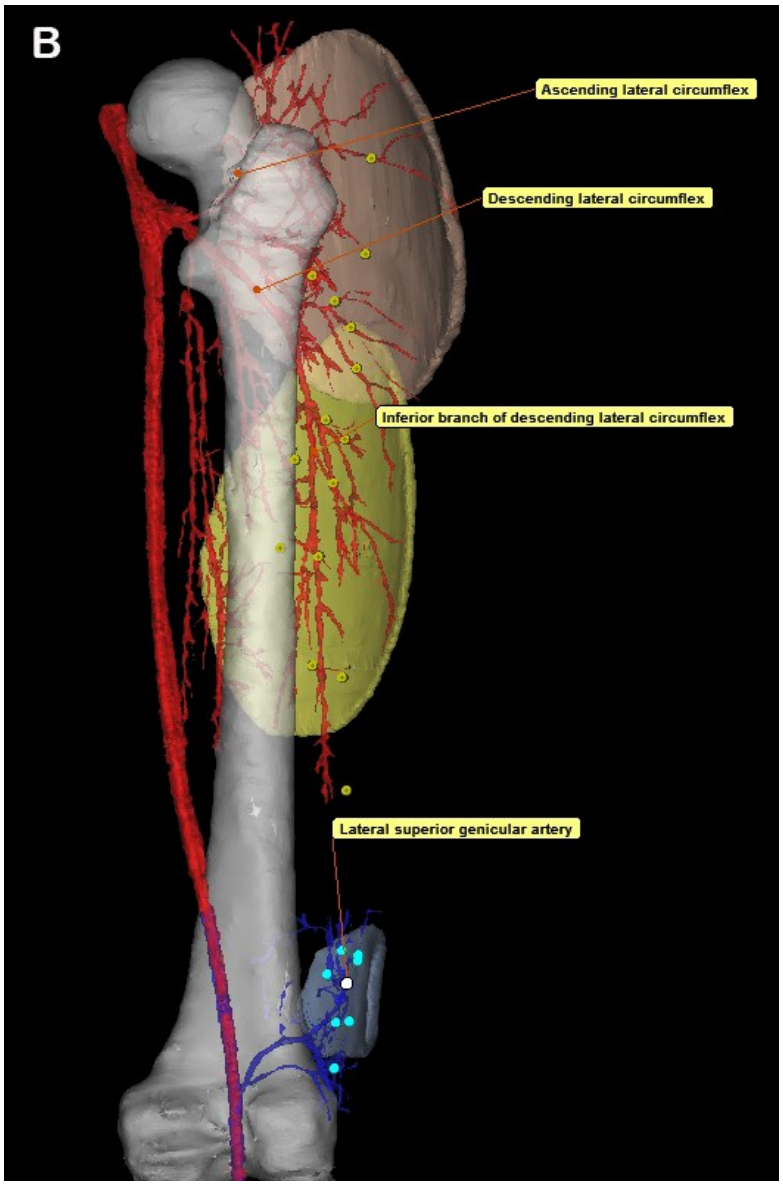

Figure 32B: the Figure shows three perforator flaps, reconstructed within the anterolatral (AL) thigh sub-region. The peach color flap is a tensor fascia lata (TFL) flap designed on a perforator of the ascending branch of the lateral circumflex femoral artery (LCFA). Other potential perforators from this source vessel are indicated with yellow-green dots .The yellow flap is an anterolateral thigh flap (ALT) designed on a perforator of the inferior branch of the descending LCFA. Other potential perforators from this source vessel are indicated with yellow-green dots. Note the perforators located within the intersection of the TFL and ALT flaps, of the transverse branch of the LCFA, can be used as bail out perforators for the ALT flap. The light blue flap is a lateral superior genicular artery (LSGA) perforator flap designed on a perforator of the LSGA. Other potential perforators from the LSGA are indicated with light blue dots.

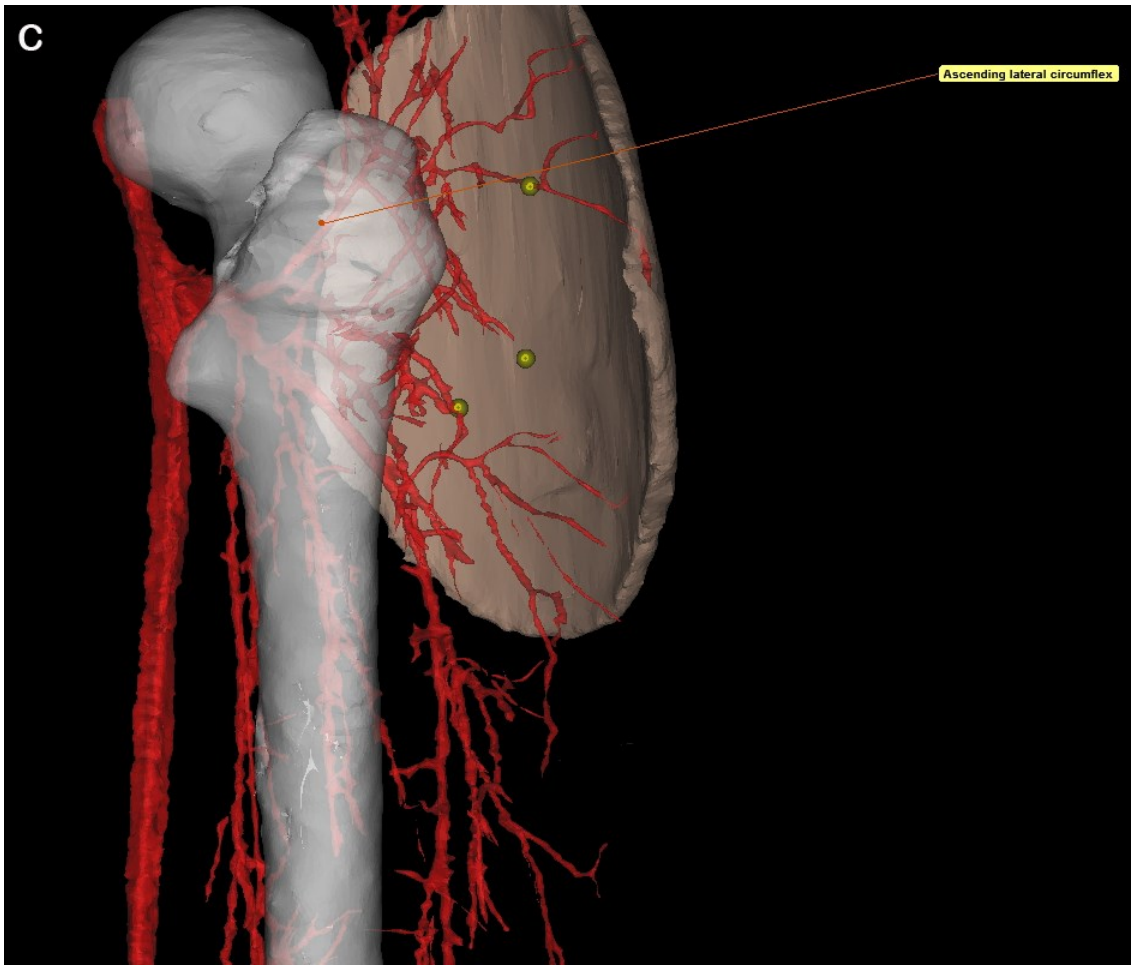

Figure 32C: the Figure shows a tensor fascia lata (TFL) perforator flap, reconstructed within the anterolateral (AL) thigh sub-region. This TFL flap is designed on a perforator of the ascending branch of the lateral circumflex femoral artery (LCFA). Other potential perforators from this source vessel are indicated with yellow-green dots.

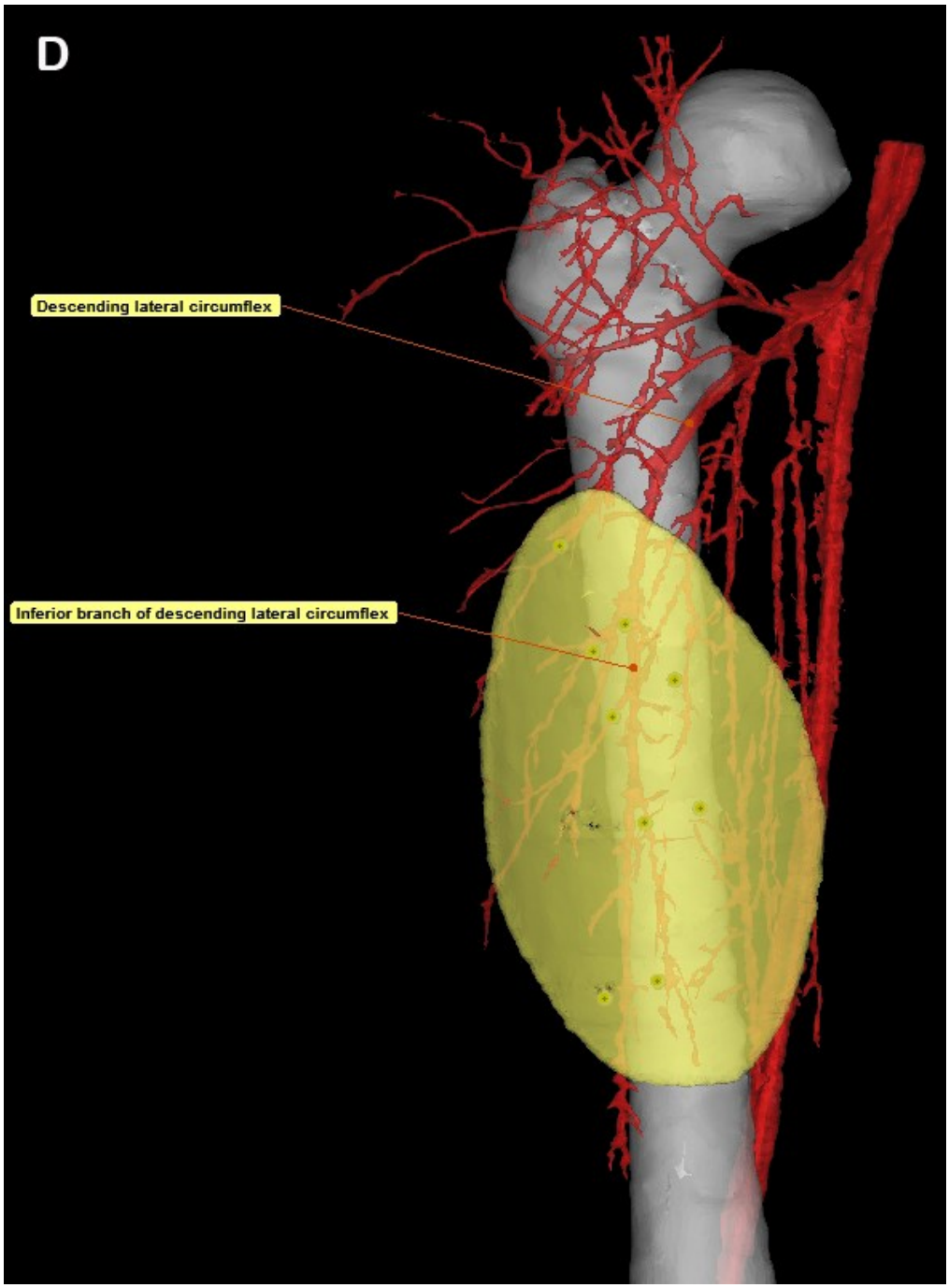

Figure 32D: the Figure shows an anterolatral thigh flap (ALT), reconstructed within the anterolateral (AL) thigh sub-region. This ALT flap is designed on a perforator of the inferior branch of the descending lateral circumflex femoral artery (LCFA). Other potential perforators from this source vessel are indicated with yellow-green dots.

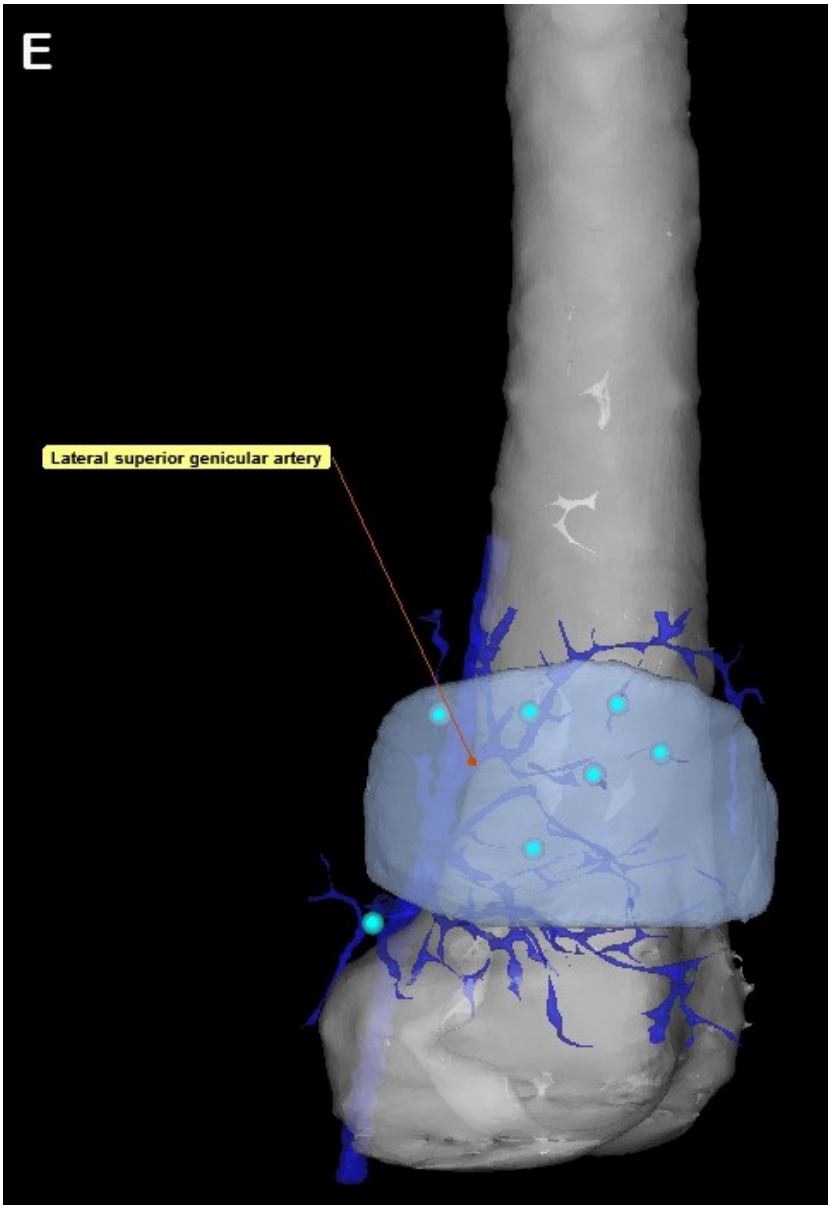

Figure 32E: the Figure shows a lateral superior genicular artery (LSGA) perforator flap, recostructed within the anterolatral (AL) thigh sub-region. This LSGA perforator flap is designed on a perforator of the LSGA. Other potential perforators from the LSGA are indicated with light blue dots.

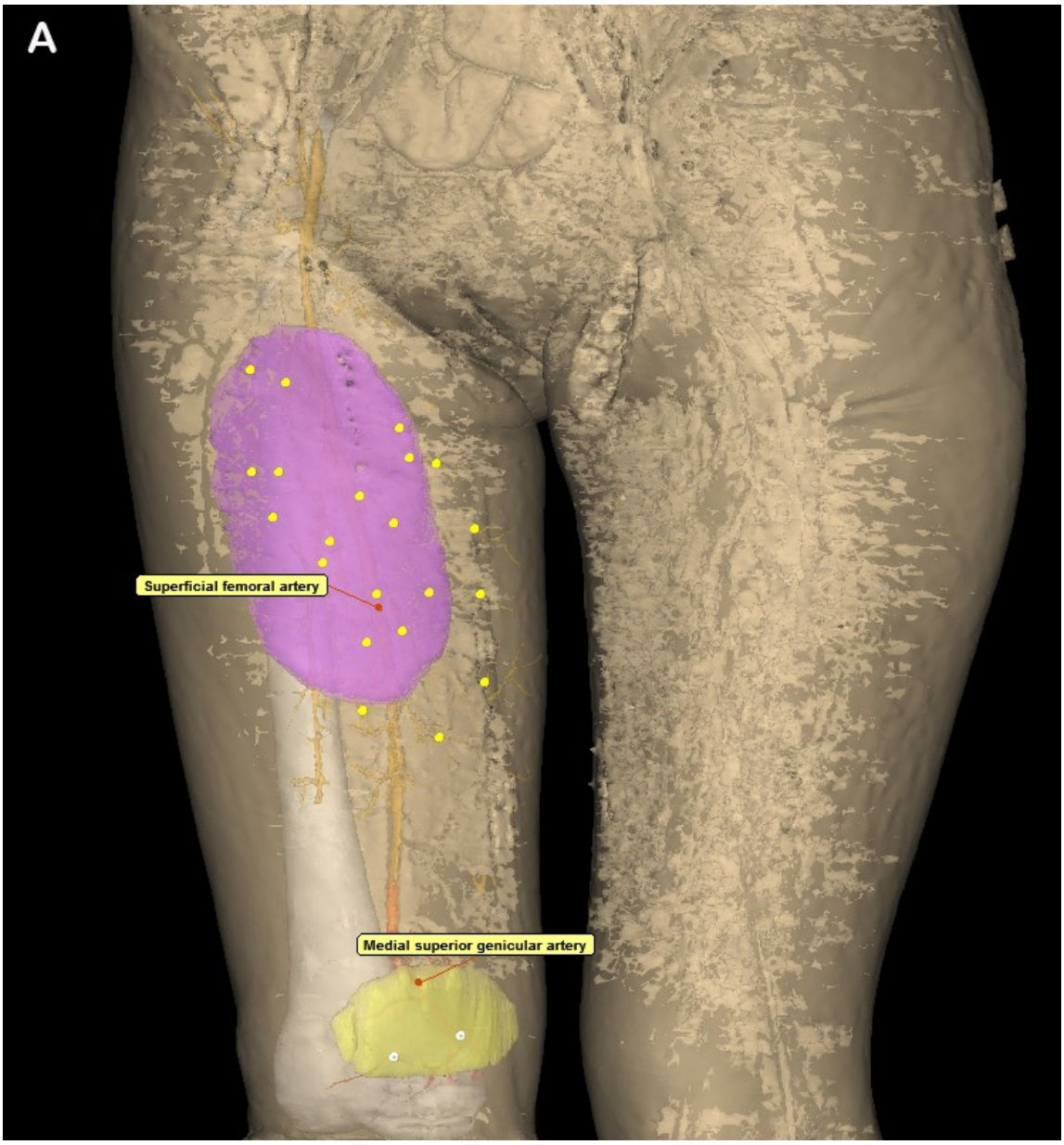

Figure 33 (A-E): Three-dimensional (3D) reconstructions of potential flaps in the anteromedial (AM) thigh sub-region. Figure 33A: the Figure shows two perforator flaps, reconstructed within the anteromedial (AM) thigh sub-region. The purple color flap is an anteromedial thigh flap (AMT) - or superficial femoral artery (SFA) perforator flap - designed on a musculocutaneous perforator of the SFA. Other potential perforators from the SFA are indicated with yellow dotes. The yellow color flap is a medial superior genicular artery (MSGA) perforator flap designed on a perforator of the MSGA. Other potential perforators from the MSGA are indicated with grey dots.

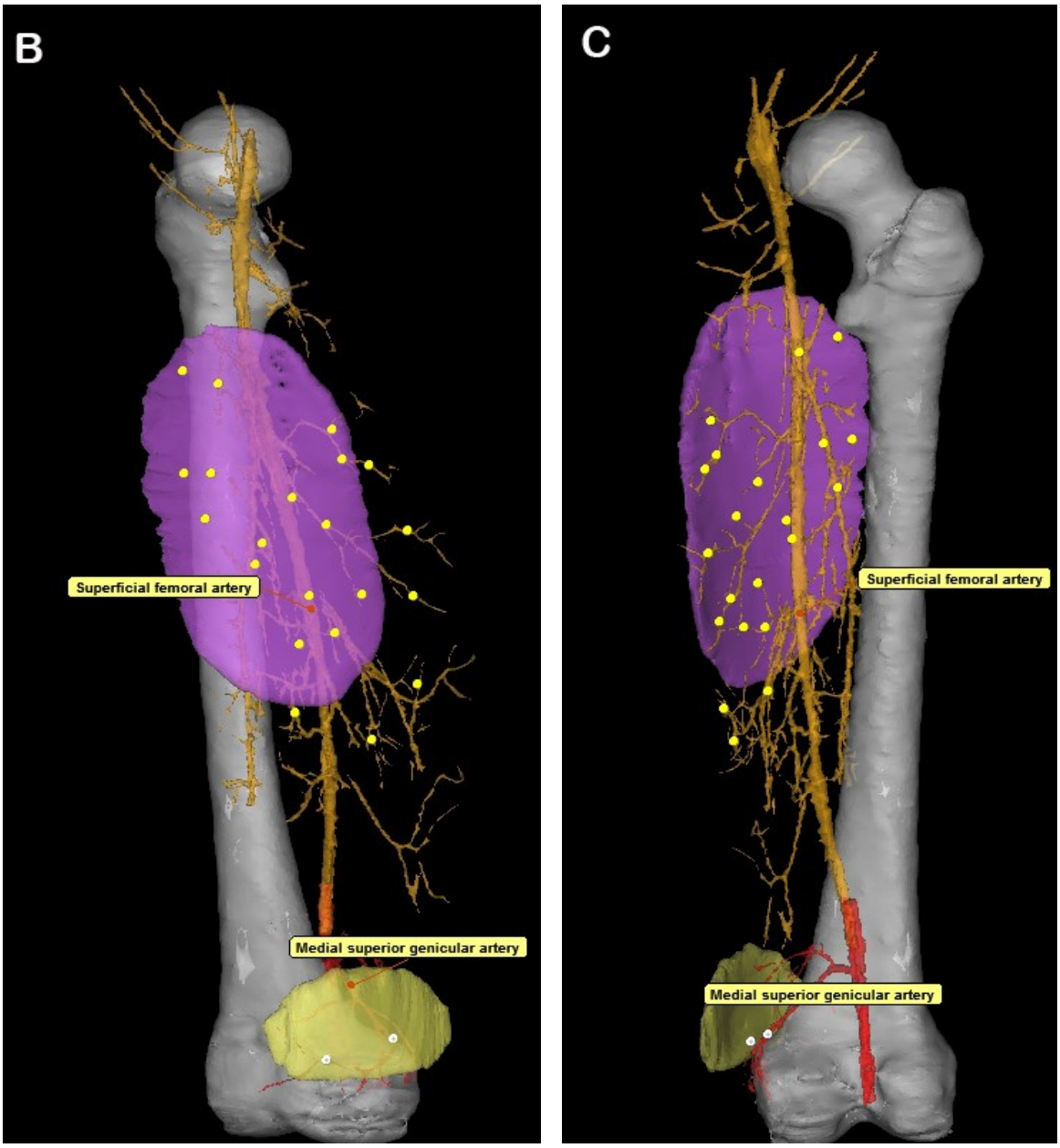

Figures 33B and 33C: the Figures show two perforator flaps, reconstructed within the anteromedial (AM) thigh sub-region. The purple color flap is an anteromedial thigh flap (AMT) - or superficial femoral artery (SFA) perforator flap - designed on a musculocutaneous perforator of the SFA. Other potential perforators from the SFA are indicated with yellow dotes. The yellow color flap is a medial superior genicular artery (MSGA) perforator flap designed on a perforator of the MSGA. Other potential perforators of the MSGA are indicated with grey dots.

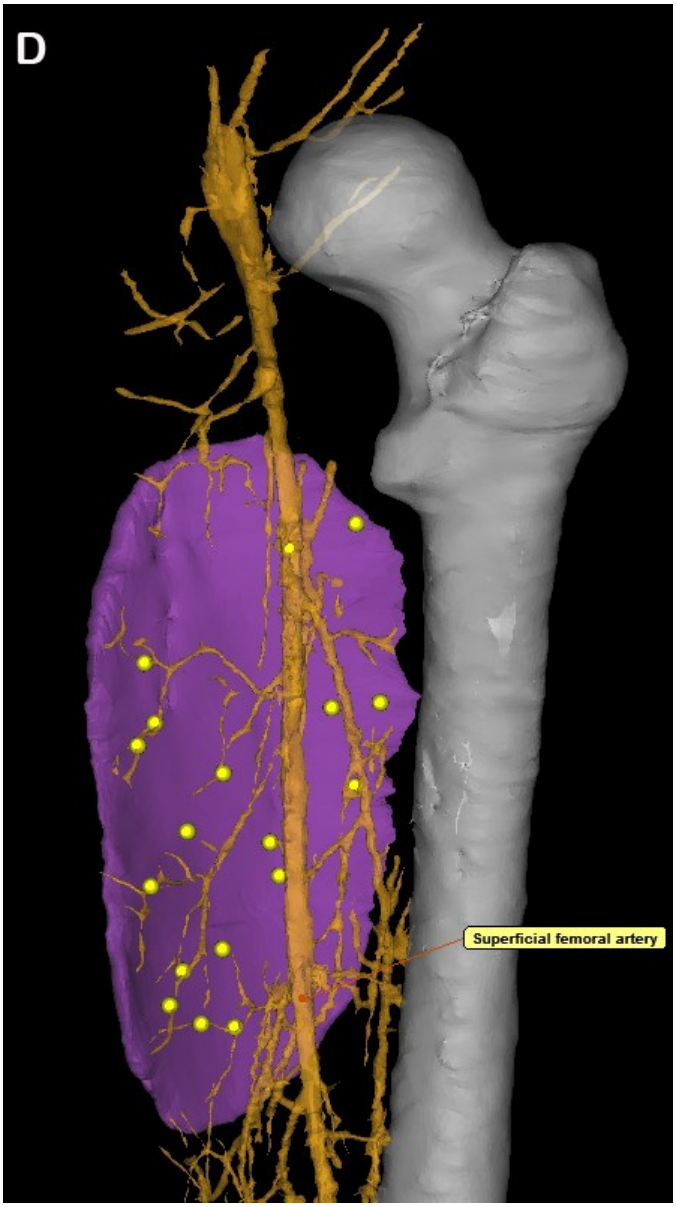

Figure 33D: the Figure shows an anteromedial thigh flap (AMT), or superficial femoral artery (SFA) flap, reconstructed within the anteromedial (AM) thigh sub-region. This flap is designed on a musculocutaneous perforator of the SFA. Other potential perforators from the SFA are indicated with yellow dotes.

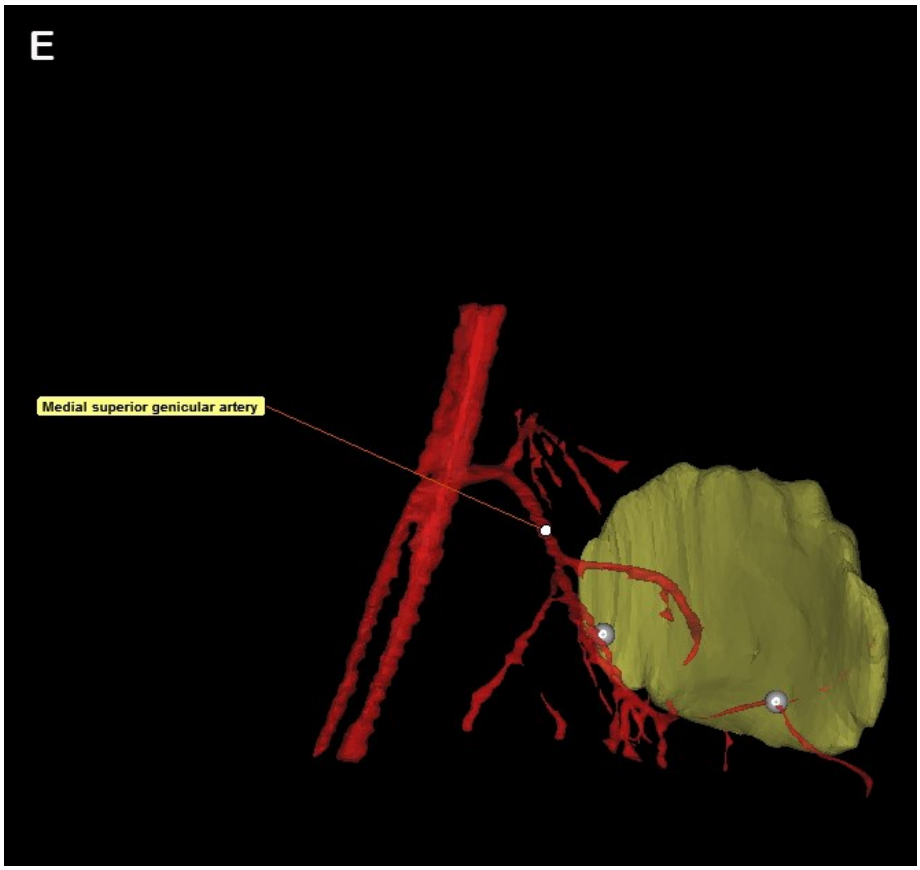

Figure 33E: the Figure shows a medial superior genicular artery (MSGA) perforator flap, reconstructed within the anteromedial (AM) thigh sub-region. This flap is designed on a perforator of the MSGA. Other potential perforators from the MSGA are indicated with grey dots.

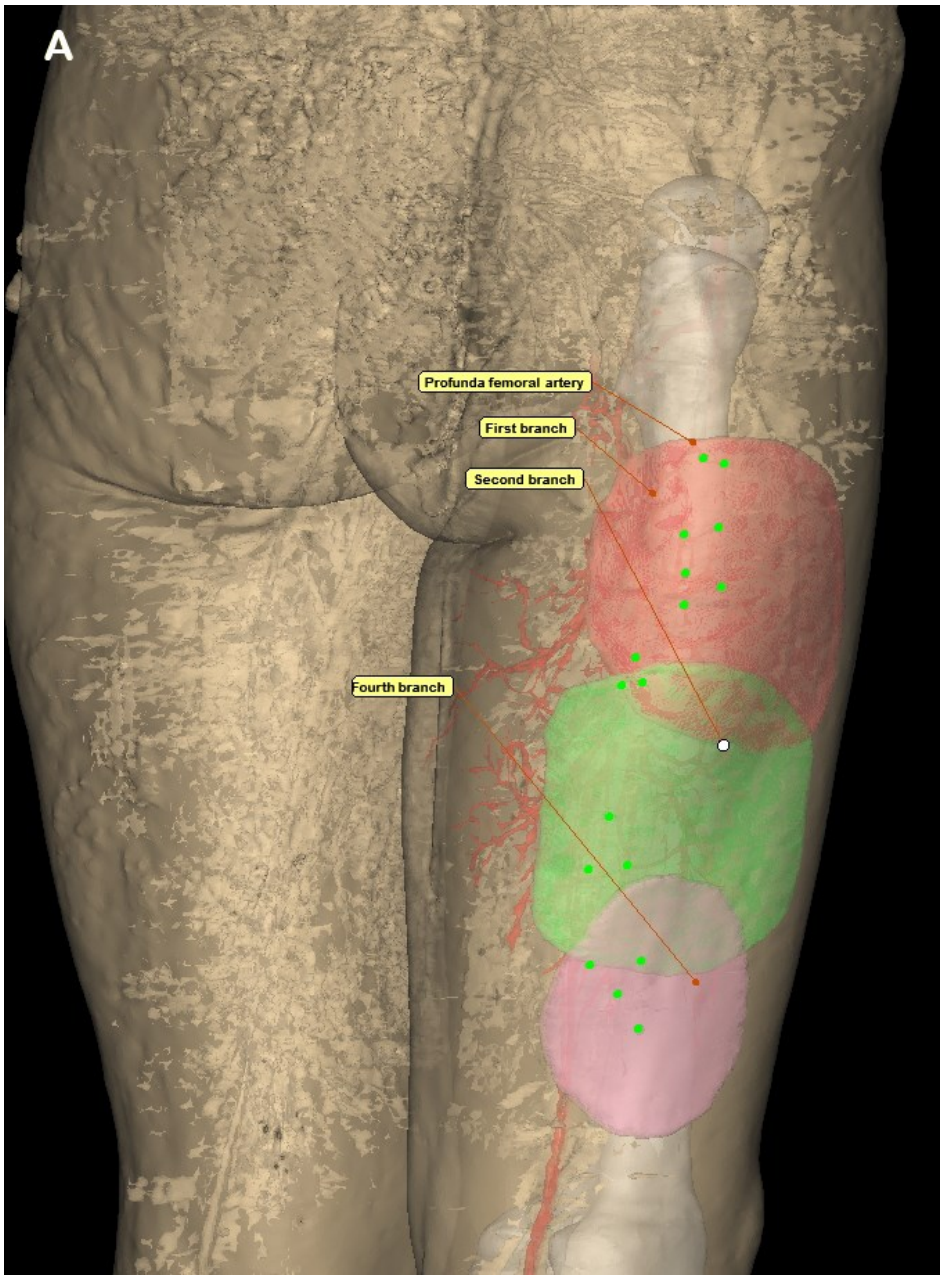

Figure 34 (A-D): Three-dimensional (3D) reconstructions of potential flaps in the posterolateral (PL) thigh sub-region. Figure 34A: the Figure shows three perforator flaps, designed within the posterolateral (PL) thigh sub-region. The red color flap is a fasciocutaneous PL flap designed on a perforator of the the first branch of the profunda femoral artery (PFA). The green color flap is a fasciocutaneous PL flap designed on a perforator of the second branch of the PFA. The pink flap is a fasciocutaneous PL flap based on a perforator from the fourth terminal branch of PFA. Other lateral potential perforators of the PFA are indicated with green dots.

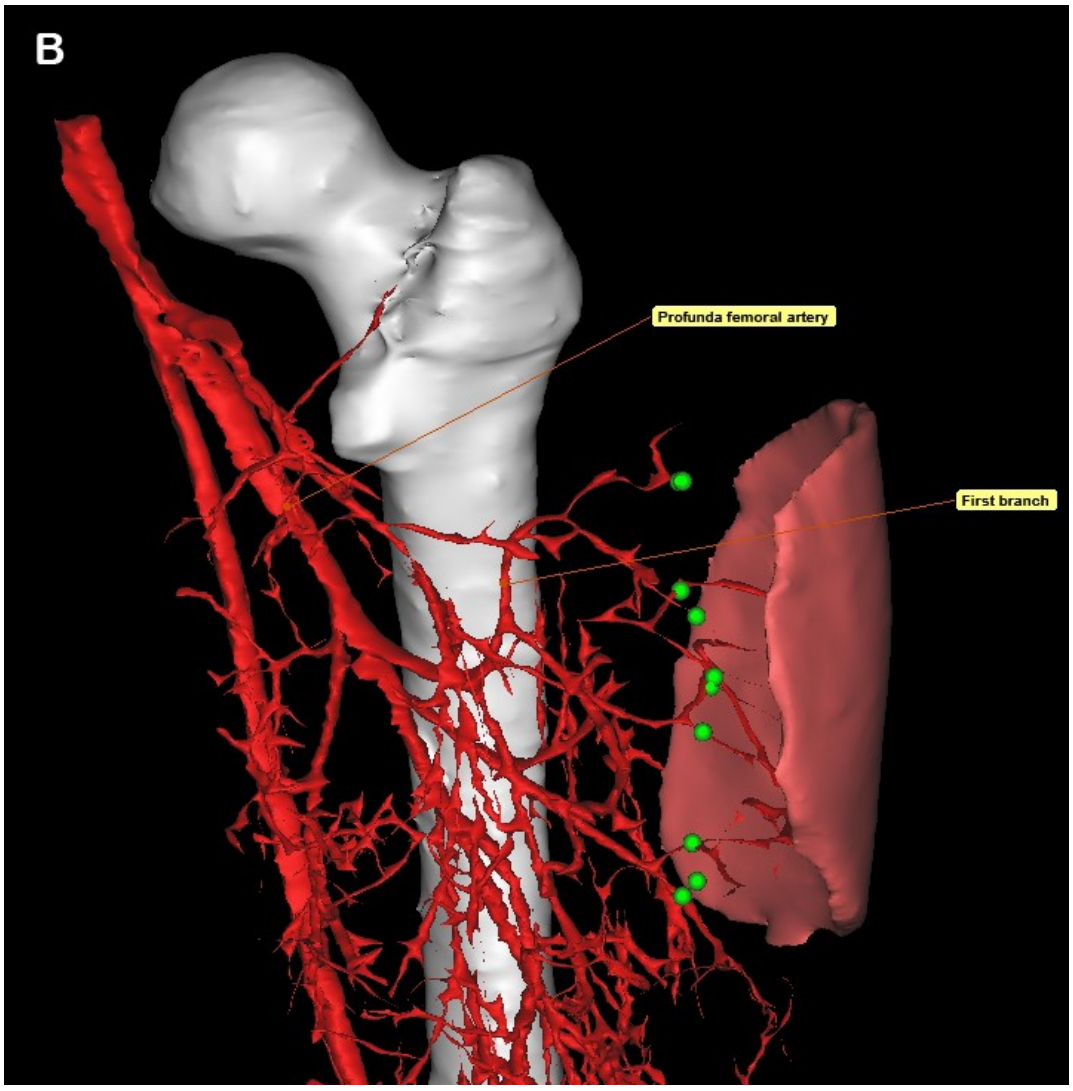

Figure 34B: the Figure shows a fasciocutaneous posterolateral (PL) flap designed on a perforator of the first branch of the profunda femoral artery (PFA) within the PL thigh sub-region. Other lateral potential perforators of the PFA are indicated with green dots.

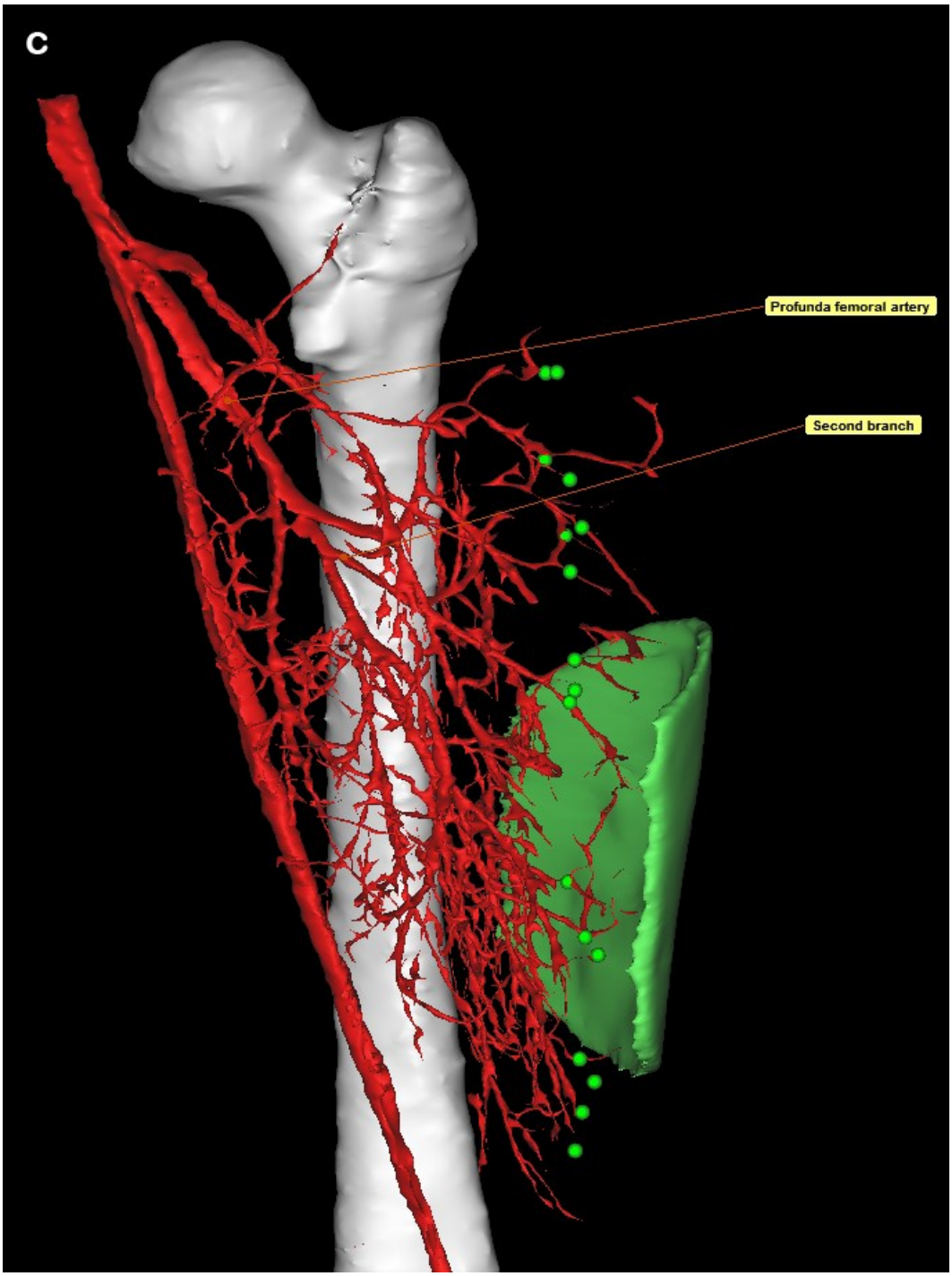

Figure 34C: the Figure shows a fasciocutaneous posterolateral (PL) flap designed on a perforator of the second branch of the profunda femoral artery (PFA) within the PL thigh sub-region. Other lateral potential perforators of the PFA are indicated with green dots.

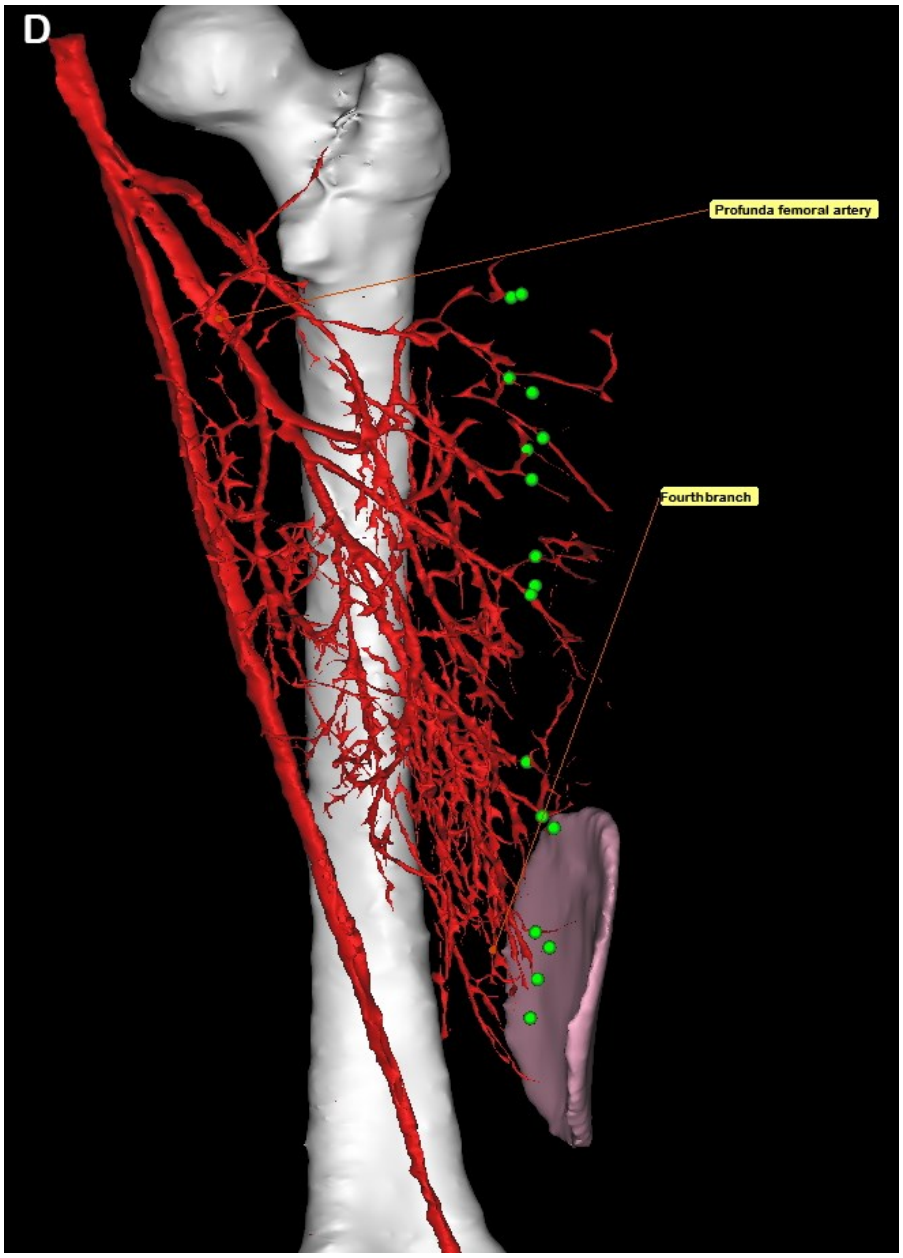

Figure 34D: the Figure shows a fasciocutaneous posterolateral (PL) flap designed on a perforator of the fourth branch of the profunda femoral artery (PFA) within the PL thigh sub-region. Other lateral potential perforators of the PFA are indicated with green dots.

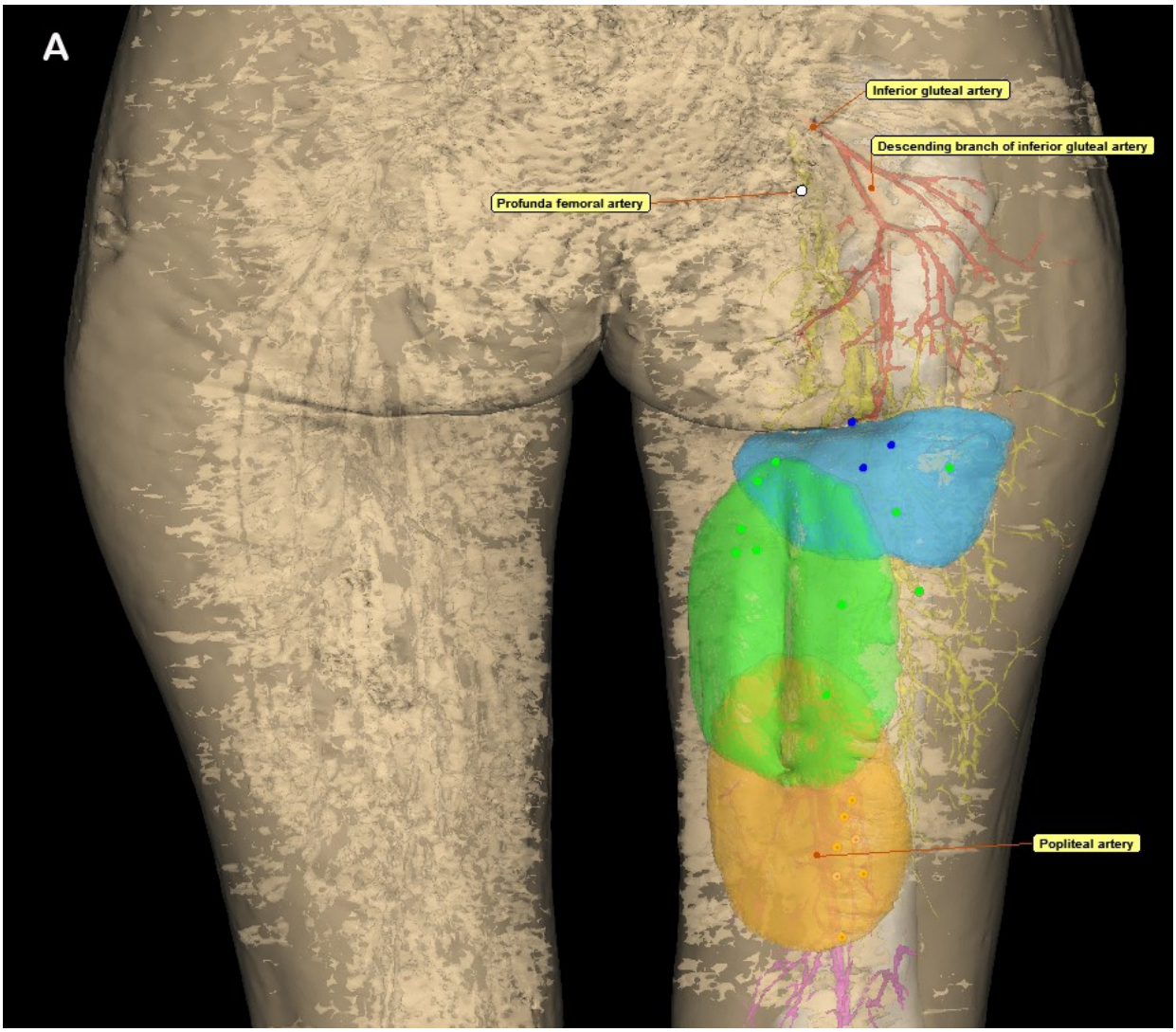

Figure 35 (A-F): Three-dimensional (3D) reconstructions of potential flaps in the posteromedian (PM*n)* thigh sub-region. Figure 35A: the Figure posteriorly views the thigh region. The blue flap is designed below the gluteal fold on two possible arterial supplies, the descending branch of the inferior gluteal artery (D-IGA) and profunda femoral artery (PFA). Potential perforators of the D-IGA and PFA to this flap are indicated with dark blue and green dots respectively. The green flap is designed on a perforator of the third branch of the PFA (known as the adductor flap). Other potential perforators from the PFA to this flap are indicated with green dots. The orange flap over the popliteal fossa is designed on two possible arterial supplies, the PFA and the popliteal artery (PA).

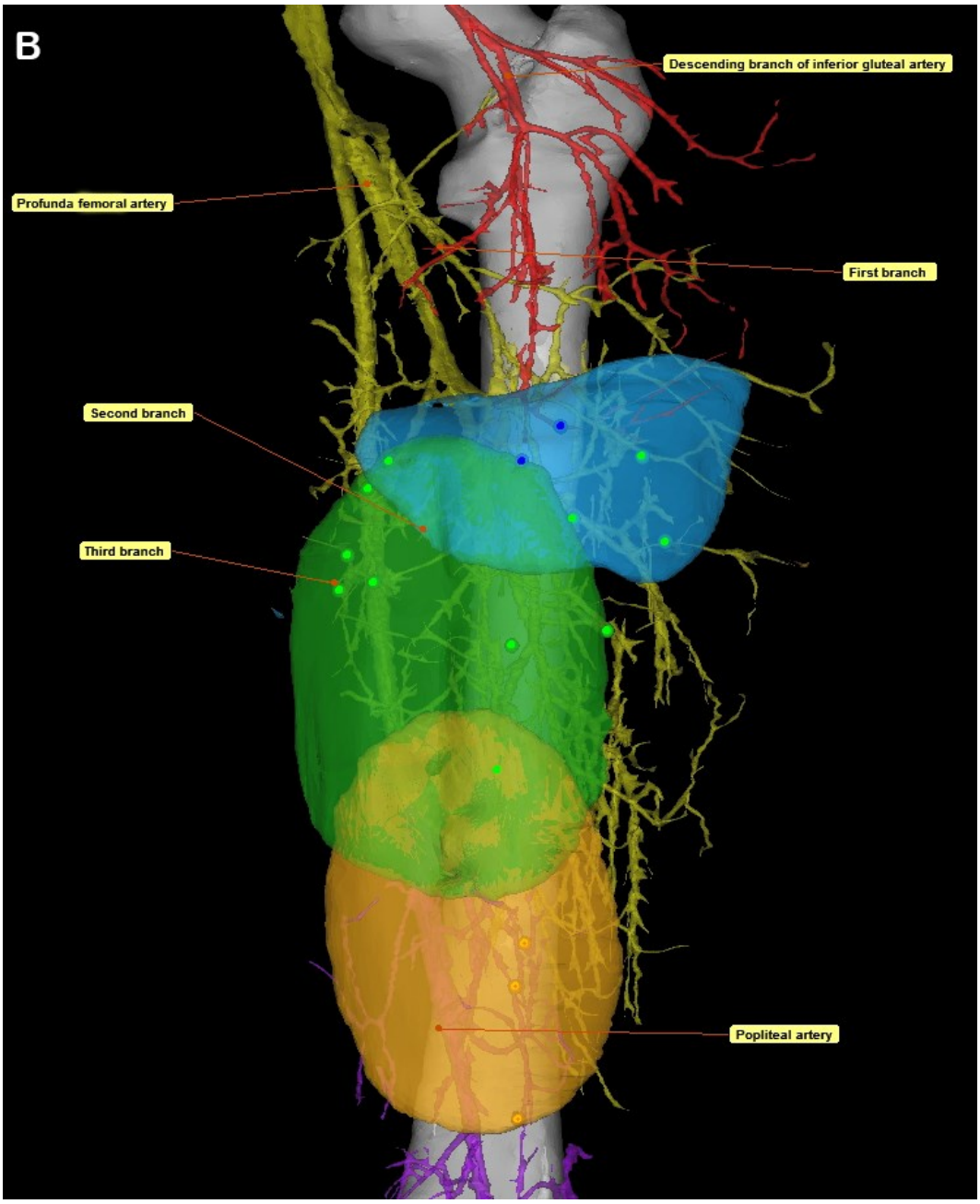

Figure 35B: posterior view of the posteromedian (PM*n*) thigh. The blue flap is designed below the gluteal fold on two possible arterial supplies, the descending branch of the inferior gluteal artery (D-IGA) and profunda femoral artery (PFA). Potential perforators of the D-IGA and PFA to this flap are indicated with dark blue and green dots respectively. The green flap is designed on a perforator of the third branch of the PFA (known as the adductor flap). Other potential perforators from the PFA to this flap are indicated with green dots. The orange flap over the popliteal fossa is designed on two possible arterial supplies, the PFA and the popliteal artery (PA).

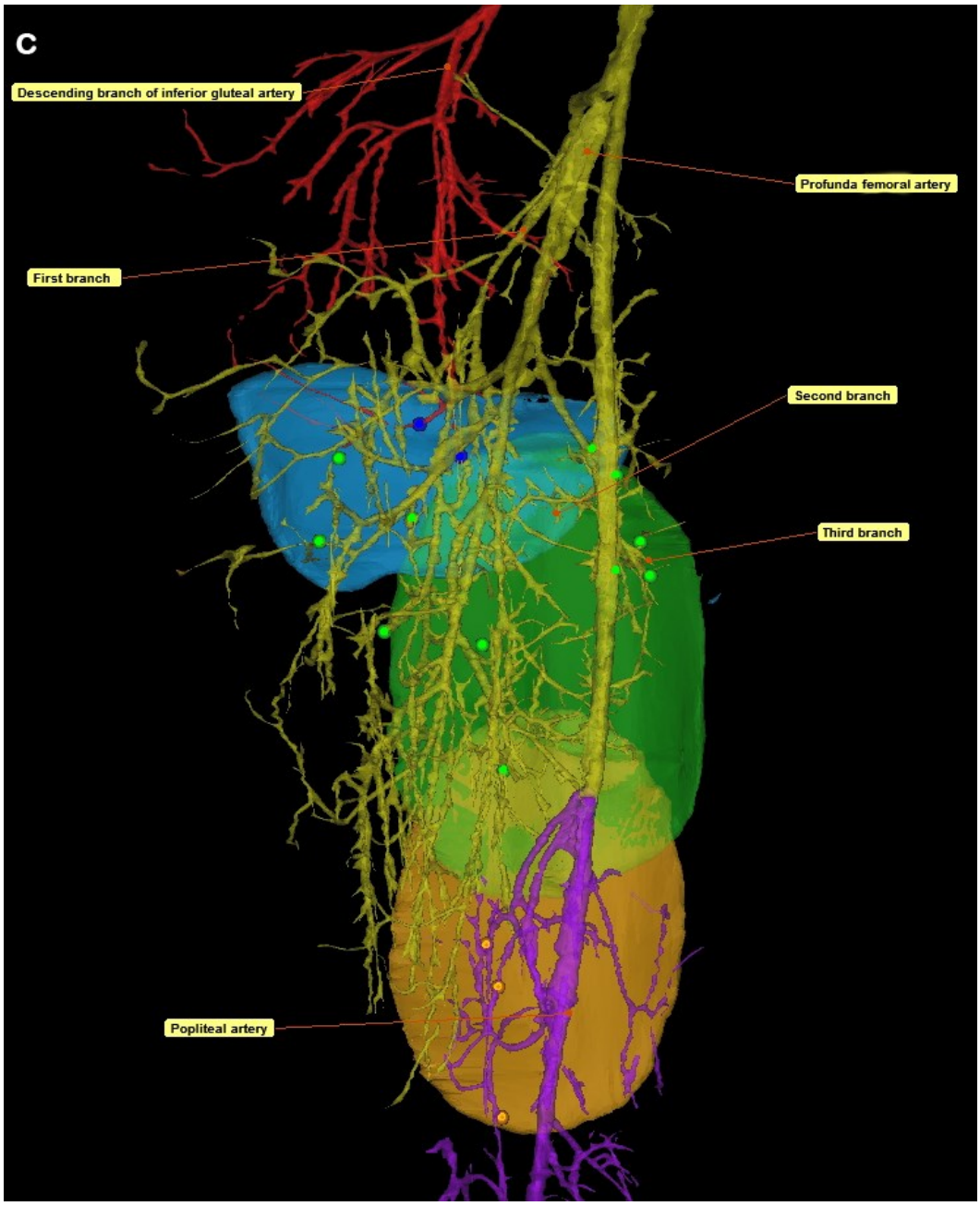

Figure 35C: anterior view of the thigh shows the underlying anatomy of the posteromedian (PM*n*) flaps. The blue flap is designed below the gluteal fold on two possible arterial supplies, the descending branch of the inferior gluteal artery (D-IGA) and profunda femoral artery (PFA). Potential perforators of the D-IGA and PFA to this flap are indicated with dark blue and green dots respectively. The green flap is designed on a perforator of the third branch of the PFA (known as the adductor flap). Other potential perforators from the PFA to this flap are indicated with green dots. The orange flap over the popliteal fossa is designed on two possible arterial supplies, the PFA and the popliteal artery (PA).

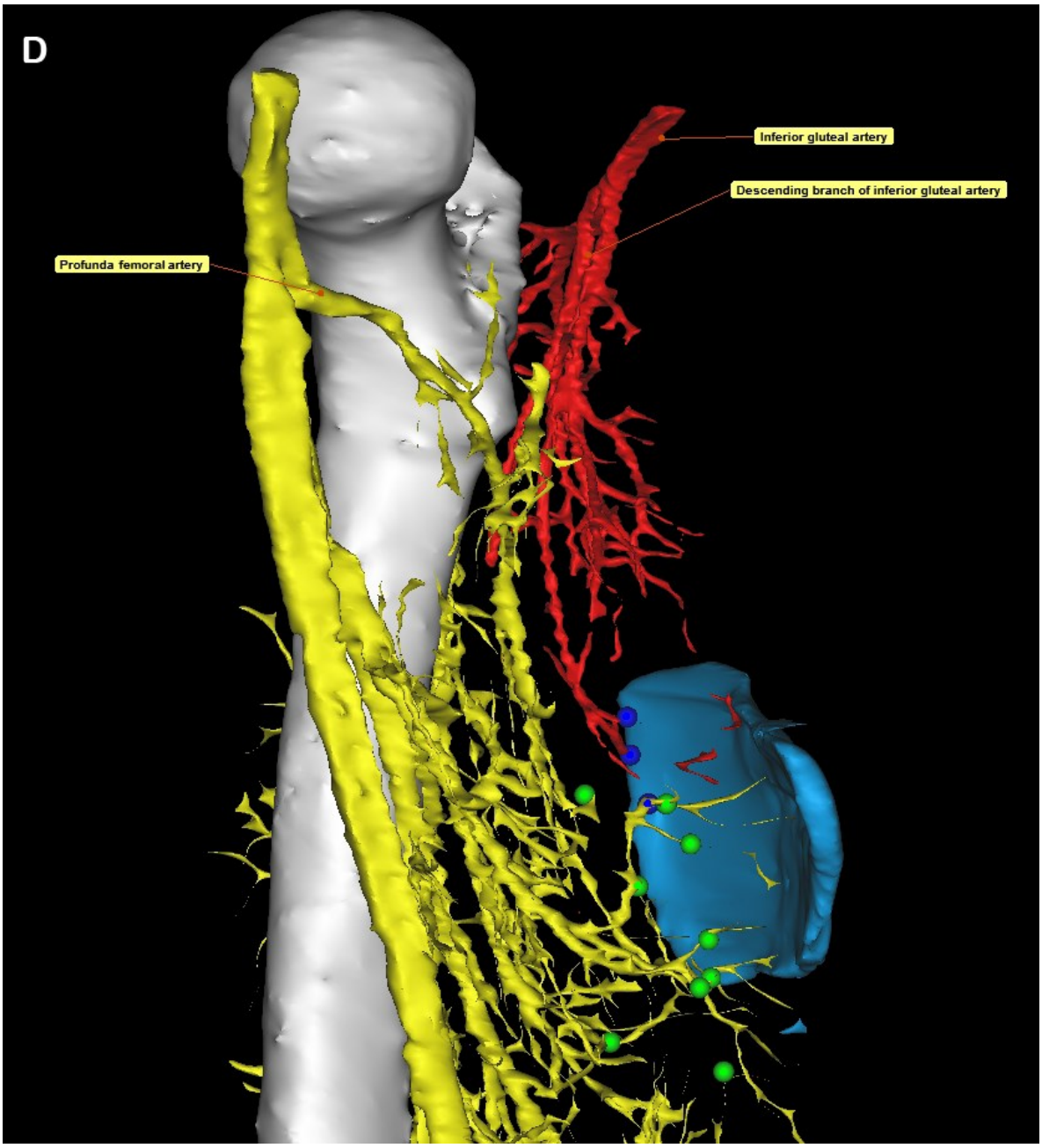

Figure 35D: medial view of the gluteal fold flap. Two arterial supplies are available to this flap, the descending branch of the inferior gluteal artery (D-IGA) and profunda femoral artery (PFA).

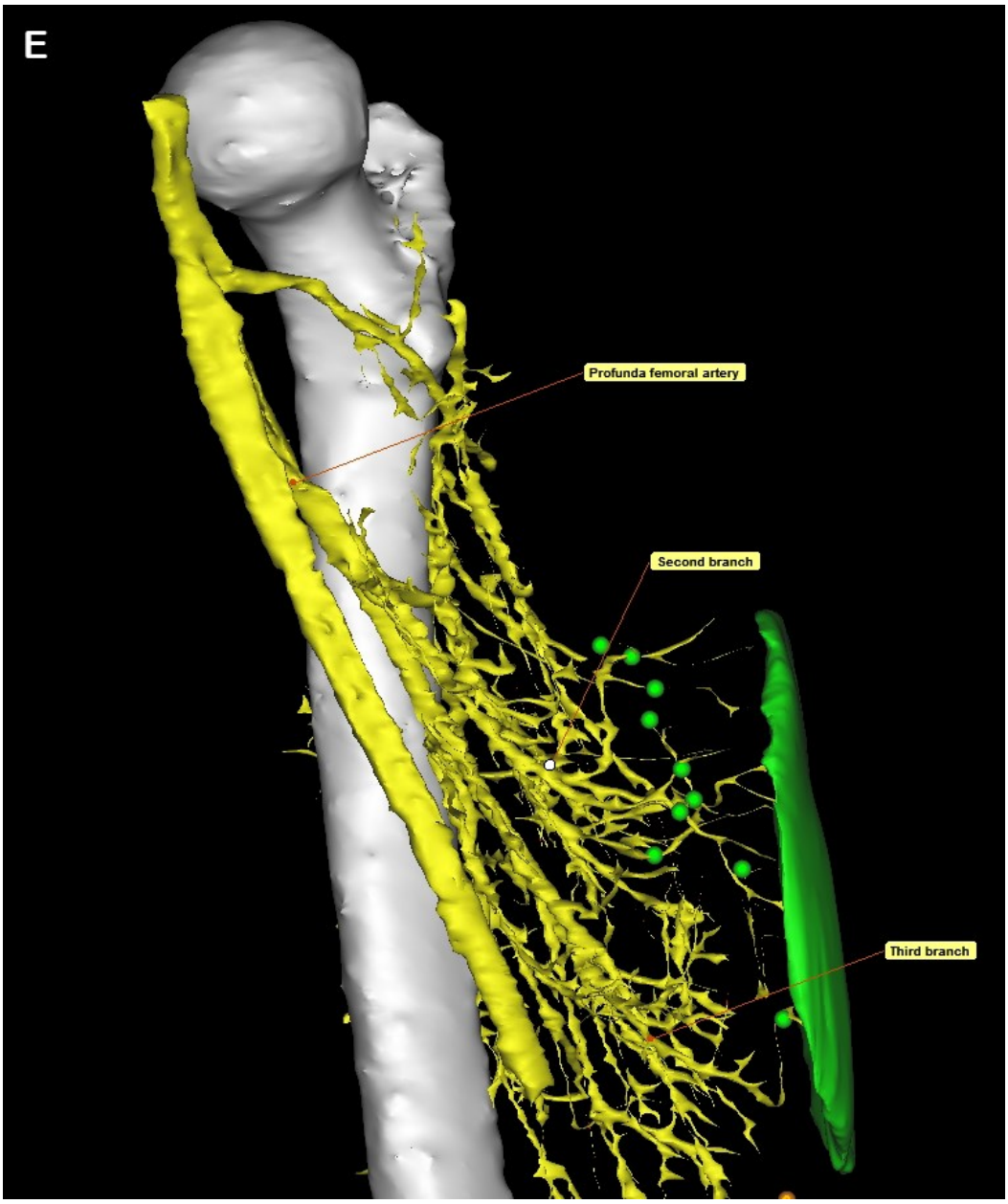

Figure 35E: medial view of a flap designed on a perforator of the third branch of the profunda femoral artery (PFA), (known as the adductor flap). Other potential perforators from the PFA to this flap are indicated with green dots.

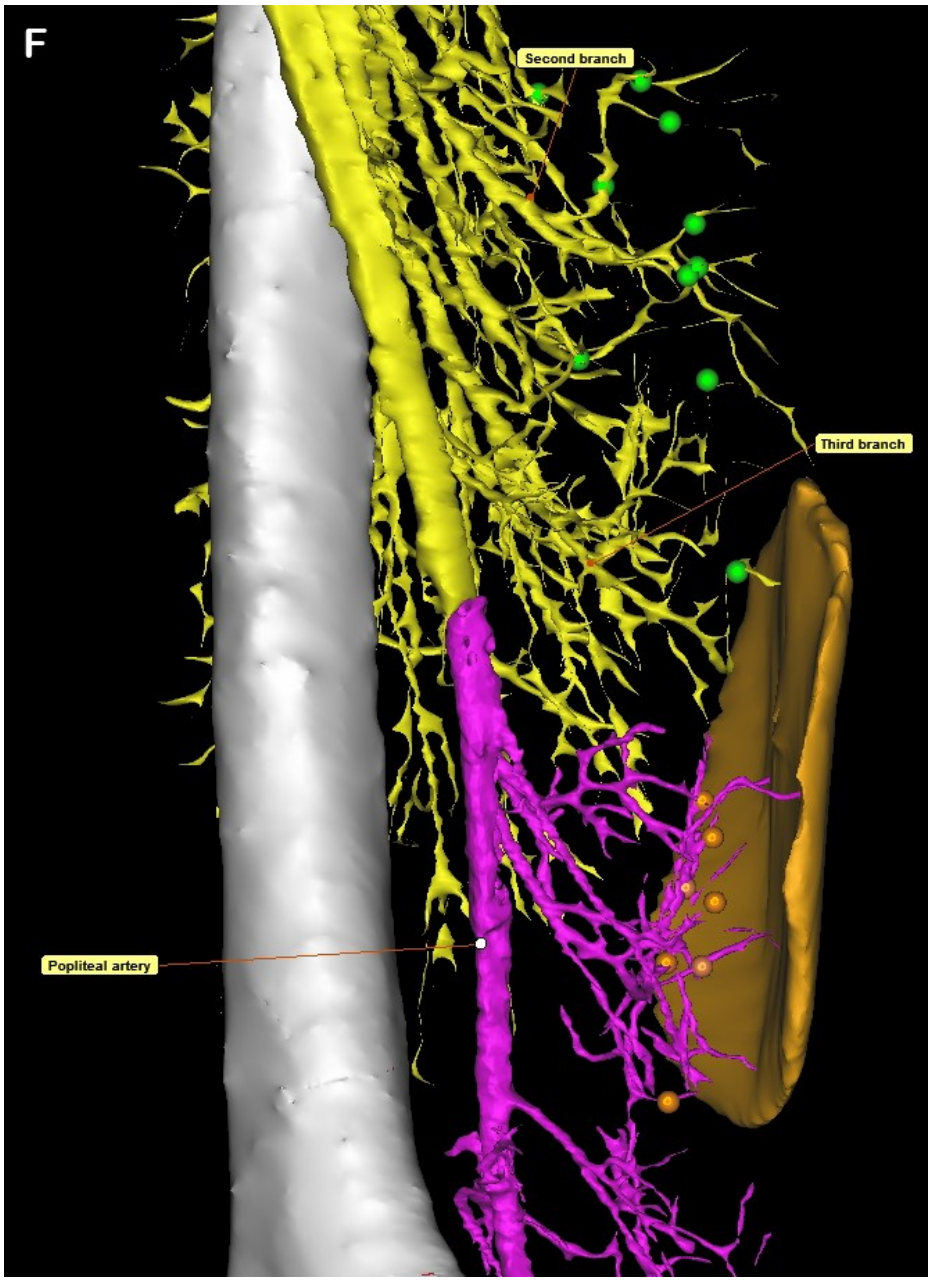

Figure 35F: the orange flap over the popliteal fossa could be designed on two arterial supplies, the profunda femoral artery (PFA) and the popliteal artery (PA).

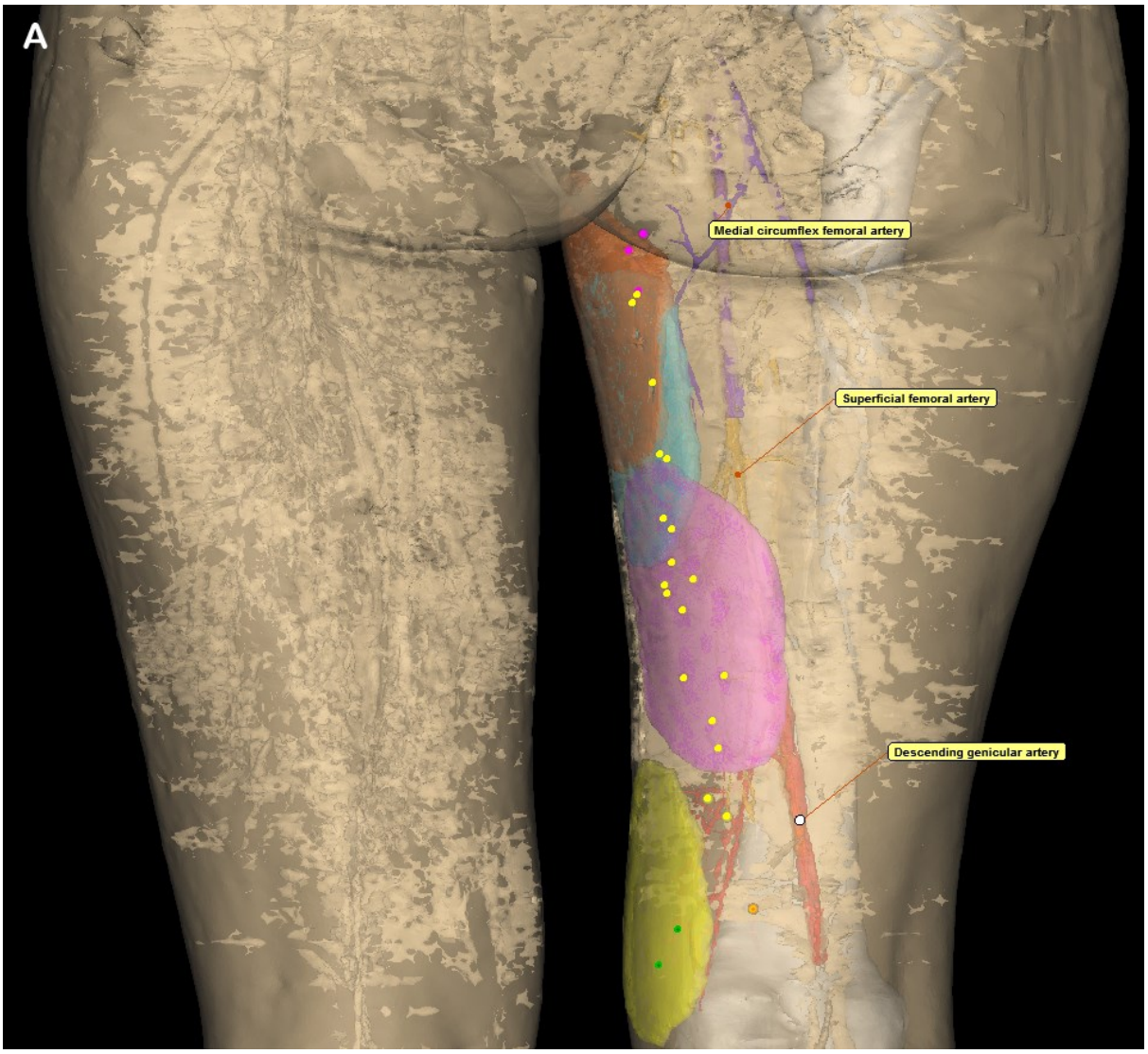

Figure 36 (A-E): Three-dimensional (3D) reconstructions of potential flaps in the posteromedial (PM*l*) thigh sub-region. Figure 36A: in this Figure, the thigh region is viewed posteriorly, the dark orange flap is a medial groin perforator flap or medial circumflex femoral artery (MCFA) flap, designed on a perforator of the MCFA. Other potential perforators from the MCFA are indicated with pink dots. The blue and purple flaps are designed on septocutaneous perforators of the superficial femoral artery (SFA). Other potential perforators from the SFA are indicated with yellow dots. The yellow flap is the saphenous flap, designed on a perforator of the saphenous branch of the descending genicular artery (DGA). Other potential perforators from the saphenous branch of the DGA are indicated with green dots.

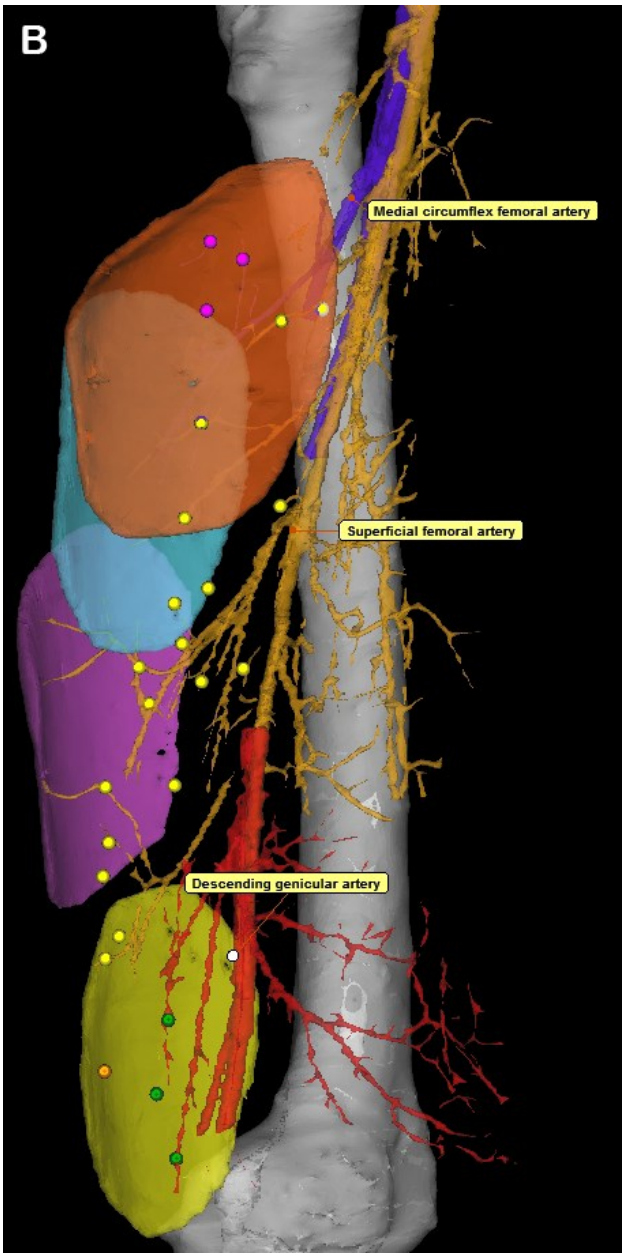

Figure 36B: lateral view of the thigh region shows the potential flaps in the posteromedial (PM*l*) thigh sub-region. The dark orange flap is a medial groin perforator flap or medial circumflex femoral artery (MCFA) flap, designed on a perforator of the MCFA. Other potential perforators from the MCFA are indicated with pink dots. The blue and purple flaps are designed on septocutaneous perforators of the superficial femoral artery (SFA). Other potential perforators from the SFA are indicated with yellow dots. The yellow flap is the saphenous flap, designed on a perforator of the saphenous branch of the descending genicular artery (DGA). Other potential perforators from the saphenous branch of the DGA are indicated with green dots.

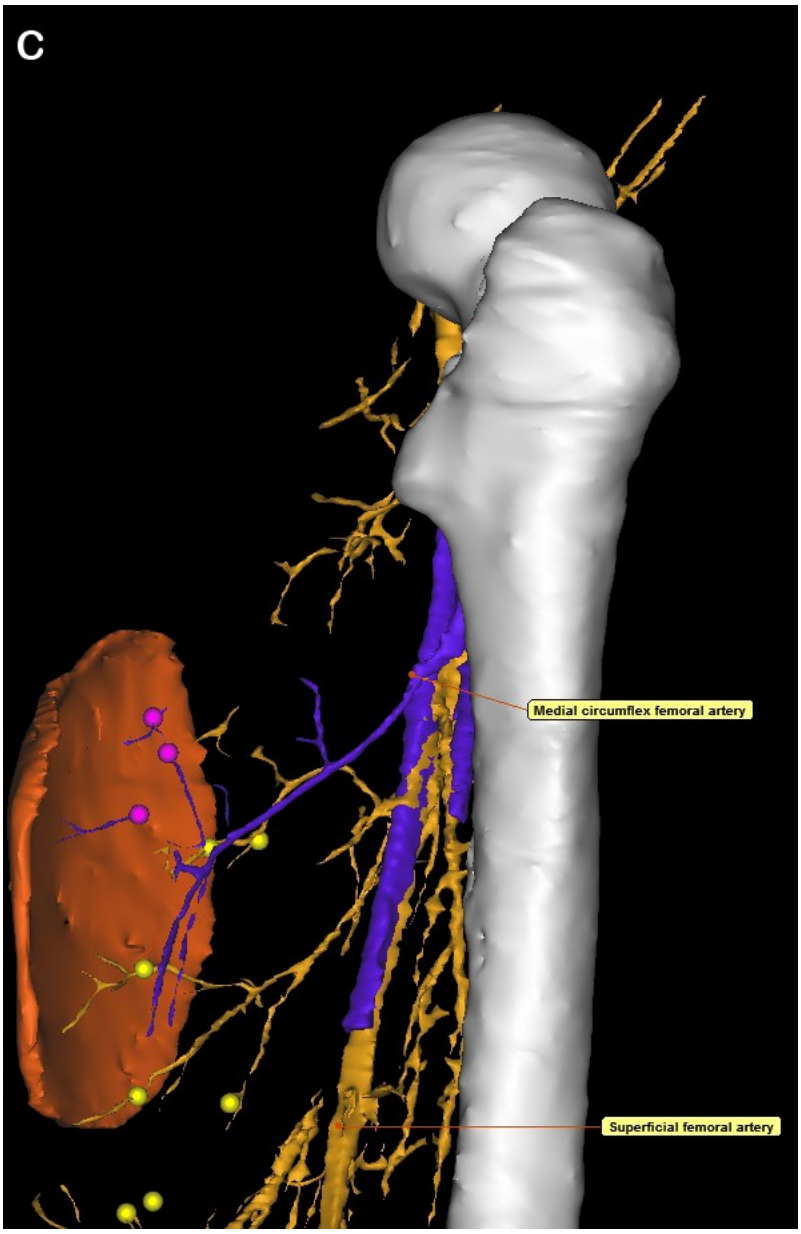

Figure 36C: the Figure shows the medial groin perforator flap. The flap is designed on a perforator of the medial circumflex femoral artery (MCFA). Other potential perforators from the MCFA are indicated with pink dots.

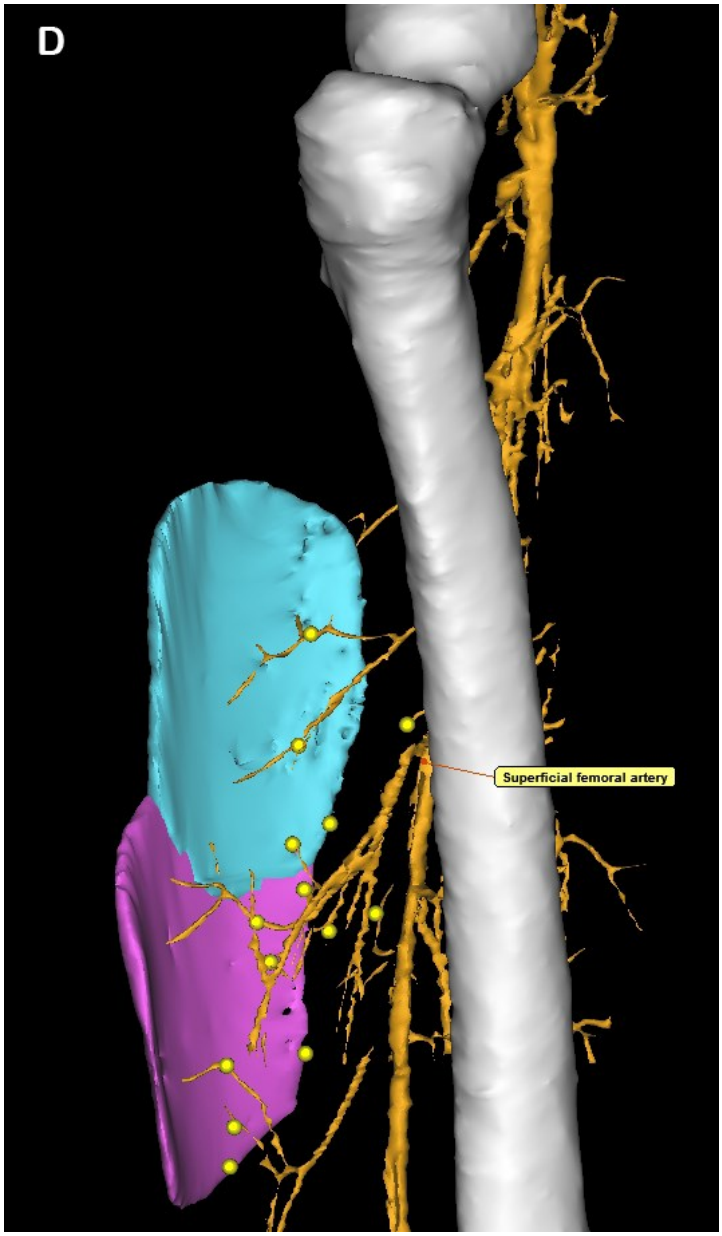

Figure 36D: the Figure shows two flaps designed on septocutaneous perforators of the superficial femoral artery (SFA). Other potential perforators from the SFA are indicated with yellow dots.

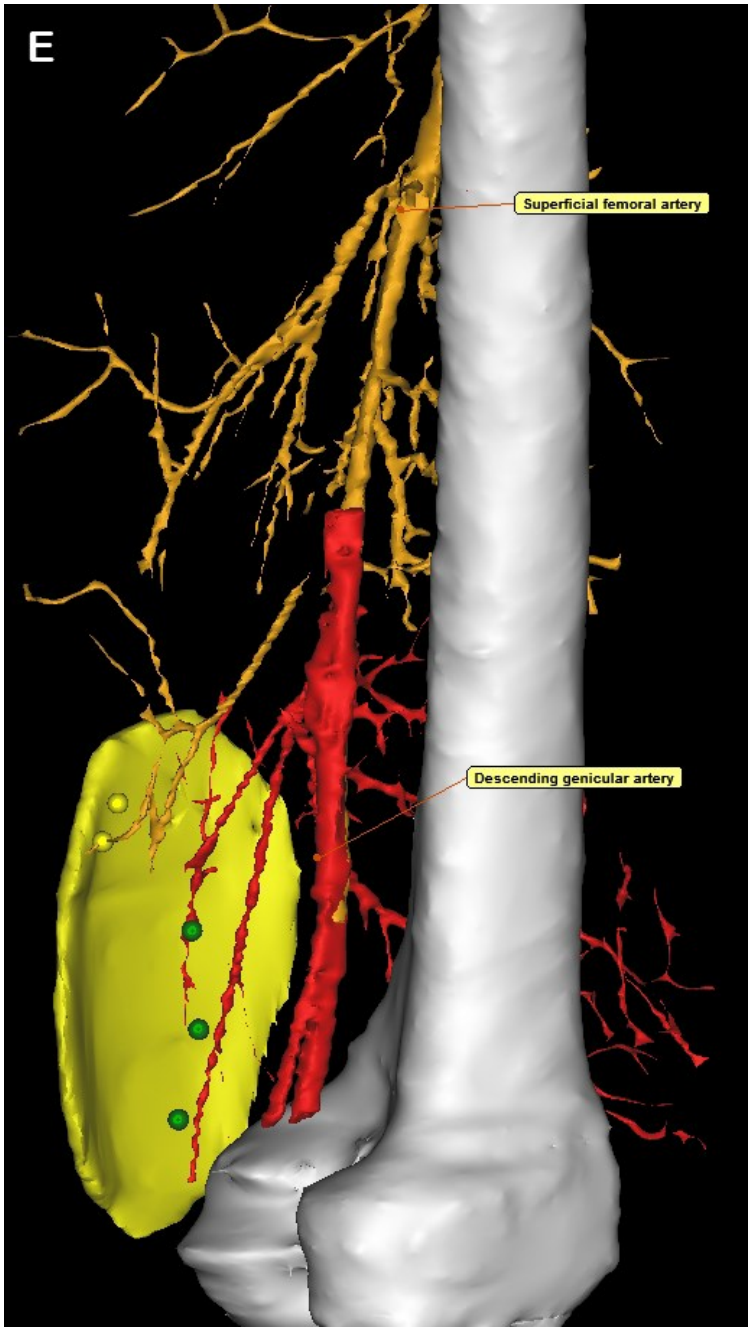

Figure 36E: the Figure shows a saphenous flap, designed on a perforator of the saphenous branch of the descending genicular artery (DGA). Other potential perforators from the saphenous branch of the DGA are indicated with green dots.

6.2 Implications of study findings on flap size prediction

In this cadaveric study (n=15), the reliability of perforator anatomy of any vascular territory of the thigh in providing "safe" (no necrosis after the reconstruction) large flaps can be estimated by the prediction of the maximum flap size, which, in turn, is reliant on factors that ultimately determine the survival rate of this flap. The prediction of the flap size can be estimated by the average perforasome area and the average area perfused per mm diameter of these vascular territories. In confirmation of previous studies, the potential vessel diameter was found to be the critical factor in the prediction of the flap size (Figure 37). The LCFA, SFA, and PFA respectively were thus found to be the most reliable vascular territories for large "safe" flap harvest.

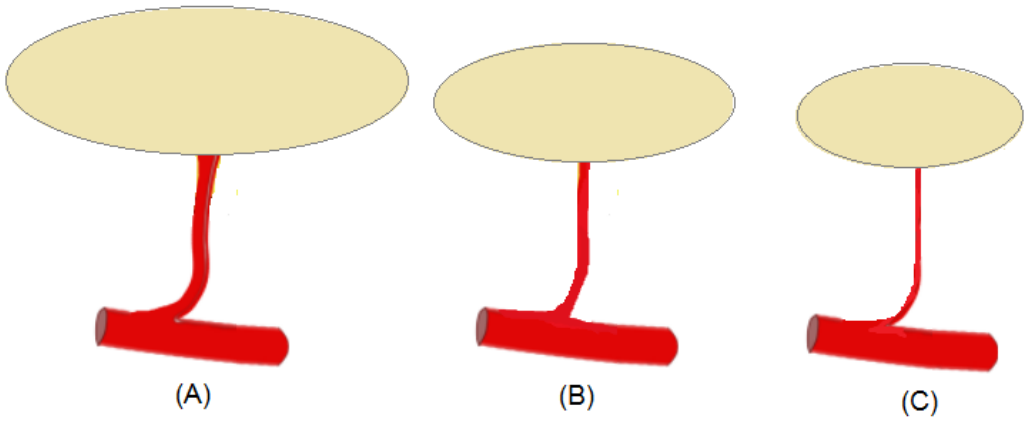

Figure 37: The relationship between perforator diameter and flap size. The Figure shows a proportional relationship between the potential perforator diameter and possible “safe” flap size. (A) Large diameter pedicle supplies a large cutaneous territory, (B) Medium diameter pedicle supplies medium cutaneous territory, (C) small diameter pedicle supplies a small cutaneous territory.

6.3 Limitations

Samples

This study is based on cadavers donated through a donation program and obtained on the basis of availability. Variable gender, age, height, and weight of the cadavers caused further variability in the results leading to many inherent restrictions characteristic of cadaveric studies. The cadavers studied were all elderly individuals and multiple pathologies were associated with causes of death including cardiovascular diseases, therefore, collected information depended on the quality of the samples and the study injections. The sample size n=15 is not enough to make conclusions for the general population.

Vessels measurements

In order to visualize and measure fine perforator arteries, the *thresholding* range in MIMICS software was expanded (below 400 HU). This may cause more pixels (tissue surrounding perforators) to be added to the reconstruction resulting in diameters that are larger than actual diameters. To address this limitation, following the method by Gillis et al.,[24] the diameter of perforators detected below the 400 HU were multiplied by a correction factor of 0.4. In this study, as a precaution to ensure the feasibility of this correction factor, approximately 20 such perforator diameters with correction factor were compared to diameter dimensions from physical dissection. Results using the correction factor were very similar to actual dimensions.

6.4 Future of 3D preoperative planning for flap surgery

3D analytical preoperative imaging is essential to the identification of the dominant potential perforator, and evaluation of the recipient site for more successful reconstructive surgeries. Flap surgery could be facilitated when 3D modeling technique, is used in vascular analysis for flap preoperative planning.

6.5 Implications for teaching and research

The 3D modeling technique, virtual dissection, would likely lead to the development of teaching videos of thigh anatomy related to reconstructive surgery and save the cadaveric educational materials for further research. One intention of this study is to share this knowledge through a website - called “Flapopedia”- accessible to educators, curious and disinterested observers alike, which will be is intended to create a one-stop platform for the fundamentals of thigh flaps and the related vascular anatomy.

CHAPTER 7 CONCLUSION

This study examined in detail the arterial vascular anatomy of the thigh integument three-dimensionally. The objective of the study was to accurately quantify and describe the location of perforators and source vessels. From a sample size of 15 thighs, all five hypotheses proposed for this study were confirmed. An average of 88 ± 16 (n=15) arterial perforators from several source vessels provides a rich vascular donor site for many potential surgical flaps. The perforators were counted and identified related to their source vessel. Then, common quantifiable characteristics of these groups were measured and calculated to ascertain the reliability.

The comprehensive knowledge of perforator anatomy combined with extrapolations from physiological studies facilitates the prediction of flap size and hence safe flap design. This method has aided in the resolution of ambiguities associated with the vascular anatomy of the thigh, and comprehensively quantified and evaluated the perforators and the associated characteristics. 3D modeling technique allowed the simulation of the design of various flaps from all the vascular territories of the thigh. Despite some limitations inherent in cadaveric studies, this study has shown clearly that 3D modeling technique provides a comprehensive spatial orientation of the thigh's vasculature allowing the simulation of safe flap surgery and providing opportunities for preoperative planning. Further, this study creates exciting implications for teaching, research and the dissemination of knowledge of flap anatomy and design.

BIBLIOGRAPHY

1. Geddes CR, Tang M, Yang D, Morris SF. 2006. Anatomy of the integument of the lower extremity. In Blondeel P, Morris SF, Hallock GG, Neligan PC, editors. *Perforator flaps: anatomy, technique and clinical applications.* St Louis: Quality Medical Publishing. p. 541-578.

2. Ahmadzadeh R, Bergeron L, Tang M, Geddes CR, Morris SF. 2007. The posterior thigh perforator flap or profunda femoris artery perforator flap. *Plast Reconstr Surg.* 119: 194-200.

3. Pan W, Taylor G I. 2009. The angiosomes of the thigh and buttock. *Plast Reconstr Surg.* 123: 236-249.

4. Moore KL, Dalley AF, Agur AMR. 2006. *Clinically oriented anatomy*. 5th ed. Baltimore: Lippincott Williams & Wilkins. p. 2.

5. McCraw JB, Vasconez LO. 1980. Musculocutaneous flaps: principles. *Clin Plast Surg.* 7: 9-13.

6. Manchot C. 1889. *Die Hautarterien des menschlichen Korpers*. Leipzig: FCW Vogel. 60 p.

7. Manchot C. 1983. *The cutaneous arteries of the human body*. Ristic J, Morain WD, translator. New York: Springer-Verlag. 149 p.

8. Spalteholz W. 1893. Die Vertheilung der Blutgefässe in der Haut. Leipzig: *Arch Anat Entwicklungsgesch (leipz).* 1:54

9. Salmon M. *Arteries of the skin*. In Taylor GI, Tempest MN, editors. 1988. London: Churchill Living-stone. 174 p.

10. Morris SF, Miller B, Taylor GI. 2006. History of Flap Surgery. In Blondeel P, Morris SF, Hallock GG, Neligan PC, editors. *Perforator flaps: anatomy, technique and clinical applications.* St Louis: Quality Medical Publishing. Fig. 2–1, p. 15; Fig. 2-8 p. 31.

11. Taylor GI, Ives A, Dhar S. 2006. Vascular territories. In: Mathes SJ, editor. *Plastic surgery.* 2nd edition, vol. 1. Philadelphia: Elsevier. Fig. 15.4; . p. 321

12. Taylor GI, Palmer JH. 1987. The vascular territories (angiosomes) of the body: experimental study and clinical applications. *Br J Plast Surg.* 40: 113-41.

13. Rees MJ, Taylor GI. 1986. A simplified lead oxide cadaver injection technique. *Plast Reconstr Surg.* 77: 141.

14. Taylor GI, Corlett RJ, Dhar SC, Ashton MW. 2011. The anatomical (angiosome) and clinical territories of cutaneous perforating arteries: development of the concept and designing safe flaps. *Plast Reconstr Surg.* 127: 1447-1459.

15. Morris SF, Taylor GI. 1993. Predicting the survival of experimental skin flaps with a knowledge of the vascular architecture. *Plast Reconstr Surg.* 7: 1352-1361.

16. Morris SF, Tang M, Almutari K, Geddes C, Yang D. 2010. The anatomic basis of perforator flaps. *Clin Plast Surg.* 37: 553-570.

17. Yang D, Tang M, Geddes CR, Morris SF. 2006. Anatomy of the integument of the head and neck. In Blondeel P, Morris SF, Hallock GG, Neligan PC, editors. *Perforator flaps: anatomy, technique and clinical applications.* St Louis: Quality Medical Publishing. p. 133-160.

18. Thomas BP, Geddes CR, Tang M, Morris SF. 2006. The vascular supply of the integument of the upper extremity. In Blondeel P, Morris SF, Hallock GG, Neligan PC, editors. *Perforator flaps: anatomy, technique and clinical applications.* St Louis: Quality Medical Publishing. p. 220–246.

19. Geddes CR, Tang M, Yang D, Morris SF. 2006. Anatomy of the integument of the trunk. In Blondeel P, Morris SF, Hallock GG, Neligan PC, editors. *Perforator flaps: anatomy, technique and clinical applications.* St Louis: Quality Medical Publishing. p. 359-384.

20. Tang M, Yin Z, Morris SF. 2008. A pilot study on three-dimensional visualization of perforator flaps by using angiography in cadavers. *Plast Reconstr Surg.* 122: 429–437.

21. Tang M, Mao Y, Almutairi K, Morris SF. 2009. Three-dimensional analysis of perforators of the posterior leg. *Plast Reconstr Surg.* 123: 1729-1738.

22. Tang M, Morris SF. Three-dimensional angiography of the deep circumflex iliac artery osteocutaneous perforator flap. A cadaver study. *Plast Reconstr Surg.* in press.

23. Tang M, Ding M, Almutairi K, Morris SF. 2011. Three-dimensional angiography of the submental artery perforator flap. *J Plast Reconstr aesthet surg.* 64: 608-613.

24. Gillis JA, Prasad V, Morris SF. 2011. Three-dimensional analysis of the internal mammary artery perforator flap. *Plast Reconstr Surg.* 128: 419-426.

25. Martin AL, Bissell MB, Al Dhamin A, Morris SF. 2013. Computed tomographic angiography for localization of the cutaneous perforators of the leg. *Plast Reconstr Surg.* 131: 792-800.

26. Haschek E, Linderthal OT. 1896. A contribution to the practical use of photography according to Roentgen. *Wien Klin Wochenschr.* 9: 63

27. Ferguson FR. 1925. Roentological Injection Masses: Old and New. *J Anat.* 59: 297-300.

28. Bergeron L, Tang M, Morris SF. 2006. A review of vascular injection techniques for the study of perforator flaps. Plast Reconstr Surg. 117: 2050-2057.

29. Trueta J, Harrison MHM. 1953. The normal vascular anatomy of the femoral head in adult man. *J Bone Joint Surg Br.* 35: 442-461.

30. Shehata R. 1974. Radio-opaque modification of Kellner's injection mass. *Acta Anat (Basel).* 87: 461-466.

31. Bulla A, Casoli C, Farace F, Mazzarello V, De Luca L, Rubino C, Montella A. 2014. A new contrast agent for radiological and dissection studies of the arterial network of anatomic specimens. *Surg Radiol Anat.* 36: 79-83.

32. Tang M, Geddes CR, Yang D, Morris SF. 2002. Modified lead oxide-gelatin injection technique for vascular studies. *Chin J Clin Anat.* 1: 73-78.

33. Suami H, Taylor GI, Pan W. 2005. A new radiographic cadaver injection technique for investigating the lymphatic system. *Plast reconstr surg.*115: 2007-2013.

34. Morris SF, Maciel-Miranda A, Hallock GG. 2013. History of perforator flap surgery. In Blondeel P, Morris SF, Hallock GG, Neligan PC, editors. *Perforator flaps: anatomy, technique and clinical applications.* 2nd ed. St Louis: Quality Medical Publishing. p. 4-24.

35. Milton SH. 1970. Pedicled skin-flaps: the fallacy of the length: width ratio. *Br J Surg.* 57: 502-508.

36. Daniel RK, Williams HB. 1972. Experimental arterial flaps. *Surg Forum.* 23: 507-509.

37. Daniel RK, Williams HB. 1973. The free transfer of skin flaps by microvascular anastomoses. An experimental study and a reappraisal. *Plast Reconstr Surg.* 52: 16-31.

38. Daniel RK, Kerrigan CL. 1979. Skin flaps: an anatomical and hemodynamic approach. *Clin Plast Surg.* 6: 181-200.

39. Bakamjian VY. 1986. Total reconstruction of pharynx with medially based deltopectoral skin flap. *N Y State J Med.* 68: 2771-2778.

40. McGregor IA, Jackson IT. 1972. The groin flap. *Br J Plast Surg.* 25: 3–16

41. Smith PJ, Foley B, McGregor IA, Jackson IT. 1972. The anatomical basis of the groin flap. *Plast Reconstr Surg.* 49: 41-47.

42. Ferreira MC, Monteiro AA, Besteiro JM. 1981. Free flaps for reconstruction of the lower extremity. *Ann Plast Surg.* 6: 475-481.

43. McCraw JB. 1980. The recent history of myocutaneous flaps. *Clin Plast Surg*. 7: 3-7

44. Mathes SJ, Nahai F. 1982. *Clinical applications for muscle, musculocutaneous flaps*. St. Louis: CV Mosby. 734 p.

45. Zhang G, Chen K, Zhang J, Wang S. 2012. Repair of a large soft tissue defect in the leg with cross-leg bridge free transfer of a latissimus dorsi myocutaneous flap: a case report. *Chin J Traumatol.* 15: 373-375.

46. Qu Z, Liu Y, He Xu, Ding X, Fang G. 2012. Use of pedicled latissimus dorsi myocutaneous flap to reconstruct the upper limb with large soft tissue defects. *Chin J Traumatol.* 15: 352-354.

47. Acarturk TO. 2009. Treatment of large ischial ulcers communicating with the hip joint with proximal femoral resection and reconstruction with a combined vastus lateralis, vastus intermedius and rectus femoris musculocutaneous flap. *J Plast Reconstr Aesthet Surg.* 62: 1497-1502.

48. Mathes SJ, Nahai F. 1997. General principles. *Reconstructive surgery: Principles, anatomy & technique.* New York: Quality Medical Publishing and Churchill Livingston. 3: 253

49. Mathes SJ, Alpert BS. 1980. Advances in muscle and musculocutaneous flaps. *Clin Plast Surg.* 7: 15-26.

50. Geddes CR, Morris SF, Neligan PC. 2003. Perforator flaps: evolution, classification, and applications. *Ann. Plast Surg* .50: 90-99.

51. Kroll SS, Rosenfield L. 1988. Perforator-based flaps for low posterior midline defects. *Plast Reconstr Surg.* 81: 561-566.

52. Koshima I, Soeda S. 1989. Inferior epigastric artery skin flaps without rectus abdominis muscle. *Br J Plast Surg.* 42: 645-648.

53. Whiteside LA. 2014. Surgical Technique: Muscle Transfer Restores Extensor Function After Failed Patella-Patellar Tendon Allograft. *Clin Orthop Relat Res*. 472: 218-226.

54. Soldado F, Bertelli J. 2013. Free gracilis transfer reinnervated by the nerve to the supinator for the reconstruction of finger and thumb extension in longstanding C7-T1 brachial plexus root avulsion. *J Hand Surg Am.* 38: 941-946.

55. Chin K, Vasdeki D, Hart A. 2013. Inverted free functional gracilis muscle transfer for the restoration of elbow flexion. *J Plast Reconstr Aesthet Surg*. 66: 144-146.

56. Whiteside LA. 2013. Surgical technique: vastus medialis and vastus lateralis as flap transfer for knee extensor mechanism deficiency. *Clin Orthop Relat Res.* 471: 221-230.

57. Xingzhou Qu, Chenping Z, Laiping Z, Min R, Shanghui Z, Mingyi W. 2011. Deep circumflex iliac artery flap combined with a costochondral graft for mandibular reconstruction. *Br J Oral Maxillofac Surg.* 49: 597-601.

58. Gaggl AJ, Burger H, Chiari FM. 2011. A combined superficial inferior epigastric artery flap and vascularized iliac crest flap in the reconstruction of extended composite defects of the posterior mandible and adjacent soft tissue: first clinical results. *Int J Oral Maxillofac Surg.* 40: 162-168.

59. Haddock NT, Wapner K, Levin LS. 2013. Vascular bone transfer options in the foot and ankle: a retrospective review and update on strategies. *Plast Reconstr Surg.* 132: 685-693.

60. Koshima I, Moriguchi T, Fukuda H, Yoshikawa Y, Soeda S. 1991. Free, thinned, paraumbilical perforator-based flaps. *J Reconstr Microsurg.* 7: 313-316.

61. Kimura N, Satoh K. 1996. Consideration of a thin flap as an entity and clinical applications of the thin anterolateral thigh flap. *Plast Reconstr Surg.* 97: 985-992.

62. Daniel RK, Taylor GI. 1973. Distant transfer of an island flap by microvascular anastomoses. A clinical technique. *Plast Reconstr Surg.* 52: 111-117.

63. Taylor GI, Daniel RK. 1973. The free flap: composite tissue transfer by vascular anastomosis. *Aust N Z J surg.* 43: 1-3.

64. Harii K, Omori K, Torii S, Murakami F, Kasai Y. 1975. Free groin skin flaps. *Br J Plast Surg.* 28: 225-237.

65. Harii K, Omori K, Omori S. 1974. Successful clinical transfer of ten free flaps by microvascular anastomoses. *Plast Reconstr Surg.* 53: 259-270.

66. Harii K, Omori K, Omori S. 1974. Free deltopectoral skin flaps. *Br J Plast Surg.* 27: 231-239.

67. Harii K, Ohmori K. 1975. Free groin flaps in children. *Plast Reconstr Surg.* 55: 588-592.

68. Koshima I, Yamamoto T, Narushima M, Mihara M, Iida T. 2010. Perforator flaps and supermicrosurgery. *Clin Plastic Surg.* 37: 683-689.

69. Baek SM. 1983. Two new cutaneous free flap: The medial, and lateral thigh flaps. *Plast Reconstr Surg.* 71: 354-65.

70. Song YG, Chen GZ, Song YL. 1984. The free thigh flap: A new concept based on the septocutaneous artery. *Br J Plast Surg.* 37: 149–159.

71. Mardini S, Lin CH, Wei FC. 2006. Lateral Circumflex femoral Artery- Vastus Lateralis Perforator Flap. . In Blondeel P, Morris SF, Hallock GG, Neligan PC, editors. *Perforator flaps: anatomy, technique and clinical applications.* St Louis (MO): Quality Medical Publishing. p. 618-633.

72. Kimura N. 2006. Lateral Circumflex femoral Artery-Tensor Fascia Lata Perforator Flap. . In Blondeel P, Morris SF, Hallock GG, Neligan PC, editors. *Perforator flaps: anatomy, technique and clinical applications*. St Louis (MO): Quality Medical Publishing. p. 636-646.

73. Hallock GG. 2006. Medial Circumflex Femoral Artery: A Medial Groin Flap. . In Blondeel P, Morris SF, Hallock GG, Neligan PC, editors. *Perforator flaps: anatomy, technique and clinical applications.* St Louis (MO): Quality Medical Publishing. p. 648-656

74. Lipa EJ. 2006. Posterior Thigh Perforator Flaps. . In Blondeel P, Morris SF, Hallock GG, Neligan PC, editors. *Perforator flaps: anatomy, technique and clinical applications.* St Louis (MO): Quality Medical Publishing. p. 597-615.

75. Yu P. 2004. Characteristics of the anterolateral thigh flap in a Western population and its application in head and neck reconstruction. *Head Neck.* 26: 759-69.

76. Xu DC, Zhong SZ, Kong JM, Wang GY, Liu MZ, Luo LS, Gao JH. 1988. Applied anatomy of the anterolateral femoral flap. *Plast Reconstr Surg.* 82: 305-310.

77. Koshima I, Fukuda H, Yamamoto H, Moriguchi T, Soeda S, Ohta S. 1993. Free anterolateral thigh flaps for reconstruction of Head and Neck defects. *Plast Reconstr Surg.* 92: 421-428; discussion 429-430.

78. Zhou G, Qiao Q, Chen GY, Ling YC, Swift R. 1991. Clinical experience and surgical anatomy of 32 free anterolateral thigh flap transplantations. *Br J Plast Surg.* 44: 91-96.

79. Kuo YR, Jeng SF, Kuo MH, Huang MN, Liu YT, Chiang YC, Yeh MC, Wei FC. 2001. Free anterolateral thigh flap for extremity reconstructions: Clinical experience and functional assessment of donor site. *Plast Reconstr Surg.* 107: 1766-1771.

80. Gedebou TM, Wei FC, Lin CH. 2002. Clinical experience of 1284 free anterolateral thigh flaps. *Handchir Mikrochir Plast Chir.* 34: 239-244.

81. Kuo YR, Seng-Feng J, Kuo FM, Liu YT, Lai PW. 2002. Versatility of the free anterolateral thigh flap for reconstructions of soft tissue defects: Review of 140 cases. *Ann Plast Surg.* 48: 161-166.

82. Wei FC, Jain V, Celik N, Chen HC, Chuang DC, Lin CH. 2002. Have we found an ideal soft- tissue flap? An experience with 672 anterolateral thigh flaps. *Plast Reconstr Surg.* 109: 2219-2226; discussion 2227-2230.

83. Chen HC, Tang YB. 2003. Anterolateral thigh flap: An ideal soft tissue flap [review]. *Clin Plast Surg.* 30: 383-401.

84. Demirkan F, Chen HC, Wei FC, Chen HH, Jung SG, Hau SP, Liao CT. 2000. The versatile anterolateral thigh flap: a musculcutaneous flap in disguise in head and neck reconstruction. *Br J Plast Surg.* 53: 30-6

85. Lakhiani C, Lee MR, Saint-Cyr M. 2012. Vascular anatomy of the anterolateral thigh flap: a systematic review. *Plast Reconst Surg.* 130: 1254-1268.

86. Wong CH, Kao HK, Fu B, Lin JY. 2009. A cautionary point in the harvest of the anterolateral thigh myocutaneous flap. Ann Plast Surg. 62: 637-639.

87. Wong CH. 2012. The oblique branch trap in the harvest of the anterolateral thigh myocutaneous flap. *Microsurg.* 32: 631-634.

88. Choi SW, Park JY, Hur MS, Park HD, Kang HJ, Hu KS, Kim HJ. 2007. An anatomic assessment of perforators of the lateral circumflex femoral artery for the anterolateral thigh flap. J Craniofacial Surg. 18: 866-871.

89. Kimata Y, Uchiyama K, Ebihara S, Nakatsuka T, Harii K. Anatomic variations and technical problems of the anterolateral thigh flap: a report of 74 cases. *Plast Reconstr Surg.* 1998;102:1517-23.

90. Wong CH, Wei FC, Fu C, Chen YA, Lin JY. 2009. Alternative vascular pedicle of the anterolateral thigh flap: the oblique branch of the lateral circumflex femoral artery. *Plast Reconstr Surg.* 123: 571-577.

91. Koshima I, Fikuda H, Utumomiya R, Soeda S. 1989. The anterolateral thigh flap: variations in its vascular pedicle. *Br J Plast Surg.* 42: 260-262.

92. Valdatta L, Tuinder S, Buoro M, Thione A, Faga A, Putz R. 2002. Lateral circumflex femoral arterial system and perforators of the anterolateral thigh flap: an anatomic study. *Ann Plast Surg.* 49: 145-150.

93. Yildrim S, Avci G, Akoz T. 2003. Soft-tissue reconstruction using a free anterolateral thigh flap: experience with 28 patients. *Ann Plast Surg.* 51: 37-44.

94. Luo S, Raffoul W, Luo J, Luo L, Gao J, Chen L, Egloff DV. 1990. Anterolateral thigh flap: a review of 168 cases. *Microsurg.* 19: 232–238.

95. Kimura N, Satoh K, Hasumi T, Otsuka T. 2001. Clinical application of the free thin anterolateral thigh flap in 31 consecutive patients. *Plast Reconstr Surg.* 108: 1197–1208.

96. Camaioni A, Loreti A, Damiani V, Bellioni M, Passali F M, Viti C. 2008. Anterolateral thigh cutaneous flap vs. radial forearm free-flap in oral and oropharyngeal reconstruction: an analysis of 48 flaps. *Acta otorhinolaryngol Ital*. 28: 7-12.

97. Hsu H, Chien S, Wang C, Cheng L, Lin C, Wu M, Huang C, Lee J. 2012. Expanding the applications of the pedicled anterolateral thigh and vastus lateralis myocutaneous flaps. *Ann Plast Surg.* 69: 643-649.

98. Wei FC, Celik N, Chen HC, Cheng MH, Huang WC. 2002. Combined anterolateral thigh flap and vascularized fibula osteoseptocutaneous flap in reconstruction of extensive composite mandibular defects. *Plast Reconstr Surg*. 109: 45-52.

99. Wei FC, Suominen S, Chen MH, Celik N, Lai YL. 2002. Anterolateral thigh flap for postmastectomy breast reconstruction. *Plast Reconstr Surg*. 110: 82-88.

100. Ross G L, Dunn R, Kirkpatrick J, Koshy C E, Alkureishi L W, Bennett N, Soutar D S, Camilleri I G. To thin or not to thin: the use of the anterolateral thigh flap in the reconstruction of intraoral defects. *Br J Plast Surg.* 56: 409-413.

101. Alkureishi LW, Shaw-Dunn J, Ross GL. 2003. Effects of thinning the anterolateral thigh flap on the blood supply of the skin. *Br J Plast Surg.* 56: 401-408.

102. Hallock GG. 2013. Tissue Expansion Techniques to Minimize Morbidity of the Anterolateral Thigh Perforator Flap Donor Site. *J Reconstr Microsurg.* 29: 565-570.

103. Tayfur V, Magdan O, Edizer M, Atabey A. 2010. Anatomy of vastus lateralis muscle flap. *J Craniofacial Surg.* 21: 1951-1953.

104. Shieh SJ, Chiu HY, Yu JC, Pan SC, Tsai ST, Shen CL. 2000. Free anterolateral thigh flap for reconstruction of head and neck defects following cancer ablation. *Plast Reconstr Surg.* 105: 2349-2357

105. Hill HL, Nahai F, Vasconez LO. 1978. The tensor fascia lata myocutaneous free flap. *Plast Reconstr Surg.* 61: 517-522.

106. Nahai F, Silverton JS, Hill HL, Vasconez LO. 1978. The tensor fascia lata musculocutaneous flap. *Ann Plast Surg.* 1: 372-379.

107. Santanelli F, Scuderi N. 2000. Neophalloplasty in female-to-male transsexuals with the island tensor fasciae latae flap. *Plast Reconstr Surg.* 105: 1990–1996.

108. Wei FC, Demirkan F, Chen HC, Ceh IH. 1999. Double free flaps in reconstruction of extensive composite mandibular defects in head and neck cancer. *Plast Reconstr Surg.* 103: 39–47.

109. Wei FC, Demirkan F, Chen HC, Chen IH, Liao CT, Hau SP. 1999. Management of secondary soft-tissue deficits following microsurgical head and neck reconstruction by means of another free flap. *Plast Reconstr Surg.* 103: 1158–1166.

110. Demirkan F, Wei FC, Chen HC, Chen IH, Hau SP, Liau CT. 1999. Microsurgical reconstruction in recurrent oral cancer: use of a second free flap in the same patient. *Plast Reconstr Surg.* 103: 829-838.

111. Bulstrode NW, Kotronakis I, Baldwin MAR. 2006. Free tensor fasciae latae musculofasciocutaneous flap in reconstructive surgery: A series of 85 cases. *J Plast Reconstr Aesthet Surg.* 59: 130–136

112. Coskunfirat OK, Ozkan O. 2006. Free tensor fasciae latae perforator flap as a backup procedure for head and neck reconstruction. *Ann Plast Surg.* 57: 159-163.

113. Ishida LH, Munhoz AM, Montag E, Alves HR, Saito FL, Nakamoto HA, Ferreira MC. 2005. Tensor fasciae latae perforator flap: Minimizing donor-site morbidity in the treatment of trochanteric pressure sores. *Plast Reconstr Surg.* 116: 1346–1352.

114. Kimura N, Saito M, Itho Y, Sumiya N. 2006. Giant combined microdissected thin thigh perforator flap. *J Plast Reconstr Aesthet Surg.* 59: 1325–1329.

115. Koshima I, Urushibara K, Inagawa K, Moriguchi T. 2001. Free tensor fasciae latae perforator flap for the reconstruction of defects in the extremities. *Plast Reconstr Surg.* 107: 1759-1765.

116. Kimura NA 2002. Microdissected thin tensor fasciae latae perforator flap. *Plast Reconstr Surg.* 109: 69-77.

117. Deiler S, Pfadenhauer A, Widmann J, Stuzle H, Kanz KG, Stock W. 2000. Tensor fasciae latae perforator flap for reconstruction of composite Achilles tendon defects with skin and vascularized fascia. *Plast Reconstr Surg.* 106: 342-349.

118. Hill H L, Hester R, Nahai F. 1979. Covering large groin defects with the tensor fascia lata musculocutaneous flap. *Br J Plast Surg.* 32: 12-14.

119. Peled IJ, Kaplan HY, Herson M, Wexler MR. 1983. Tensor fascia lata musculocutaneous flap for abdominal wall reconstruction. *Ann Plast Surg.* 11: 141-143.

120. Luce EA, Hyde G, Gottlieb SE, Romm S. 1983. Total abdominal wall reconstruction. *Arch Surg.* 118: 1446-1448.

121. Riebelova V. 1985. The tensor fasciae latae musculocutaneous flap in operations for trochanteric decubitus ulcers. *Acta Chir Plast*. 27: 17-25.

122. Krupp S, Kuhn W, Zaech GA. 1983. The use of innervated flaps for the closure of ischial pressure sores. *Paraplegia.* 21: 119-126.

123. Ihara K, Doi K, Shigetomi M, Kawai S. 1997. Tensor fasciae latae flap: alternative donor as a functioning muscle transplantation. *Plast Reconstr Surg.* 100: 1812-1816.

124. Kind GM, Foster RD. 2011. Breast reconstruction using the lateral femoral circumflex artery perforator flap. *J Reconstr Microsurg.* 27: 427-432.

125. Lin CH, Wei FC, Lin YT, Yeh JT, Rodriguez E, Chen CT. 2006. Lateral circumflex femoral artery system: Warehouse for functional composite free-tissue reconstruction of the lower leg. *J Trauma.* 60: 1032–1036

126. Dabernig J, Shilov B, Schumacher O, Lenz C, Dabernig W, Schaff J. 2006. Functional reconstruction of Achilles tendon defects combined with overlying skin defects using a free tensor fasciae latae flap. *J Plast Reconstr Aesthet Surg.* 59: 142– 147.

127. Laitung JK. 1989. The lower posterolateral thigh flap. *Br J Plast Surg.* 42: 133-139.

128. Hayashi A, Maruyama Y. 1990. The lateral genicular artery flap. *Ann. Plast Surg.* 24: 310-317.

129. Spokevicius S, Jankauskas A. 1995. Anatomy and clinical applications of a composite cutaneo-subcutaneous flap based on the lateral superior genicular vessels. *J Reconstr Microsurg.* 11: 15-20.

130. Taniguchi Y, Kitano T, Shimoe T, Asai Y, Yoshida M. 2009. Superior lateral genicular artery flap for coverage of a soft tissue defect after total knee arthroplasty. *J Reconstr Microsurg.* 25: 479-482.

131. Koshima I, Yamamoto H, Hosoda M, Moriguchi T, Orita Y, Nagayama H. 1993. Free combined composite flaps using the lateral circumflex femoral system for repair of massive defects of the head and neck regions: an introduction to the chimeric flap principle. *Plast Reconstr Surg.* 92: 411 420.

132. Koshima I, Hosoda M, Inagawa K, Moriguchi T, Orita Y. 1996. Free medial thigh perforator-based flaps: new definition of the pedicle vessels and versatile application. *Ann Plast Surg.* 37: 507-15.

133. Ao M, Nagase Y, Mae O, Namba Y. 1997. Reconstruction of posttraumatic defects of the foot by flow-through anterolateral or anteromedial thigh flaps with preservation of posterior tibial vessels. *Ann Plast Surg.* 38:598-603

134. Ao M, Uno K, Maeta M, Nakagawa F, Saito R, Nagase Y. 1999. De-epithelialised anterior (anterolateral and anteromedial) thigh flaps for dead space filling and contour correction in head and neck reconstruction. *Br J Plast Surg.* 52: 261-267

135. Schoeller T, Huemer G M, Shafighi M, Gurunluoglu R, Wechselberger G, Piza Katzer H. 2004. Free anteromedial thigh flap: clinical application and review of literature. *Microsurg*. 24: 43-48.

136. Shimizu T, Fisher DR, Carmichael SW, Bite U. 1997. An anatomic comparison of septocutaneous free flaps from the thigh region. *Ann Plast Surg.* 38: 604-610

137. Hayashi A, Maruyama Y. 1990. The medial genicular artery flap. *Ann. Plast Surg.* 25: 174-180.

138. Acland RD, Schusterman M, Godina M, Eder E, Taylor GI, Carlisle I. 1981. The saphenous neurovascular free flap. *Plast Reconstr Surg.* 67: 763-774.

139. Koshima I, Endou T, Soeda S, Yamasaki M. 1988. The free or pedicled saphenous flap. *Ann Plast Surg.* 21: 369-374.

140. Tsai CC, Lin SD, Lai CS, Chou CK, Lin TM. 1995. Reconstruction of the upper leg and knee with a reversed flow saphenous island flap based on the medial inferior genicular artery. *Ann Plast Surg.* 35: 480-484.

141. Regnard P J, Bensa P, Zilliox R. 1990. The saphenous flap called the *Acland. Ann Chir Plast Esthet.* 35: 313-316.

142. Karamursel S, Celebioglu S. 2006. Use of the medial side of the knee skin as a free flap: saphenous flap. *Plast Reconstr Surg.* 117: 1308-1314.

143. Lykoudis EG, Spyropoulou GC, Vlastou C. 2005. The anatomic basis of the gracilis perforator flap. *Br J Plast Surg.* 58: 1090-1094.

144. Orticochea M. 1972. The musculo-cutaneous flap method: an immediate and heroic substite for the method of delay. *Br J Plast Surg.* 25: 106-110

145. Mathes SJ, McCraw JB, Vasconez LO. 1974. Muscle transposition flaps for c overage of lower extremity defects: Anatomic considerations. *Surg Clin North Am.* 54: 1337–1354.

146. Wang TN, Whetzel T, Mathes SJ, Vasconez LO. 1987. A fasciocutaneous flap for vaginal and perineal reconstruction. *Plast Reconstr Surg.* 80: 95-103.

147. McCraw JB, Dibbell DG, Carraway JH. 1977. Clinical definition of independent myocutaneous vascular territories. *Plast Reconstr Surg.* 60: 341-352.

148. Yousif NJ, Matlob HS, Kolachalam R, Grunert BK, Sanger JR. 1992. The transverse gracilis musculocutaneous flap. *Ann Plast Surg.* 29: 482-490.

149. Peek A, Muller M, Ackermann G, Exner K, Baumeister S. 2009. The free gracilis perforator flap: anatomical study and clinical refinements of a new perforator flap. *Plast Reconstr Surg.* 123: 578-588.

150. Hallock GG. 2003. The gracilis (medial circumflex femoral) perforator flap: A medial groin free flap? *Ann Plast Surg.* 51: 623–626.

151. Peek A, Muller M, Exner K. 2002. The free gracilis perforator flap for autologous breast reconstruction. *Handchir Mikrochir Plast Chir.* 34: 245-250.

152. Hallock GG. 2006. Scrotal reconstruction following fournier gangrene using the medial circumflex femoral artery perforator flap. *Ann Plast Surg*. 57: 333-335.

153. Hallock GG. 2003. The medial circumflex femoral (gracilis) local perforator flap_ A local medial groin perforator flap. *Ann Plast Surg.* 51: 460-464.

154. Fansa H, Schirmer S, Warnecke I C, Cervelli A, Frerichs O. 2008. The transverse myocutaneous gracilis muscle flap: a fast and reliable method for breast reconstruction. *Plast Reconstr Surg.* 122: 1326-1333.

155. Hurwitz DJ. 1980. Closure of a large defect of the pelvic cavity by an extended compound myocutaneous flap based on the inferior gluteal artery. *Br J Plast Surg.* 33: 256-261.

156. Hurwitz DJ, Swartz WM, Mathes SJ. 1981. The gluteal thigh flap: a reliable, sensate flap for the closure of buttock and perineal wounds. *Plast Reconstr Surg.* 68: 521-532.

157. Zenn MR, Millard JA. 2006. Free inferior gluteal flap harvest with sparing of the posterior femoral cutaneous nerve. *J Reconstr Microsurg.* 22: 509-512.

158. Paletta C, Bartell T, Shehadi S. 1993. Applications of the posterior thigh flap. *Ann Plast Surg.* 30: 41-47.

159. Hurteau JE, Bostwick J, Nahai F, Hester R, Jurkiewicz MJ. 1981. V-Y advancement of hamstring musculocuataneous flap for coverage of ischial pressure sores. *Plast Reconstr Surg.* 68: 539-542.

160. Ramirez OM, Hurwitz DJ, Futrell JW. 1984. The expansive gluteus maximus flap. *Plast Reconstr Surg.* 74: 757-770.

161. Maruyama Y, Ohnishi K, Takeuchi S. 1984. The lateral thigh fascio-cutaneous flap in the repair of ischial and trochanteric defects. *Br J Plast Surg.* 37:103-107.

162. Rozen WM, Donahoe S, Wilson JL. 2011. The profunda femoris artery "fourth perforator" island flap: a new perforator flap in lower-limb reconstruction. *J Reconstr Microsurg.* 27: 273-276.

163. Angrigiani C, Grilli D, Thorne C H. 2001. The adductor flap: a new method for transferring posterior and medial thigh skin. *Plast Reconstr Surg.* 107: 1725-1731.

164. Allen RJ, Haddock NT, Ahn C Y, Sadeghi A. 2012. Breast reconstruction with the profunda artery perforator flap. *Plast Reconstr Surg.* 129: 16e-23e.

165. Haddock NT, Greaney P, Otterburn D, Levine S, Allen RJ. 2012. Predicting perforator location on preoperative imaging for the profunda artery perforator flap. *Microsurg.* 32: 507-511.

166. Saad A, Sadeghi A, Allen RJ. 2012. The anatomic basis of the profunda femoris artery perforator flap: a new option for autologous breast reconstruction--a cadaveric and computer tomography angiogram study. *J Reconstr Microsurg.* 28: 381-386.

167. Maruyama Y, Iwahira Y. 1989. Popliteo-posterior thigh fasciocutaneous island flap for closure around the knee. *Br J Plast Surg.* 42: 140-143.

168. Lambert F, Cariou J L, Couturaud B, Bellavoir A. 1996. Fasciocutaneous flap of the posterior surface of the thigh with distal pedicle. Anatomical study and surgical value. A propos of 3 cases. *Ann Chir Plast Esthet.* 41: 145-154.

169. Bergeron L. 2006. *The anatomical basis of the deep circumflex iliac artery perforator flap with iliac crest.* (Masters thesis). Montreal (QC): University of Montreal. 3: 33.

170. Cormack GC, Lamberty BG. 1986. Cadaver studies of correlation between vessel size and anatomical territory of cutaneous supply. *Br J Plast Surg.* 39: 300-306.

171. Chen SY, Lin WC, Deng SC, Chang SC, Fu JP, Dai NT, Chen SL, Chen TM, Chen SG. 2012. Assessment of the perforators of anterolateral thigh flaps using 64-section multidetector computed tomography angiography in head and neck cancer reconstruction. *Eur J of Surg Oncol.* 36: 1004-1011.

172. Chou EK, Ulusal B, Ulusal A. Wei FC, Lin CH, Taso CK. 2006. Using the descending branch of the lateral femoral circumflex vessel as a source of two independent flaps. *Plast Reconstr Surg.* 117: 2059-2063.

173. Tsai FC, Yang JY, Mardini S, Chuang SS, Wei FC. 2004. Free split-cutaneous perforator flaps procured using a three-dimensional harvest technique for the reconstruction of postburn contracture defects. *Plast Reconstr Surg.* 113: 185-193; discussion 194-195.

174. Yun I S, Lee J H, Rah D K, Lee W J. 2010. Perineal reconstruction using a bilobed pudendal artery perforator flap. *Gynecol Oncol.* 118: 313-316.